

AN ENERGY STUDY OF THE GROUND STATE OF  
SOME FOUR ELECTRON COMPLEXES

by

ANTHONY WEST

A thesis submitted to  
THE UNIVERSITY OF LEICESTER  
for the degree of Ph.D.  
in the Faculty of Science

1970

UMI Number: U376989

All rights reserved

INFORMATION TO ALL USERS

The quality of this reproduction is dependent upon the quality of the copy submitted.

In the unlikely event that the author did not send a complete manuscript and there are missing pages, these will be noted. Also, if material had to be removed, a note will indicate the deletion.



UMI U376989

Published by ProQuest LLC 2015. Copyright in the Dissertation held by the Author.  
Microform Edition © ProQuest LLC.

All rights reserved. This work is protected against  
unauthorized copying under Title 17, United States Code.



ProQuest LLC  
789 East Eisenhower Parkway  
P.O. Box 1346  
Ann Arbor, MI 48106-1346

X753052023

## A C K N O W L E D G M E N T S

The author would like to thank Professor E.A.Stewardson for the opportunity to work in the Physics Department of the Leicester University.

Thanks are also due to Mr.A.D.Tait for his assistance with NSO theory and to the Quantum Molecular Physics Group as a whole for much useful discussion on a number of aspects of this work.

The receipt of a maintenance award from the S.R.C. is gratefully acknowledged.

Above all, thanks are extended to Dr.K.E.Banyard for his supervision throughout this research, and for many hours of helpful and stimulating discussion on every aspect of this work.

---

THESIS  
H 04793  
25.11.71

## C O N T E N T S

	Page
ACKNOWLEDGMENTS	
ABSTRACT	
CHAPTER 1 - INTRODUCTION .....	1
CHAPTER 2 - COMPLEXES INVESTIGATED .....	6
CHAPTER 3 - THE METHOD OF CALCULATION -	
Background Development .....	11
The Hamilton Operator .....	14
The Geometry of the System .....	15
Construction of the Wave Function...	17
Construction of the Matrix Elements.	22
CHAPTER 4 - TESTING THE PROGRAMME .....	27
CHAPTER 5 - RESULTS AND DISCUSSION -	
The $ZHZH^{+2Z-2}$ System .....	36
The Hamilton-like System .....	70
Summary .....	84
APPENDIX I - EVALUATION OF INTEGRALS .....	86
APPENDIX II - THE EIGENVALUE PROBLEM .....	90
APPENDIX III - NSO's and ELECTRON DENSITY DISTRIBUTION	98
REFERENCES .....	112

## A B S T R A C T

The work of Banyard and Shull on a series of two-electron pseudomolecular ions  $ZHZ^{+2Z-1}$  has been extended to four electron systems of the form  $ZHZH^{+2Z-2}$ . These systems may be regarded as an approximate representation of a fragment of a more complex molecule, therefore, noninteger  $Z$  values were used in an attempt to make some allowance for the nuclear shielding caused by the presence of other electrons which were otherwise unaccounted for in the calculations. The effective nuclear charge  $Z$  was allowed to take values of 1.0, 1.2, 1.4, 1.8 and 2.2 and the optimum bond angle  $ZHZ$  was studied as a function of  $Z$ . Within a limited basis set of Slater-type  $1s$  orbitals, the calculations were complete configuration interaction treatments. The C.I. wave functions were reformulated in terms of natural spin orbitals. Consequently, changes in the electron density distributions have been investigated as a function of  $Z$  and bond angle. For  $Z = 1.0, 1.4, 1.8$  and  $2.2$ , and  $\widehat{ZHZ} = 100^\circ$  and  $120^\circ$ , the electron densities of the  $ZHZH^{+2Z-2}$  ion have been compared with those of the  $ZHZ^{+2Z-1}$  systems.

The nuclear framework of the diborane "bridge" was adopted for a second series of four-centre, four-electron calculations: a similar investigation has been carried out by Hamilton. Once again an allowance was made for nuclear shielding by using effective nuclear charges - the boron nuclear charge,  $B_Z$ , was given values of 2.0, 2.5 and 3.0. Slater-type  $1s$  orbitals were centred on the hydrogen nuclei and  $2s$  orbitals on the boron nuclei. For each value of  $B_Z$  the energy was minimized with respect to the orbital exponents. The electron density at points along the internuclear axes was then evaluated for the optimized systems.

CHAPTER 1

INTRODUCTION

The discovery, by Schrodinger in 1926<sup>(1)</sup>, of a fundamental differential equation describing the motion of an electron and accounting for its wave-like nature laid the foundations of present day wave mechanics. The Schrodinger equation

$$\nabla^2 \Phi + \frac{2M}{\hbar^2} [E - V] \Phi = 0 \quad (1.1)$$

stands in approximately the same relation to the Hamilton-Jacobi<sup>(2)</sup> equations as does wave optics to geometrical optics. In fact, the Schrodinger equation is often written in Hamilton-like form

$$H \Phi(\vec{q}) = E \Phi(\vec{q}) \quad (1.2)$$

where  $\Phi(\vec{q})$  is a function of the coordinates of all the particles of the system. The Hamiltonian operator H can be defined by referring to one of the basic postulates of the new quantum theory:- "for every physically measurable property of a system there corresponds a linear operator such that the eigenvalues of that operator are the possible results of measurement of the observable property<sup>(3)</sup>". If the time independent energy levels of a system are the desired physical observables, the corresponding linear operator is the Hamiltonian, H, and if one can find the eigenfunctions  $\Phi(\vec{q})$ , of H, then the desired stationary energy levels can be calculated.

Assuming then that Schrodinger's equation does describe atomic-scale systems correctly, it might appear, at first sight, that the calculation of atomic and molecular structure is merely an exercise in applied mathematics; however, this is not so. The wave equation for

a molecule, for example, is a second order differential equation in  $3N$  variables, where  $N$  is the number of particles in the molecule. No general analytical solution can be found for such an equation, and the use of direct numerical solutions does not help; the amount of numerical data required to specify the wave function of comparatively simple molecules, would be enormous. In order to make the problem tractable it is necessary to have recourse to the use of approximate methods. This is where a knowledge of the physics of the problem becomes important. Any approximations which are made in solving the problem must be physically reasonable if meaningful results are to be obtained.

The approximation developed by Hartree<sup>(4)</sup> and Fock<sup>(5)</sup> was a major step in simplifying the solution of the many-electron atom wave equation. The essence of the approximation - now known as the Hartree-Fock method - is that each electron is considered to be under the influence of the nuclear potential field and the total average charge distribution of all the other electrons in the atom. Each electron is thus considered to be independent of the instantaneous position of the others. When this independent particle approximation is used the total wave function for the atom (at least one with a closed shell structure) may be written as a single determinant, that is

$$\Psi = \begin{vmatrix} \psi_1(1) & \psi_2(1) & \dots & \psi_N(1) \\ \psi_1(2) & \psi_2(2) & \dots & \psi_N(2) \\ \vdots & \vdots & \ddots & \vdots \\ \psi_1(N) & \psi_2(N) & \dots & \psi_N(N) \end{vmatrix} \quad (1.3)$$

where  $\Psi$  is the total wave function of the system and  $\psi_1, \psi_2, \dots, \psi_N$  are one-electron wave functions known as atomic orbitals. Using this type of wave function and applying the variational method the problem reduces to the solution of a set of equations

$$F \psi_i = \epsilon_i \psi_i \quad (1.4)$$

known as the Fock equations.  $F$  is an operator defined in terms of the  $\psi_i$ , so the equations must be solved iteratively until a self-consistent set of orbitals is obtained.

Due to the nature of its basic approximation the Hartree-Fock method incorporates an inherent error known as the correlation error. The distribution of electrons within the atomic system will be such that they tend to avoid each other in their motion about the nucleus, that is their motion is correlated. The Hartree-Fock method does not take sufficient account of this and consequently will always predict an energy value which is too high. But even so this method has been widely applied to calculations on atomic structure, and seems to give an accurate description of the distribution of electrons within an atom. However its application is still tedious and complicated, and attempts have been made to simplify the problem. This has been done by replacing the copious numerical data obtained by the Hartree-Fock method by simple analytical one-electron functions which approximately reproduce the self-consistent field atomic orbitals. These attempts have met with a good deal of success and as a result these simple functions, in particular those of Slater<sup>(6)</sup>, have been applied extensively in atomic problems.

The problem of solving the wave equation of a molecule is complicated by the presence of the atomic nuclei. Fortunately, because of the great disparity between the electronic and nuclear masses the total wave equation of a molecule may be separated into two parts, one describing the nuclear motion and the other the distribution of the electrons. The electronic wave equation arising from the application of this approximation may be solved by the Hartree-Fock method. However, because of the many-centre nature of the nuclear potential field this is an extremely complex problem. As a result either the approximation developed by Roothaan<sup>(7)</sup> or a complete configuration interaction method is usually used. In Roothaan's method the one-electron wave functions, which are now molecular orbitals, are written as linear combinations of atomic orbitals (the LCAO approximation)

$$\Psi_i = \sum_j a_{ij} \psi_j \quad (1.5)$$

Using this approximation a set of equations analogous to the Fock equations (1.4) is obtained, and these are solved by varying the coefficients  $a_{ij}$  until self consistency is achieved. The configuration interaction method, the one used in this work, builds up the total wave function in a somewhat different way. Slater determinantal wave functions  $\phi$  are constructed for each electronic configuration. The total wave function  $\Psi_k$  for the  $k_{th}$  energy state of the system is expressed as

$$\Psi_k = \sum_i c_{ki} \phi_i \quad (1.6)$$

where  $c_{ki}$  are coefficients to be determined. Once the detailed forms of the configurations  $\phi_i$  are specified the molecular energy and the

corresponding total wave function may be obtained by application of the variation method.

The chief difficulty in both the configuration interaction and Roothaan's method lies in the evaluation of the many-centre integrals which arise. However, the advent of high speed digital computers have made these calculations possible. For this same reason the theoretical study of the structure and physical properties of small molecules has received a great deal of attention in recent years. A major part of the work has been centred around the study of the "normal" two-electron bond. However, as early as 1927 it was recognised that there were some relatively simple substances which defy classification within the Lewis-Langmuir-Sidgwick scheme. These substances are classified as being electron deficient<sup>(A)</sup>, and the work described here attempts to further our understanding of the three-centre two-electron bond. The four-electron systems studied in this work may be regarded as an approximate representation of a fragment of a more complex molecule which is itself electron deficient. The systems which have been investigated in this work and the reasons for doing so are discussed in Chapter 2.

Footnote A. The most restrictive and perhaps the most clear cut definition of electron deficiency is that, in general, the number of valence electrons in a molecule is less than  $2(n-1)$ , where  $n$  is the number of atoms contained in the molecule. In such molecules the idea of an electron pair bond can be retained if we allow that some bonds involve atomic orbitals from more than two atoms of the molecule.

CHAPTER 2

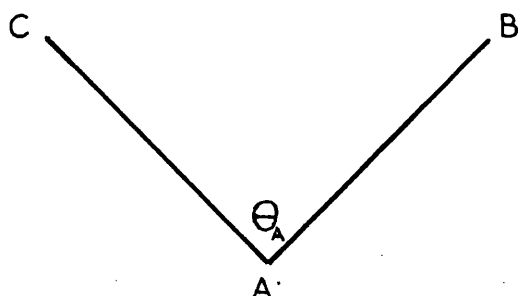
COMPLEXES INVESTIGATED

The electron deficient bonds which occur in the boron hydrides and certain aluminium and beryllium hydrides are also present in the  $H_3^+$  molecular ion. It is for this reason that the  $H_3^+$  ion has been the subject of several recent investigations<sup>(8-11)</sup>. One of these calculations, that of Christoffersen, is of particular significance with regard to this study; this is revealed in the work on Banyard and Shull<sup>(12)</sup> and Banyard and Tait<sup>(13)</sup>. The details of the connections between the four-electron complexes investigated here and the work of Christoffersen are outlined below.

The  $H_3^+$  molecular ion is the simplest of the electron deficient systems and the work of Christoffersen was concerned with the geometry and stability of this molecule. A similar type of bonding to that of  $H_3^+$  is probably the diborane bridge. A detailed study of the "bridge" or "banana" bond in diborane is naturally a difficult problem. Ideally, for each boron atom, the conventional bonds with the terminal hydrogen atoms and also the relatively unperturbed inner-shell electrons should be considered. However, as an initial attempt to contribute towards the understanding of the three-centre two-electron bonds, Banyard and Shull extended Christoffersen's treatment of  $H_3^+$  to a series of pseudomolecular ions of the form  $ZHZ^{+2Z-1}$ .

The two-electron systems  $ZHZ^{+2Z-1}$  were regarded as an approximate representation of a fragment of a more complex molecule. The system contained two outer nuclei which had identical, non-integer charges  $Z$ . The "central" nucleus always had a charge of unity and was, therefore, a bare hydrogen nucleus. The use of non-integer  $Z$  values was an attempt

to create an approximate nuclear framework which allowed, in part, for the nuclear shielding caused by the presence of electrons which were otherwise unaccounted for in the calculation.



Nuclear Charges  $Z_B = Z_C = Z$   
Distances  $AB = AC = 1.66$  au.  
Bond Angle  $ZHZ = \theta_A$

Figure 201. Geometry of the  $ZHZ^{+2Z-1}$  ions

By studying the behaviour of the two electrons within such a modified nuclear framework, Figure 201, it was hoped that some understanding of the nature of the electron deficient bond could be obtained. To this end, the effective nuclear charge  $Z$  was allowed to take values of 0.80 (0.2) 2.2 and the optimum bond angle  $ZHZ$  was investigated as a function of  $Z$ . For each  $Z$  a study was also made of the angular dependence of the molecular energy for a fixed value of the bond length  $AB$ .

The study gave rise to several interesting features, two of which were the initial decrease in the optimum bond angle  $ZHZ$  as the effective nuclear charge  $Z$  was increased, and the occurrence of a double minimum in the angular dependence of the molecular energy for  $Z \sim 1.8$ . It was found that, in general, all the results could be understood by making the tentative suggestion that the electron density was composed of two main components. For convenience, these two forms of the electron density were referred to as the "shared" density and the "local" density:

the former was associated with the inter-nuclear regions and the latter was situated, primarily, about each nucleus.

The initial intention of the  $ZHZ^{+2Z-1}$  investigation was to obtain some understanding of the diborane - like bridge bond. In spite of the interesting results, this work revealed that the behaviour and nature of the bridge bond was still left in considerable doubt. The sizeable initial decrease in the bond angle with increasing effective nuclear charge indicated that the three-centre model was unable to simulate the bridge bond. Consequently there were two paths open for the furtherance of the  $ZHZ^{+2Z-1}$  work; the unusual and rather intriguing results obtained from this work and the problem of the bridge bond representation both required further investigation.

The first path was followed by Banyard and Tait. The configuration-interaction wave functions for the pseudomolecular ions  $ZHZ^{+2Z-1}$  were reformulated in terms of natural orbitals<sup>(14)</sup>. Consequently, changes in the one-particle electron density due to variation of  $Z$  and the bond angle  $ZHZ$  were able to be investigated by means of the population analysis suggested by Mulliken<sup>(15)</sup>. The "local" and "shared" densities interpretation of results was given reasonable support by this work and, in particular, it was of real interest to observe how the systematic variations of  $Z$  and  $\theta_A$  were reflected in the movements of electronic charge throughout the system.

Since the three-centre approach to the diborane-like bridge system was unsatisfactory, it was decided that a different model should be used. The obvious extension of the  $ZHZ^{+2Z-1}$  arrangement was to consider both bridge bonds together. Clearly, it was also of great interest to ask how the presence of the "other bridge" would affect the

findings and analysis of the previous calculation, since, within a constrained system, such calculations present an intriguing picture of charge movement and consequent energy changes due to variations in either nuclear charge or bond angles, or both. The two bridge bonds together constitute a four-electron four-centre problem - the subject of the present investigation.

The four-centre four-electron investigation was conducted in a similar manner to that adopted for the  $ZHZ^{+2Z-1}$  investigation. Non-integer  $Z$  values were once again used to make some allowance for nuclear shielding effects. To enable comparison to be made with the earlier work, the bond lengths AB, BC, CD and AD, Figure 302, were set at 1.66 au, the value used in the  $ZHZ^{+2Z-1}$  calculations. Slater-type 1s atomic orbitals were centred on each nucleus and within this minimal basis set the calculation was a complete four-centre configuration interaction treatment. The effective nuclear charge  $Z$  was allowed to take values of 1.0, 1.2, 1.4, 1.8 and 2.2. It was then possible to study the optimum bond angle  $ZHZ$  as a function of  $Z$ . The method of calculation and the results are described in the later chapters.

The four-centre four-electron work described so far is an extension of the  $ZHZ^{+2Z-1}$  calculations rather than a schematic representation of the "diborane bridge" complex since the details of the geometrical arrangements of the two systems are somewhat different. For this reason, a second series of calculations were carried out using the diborane bridge geometry determined by electron diffraction methods<sup>(16)</sup>. These calculations were similar to those of Hamilton<sup>(17)</sup> since both were four-centre four-electron studies and both used the true geometry. The main differences between the two studies was that Hamilton used a "Roothaan

self consistent field, linear combination of atomic orbitals" method of calculation and hybridized orbitals on the boron atoms. However, in his work the three and four-centre integrals were evaluated using the approximation suggested by Mulliken<sup>(18)</sup>, rather than evaluated explicitly. In the present calculations a 1s Slater-type orbital was centred on the hydrogen nuclei and a 2s Slater-type orbital on the boron nuclei. By introducing the 2s orbital, an attempt was being made to obtain a more realistic model of the diborane bridge<sup>(B)</sup>. The boron nuclear charge was replaced by a series of "effective" values, i.e. 2.0, 2.5 and 3.0, which make some partial allowance for inner-shell nuclear shielding. The variation of the energy with respect to the effective nuclear charge was then investigated.

Where possible the results of the energy calculations were compared with the results of Hamilton. The full extent of these comparisons, along with the results, are described in the later chapters. Subsequent analysis of the wave function in terms of charge distribution should also be of some considerable interest, especially when compared with earlier work.

Footnote (B) Although the introduction of  $2p\sigma$  and  $2p\pi$  orbitals would have been desirable, at the time of calculation the programmes available for evaluating four-centre electron repulsion integrals were restricted to s-type Slater orbitals only. It was for this reason that the calculations were limited to s-type orbitals.

CHAPTER 3

THE METHOD OF CALCULATION

3.1 Background Development

If relativistic effects, spin-orbit and orbit-orbit interactions are ignored, the Hamiltonian operator for an n-particle system can be written as

$$H = \frac{\hbar^2}{2} \sum_{i=1}^n \frac{1}{m_i} \nabla^2(\vec{r}_i) + \sum_{i < j} \frac{Z_i Z_j}{|\vec{r}_i - \vec{r}_j|}, \quad (3.1)$$

where  $\hbar = \frac{h}{2\pi}$ , h is Plank's constant,  $\vec{r}_i$  is the vector distance from some reference coordinate system to particle i, and  $m_i$  and  $Z_i$  are the mass and charge, respectively, of the  $i_{th}$  particle. The first term represents the kinetic energy of the system and the second the potential energy.

On account of the mass of the proton being about 1836 times as great as the mass of the electron, the nuclei move much more slowly than the electrons. This means that when calculating the energy of electrons, the nuclei within a molecule may be treated as fixed. Such an approach, known as the Born-Oppenheimer<sup>(19)</sup> approximation, means that the vibrational and rotational motions of a molecule are effectively quite separate from the electronic motions. Hence, corresponding to any given position of the nuclei, there is a definite energy or set of energies for the electrons. Despite this, only in the case of molecules with a single electron can the wave equation be solved exactly. A means of obtaining energies of any desired accuracy, even through the exact

wave function is not known is provided by the variation theorem. This theorem states that, if  $\Psi$  is an approximation of the exact wave function  $\Phi$ , then the following condition will always be observed:

$$E = \frac{\int \Psi^* H \Psi d\tau}{\int \Psi^* \Psi d\tau} \geq E_0 \quad (3.2)$$

where  $E_0$  is an eigenvalue of the operator  $H$  for the system; the integration is over the total electron configuration space. There is one particular form of the variation method, called the "Method of Linear Combinations", which is outstandingly convenient to use and is most pertinent for the study of molecular systems. With this method the eigenfunction  $\Phi$  associated with the operator  $H$  is approximated by a function  $\Psi$ , which is turn is written as a linear combination of functions  $\phi$ , i.e.

$$\Psi_k = \sum_i c_{ki} \phi_i \quad (3.3)$$

The functions  $\phi_i$  are linearly independent functions appropriate to the system under consideration. By requiring that the energy which is calculated from  $\Psi$  be a minimum, a system of linear equations is obtained which must be solved for the coefficients  $c_{ki}$  and the energy  $E_k$ . The system of equations which arises can be conveniently written out in matrix form as

$$(\underset{\sim}{H} - \lambda \underset{\sim}{S}) \underset{\sim}{C} = 0 \quad (3.4)$$

and are commonly referred to as the secular equations. The above mentioned matrix equation represents the familiar matrix eigenvalue problem. Written out in full the matrix elements  $H_{ij}$  and  $S_{ij}$  are

$$\begin{aligned} H_{ij} &= \int \phi_i^* H \phi_j d\tau \\ S_{ij} &= \int \phi_i^* \phi_j d\tau \end{aligned} \quad (3.5)$$

and  $\underline{C}$  is a column vector of the coefficients  $C_{ki}$ . If the eigenvalues  $\lambda_k$  are arranged in ascending order, then  $\lambda_0$  represents the ground state energy of the system described by the approximate wave function  $\Psi$ . The remaining eigenvalues  $\lambda_i$  ( $i = 1, \dots, n$ ) are approximations to the excited state energies.

The methods and theorems described above were employed in constructing the secular equations which describe a molecular complex of four electrons and four nuclei. Each procedure was systematically followed and a detailed account of the results appears in the following sections.

### 3.2 The Hamiltonian Operator

The Born-Oppenheimer approximation was adopted, and the total molecular Hamiltonian  $H$  for a system of four nuclei and four electrons was written in atomic units<sup>(20)</sup> as:

$$\begin{aligned}
 H = & \sum_{i=1}^4 \left( \frac{1}{2} \nabla_i^2 \right) - \sum_{i=1}^4 \left( \frac{Z_A}{r_{Ai}} + \frac{Z_B}{r_{Bi}} + \frac{Z_C}{r_{Ci}} + \frac{Z_D}{r_{Di}} \right) \\
 & + \left( \frac{Z_A \cdot Z_B}{R_{AB}} + \frac{Z_A \cdot Z_C}{R_{AC}} + \frac{Z_A \cdot Z_D}{R_{AD}} + \frac{Z_B \cdot Z_D}{R_{BD}} + \frac{Z_C \cdot Z_D}{R_{CD}} + \frac{Z_B \cdot Z_C}{R_{BC}} \right) \quad (3.6) \\
 & + \sum_{i>j}^4 \frac{1}{r_{ij}}
 \end{aligned}$$

There are four groups of terms.

The first group represents the kinetic energy of the electrons, the second represents the attraction of the  $i_{th}$  electron to each of the nuclei (A, B, C and D), the third represents the mutual repulsion of the nuclei and the last, the mutual repulsion of the electrons. This particular form of the Hamiltonian was generated from the general form described in section 3.1. The Born-Oppenheimer approximation allowed the terms representing the kinetic energy of the nuclei to be neglected.

### 3.3 The Geometry of the System

In molecular calculations Group Theory provides a powerful tool for utilising the symmetry properties of the molecule. The diborane-like bridge, whose geometry is shown below, belongs to the point group  $D_{2h}$ .

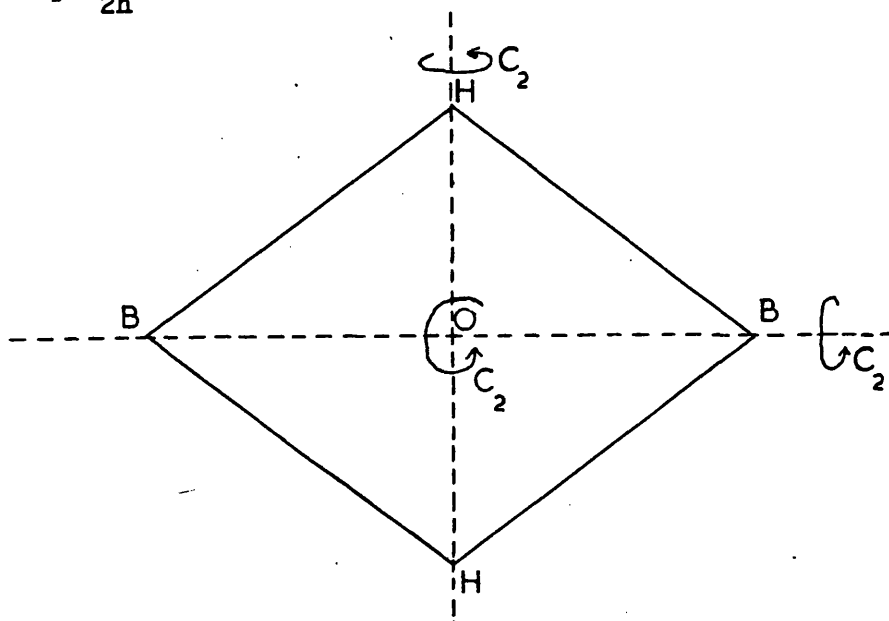


Figure 301. Geometry of the Diborane Bridge

This is a highly symmetrical group with three  $C_2$  axes of symmetry and three reflection planes which intersect at right angles at the point O. If this geometry had been adopted the possible applications of the work would have been greatly reduced. A much lower symmetry was thought to be useful in order to encompass as many molecular complexes as possible. For this reason the geometry shown below was chosen.

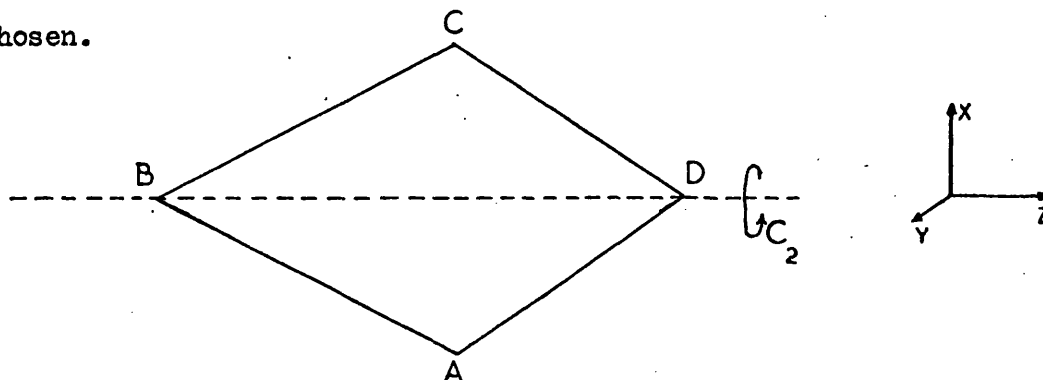


Figure 302. The Geometry of the 'General' System

Centres A and C are identical. The distances AB and BC are equal, so too are CD and AD. The plane of the molecule is a reflection plane and a  $C_2$  axis of symmetry passes through the centres B and D. A second reflection plane perpendicular to the plane of the molecule also passes through centres B and D. This molecular configuration belongs, therefore, to the point group  $C_{2v}$ . Since the symmetry operations which form the  $C_{2v}$  group are contained within the  $D_{2h}$  group, the former is a sub-group of the latter. Because the lower symmetry had been chosen the following systems were also within the scope of this work:-

1. The  $H_3^-$  ion.
2. The  $H_4$  complex.
3. The molecular ion complex  $LiH_2^+$ .
4. The beryllium hydride ion  $BeH^+$ .

Systems 1 and 2 were investigated for the purpose of checking the computer programmes used in this work. A detail account of these calculations can be found in Chapter 4. Unfortunately time did not allow systems 3 and 4 to be investigated. The way in which the symmetry properties were used in the construction of the wave function for the four-centre four-electron system of  $C_{2v}$  symmetry, Figure 302, is discussed in the next section.

### 3.4 Construction of the Wave Function

The most efficient way of constructing the total wave function was through the methods of group theory. The advantages of adopting this formalism can be seen in the following discussion. The Hamiltonian for the system shown in Figure 302 is invariant under four symmetry operation, E,  $C_2$ ,  $\sigma_{xy}$  and  $\sigma_{yz}$ . These operations form the group  $C_{2v}$ , the character table for this group is given in Table 301.

Table 301. The Character Table of the Group  $C_{2v}$ .

$C_{2v}$	E	$C_2$	$\sigma_v(xz)$	$\sigma_v(yz)$
$A_1$	1	1	1	1
$A_2$	1	1	-1	-1
$B_1$	1	-1	1	-1
$B_2$	1	-1	-1	1

An s-type Slater orbital was centred on each nucleus and the usual methods of group theory were used to construct the symmetry adapted molecular orbitals describing this system. Since four basis functions were being considered four symmetry adapted molecular orbitals  $\psi_i$  should result. These were

$$\begin{array}{lcl}
 \psi_1 = 1sb & & \\
 \psi_2 = 1sd & & \\
 \psi_3 = (1sa + 1sc) & & \\
 \psi_4 = (1sa - 1sc) & & 
 \end{array}
 \left. \vphantom{\begin{array}{l} \psi_1 \\ \psi_2 \\ \psi_3 \\ \psi_4 \end{array}} \right\}
 \begin{array}{l}
 A_1 \text{ symmetry} \\
 \\
 \\
 B_2 \text{ symmetry}
 \end{array}
 \quad (3.7)$$

for the case of 1s orbitals being centred on each nucleus. The symmetry adapted molecular orbital  $\psi_4$  is orthogonal to  $\psi_1, \psi_2$  and  $\psi_3$  because it belongs to a different irreducible representation.

The problem was now at the stage where the total wave function for the system,  $\Psi_k = \sum_i c_{ki} \phi_i$ , could be constructed. Since only one state was being investigated, only those  $\phi_i$  which transformed in the same manner as this state needed to be considered. The ground state was the state of interest and it was assumed to belong to the  $A_1$  irreducible representation. Thus, only the configurations which transformed under the various symmetry operations in the same manner as the  $A_1$  irreducible representation were constructed. Table 302 was employed in formulating these configurations. Each acceptable configuration was formed from a product of symmetry adapted molecular orbitals  $\psi_i$ , whose direct product of irreducible representations contained only an  $A_1$  component.

Table 302. Direct Product Table

$C_{2V}$	$A_1$	$A_2$	$B_1$	$B_2$
$A_1$	$A_1$	$A_2$	$B_1$	$B_2$
$A_2$	$A_2$	$A_1$	$B_2$	$B_1$
$B_1$	$B_1$	$B_2$	$A_1$	$A_2$
$B_2$	$B_2$	$B_1$	$A_2$	$A_1$

The Pauli principle<sup>(21)</sup> demands that the total wave function describing the motion of electrons must be antisymmetric with respect to interchange of any two electrons. It is a property of determinants that, if any two rows or columns are interchanged, the sign of the

determinant changes, but the numerical value is unaffected. Therefore, the configurations  $\phi_i$  were set up in the form of determinants in which the permutation of a pair of electrons was equivalent to the interchange of a pair of rows. The Pauli principle was thereby automatically satisfied.

Two restrictions have been placed on the total wave function, it must be antisymmetric with respect to interchange of electrons and it must belong to the  $A_1$  irreducible representation. The spacial part of the total wave function was constructed in such a way that these rules were obeyed. The term "spacial part" is used because an electron has four degrees of freedom, three associated with its position in space and the fourth arising from the possibility of different orientations of the spin axis<sup>(22)</sup>. The consequence of spin had to be investigated next<sup>(C)</sup>. Each of the orbital configurations was multiplied by a spin function. A singlet state was being considered, therefore, the spin functions were such that -

a) The total wave function was an eigenfunction of the  $S^2$  and  $S_z$  operators<sup>(23)</sup>.

b) The eigenvalue of the  $S^2$  and  $S_z$  operators was zero.

Lowdins' projection operator technique<sup>(24)</sup> was used to construct the spin functions which satisfied the above conditions. The total wave function, constructed from symmetry adapted spin orbitals was, therefore,

of the form  $\Psi_k = \sum_{i=1}^{12} C_{ki} \phi_i$ , where

Footnote C. Spin-orbit interaction causes a small term containing the spin operator<sup>(25)</sup> to appear in the Hamiltonian of atoms and molecules. However, for calculations such as ours, this term is normally neglected. To this approximation the Hamiltonian is independent of spin.

$$\begin{aligned}
 \phi_1 &= \begin{vmatrix} \psi_\alpha & \psi_\beta & \psi_\alpha & \psi_\beta \\ 1 & 1 & 2 & 2 \end{vmatrix} \\
 \phi_2 &= \begin{vmatrix} \psi_\alpha & \psi_\beta & \psi_\alpha & \psi_\beta \\ 1 & 1 & 3 & 3 \end{vmatrix} \\
 \phi_3 &= \begin{vmatrix} \psi_\alpha & \psi_\beta & \psi_\alpha & \psi_\beta \\ 2 & 2 & 3 & 3 \end{vmatrix} \\
 \phi_4 &= \begin{vmatrix} \psi_\alpha & \psi_\beta & \psi_\alpha & \psi_\beta \\ 1 & 1 & 2 & 3 \end{vmatrix} - \begin{vmatrix} \psi_\alpha & \psi_\beta & \psi_\beta & \psi_\alpha \\ 1 & 1 & 2 & 3 \end{vmatrix} \\
 \phi_5 &= \begin{vmatrix} \psi_\alpha & \psi_\beta & \psi_\alpha & \psi_\beta \\ 2 & 2 & 1 & 3 \end{vmatrix} - \begin{vmatrix} \psi_\alpha & \psi_\beta & \psi_\beta & \psi_\alpha \\ 2 & 2 & 1 & 3 \end{vmatrix} \\
 \phi_6 &= \begin{vmatrix} \psi_\alpha & \psi_\beta & \psi_\alpha & \psi_\beta \\ 3 & 3 & 1 & 2 \end{vmatrix} - \begin{vmatrix} \psi_\alpha & \psi_\beta & \psi_\beta & \psi_\alpha \\ 3 & 3 & 1 & 2 \end{vmatrix} \quad (3.8) \\
 \phi_7 &= \begin{vmatrix} \psi_\alpha & \psi_\beta & \psi_\alpha & \psi_\beta \\ 1 & 1 & 4 & 4 \end{vmatrix} \\
 \phi_8 &= \begin{vmatrix} \psi_\alpha & \psi_\beta & \psi_\alpha & \psi_\beta \\ 2 & 2 & 4 & 4 \end{vmatrix} \\
 \phi_9 &= \begin{vmatrix} \psi_\alpha & \psi_\beta & \psi_\alpha & \psi_\beta \\ 3 & 3 & 4 & 4 \end{vmatrix} \\
 \phi_{10} &= \begin{vmatrix} \psi_\alpha & \psi_\beta & \psi_\alpha & \psi_\beta \\ 4 & 4 & 1 & 2 \end{vmatrix} - \begin{vmatrix} \psi_\alpha & \psi_\beta & \psi_\beta & \psi_\alpha \\ 4 & 4 & 1 & 2 \end{vmatrix} \\
 \phi_{11} &= \begin{vmatrix} \psi_\alpha & \psi_\beta & \psi_\alpha & \psi_\beta \\ 4 & 4 & 1 & 3 \end{vmatrix} - \begin{vmatrix} \psi_\alpha & \psi_\beta & \psi_\beta & \psi_\alpha \\ 4 & 4 & 1 & 3 \end{vmatrix} \\
 \phi_{12} &= \begin{vmatrix} \psi_\alpha & \psi_\beta & \psi_\alpha & \psi_\beta \\ 4 & 4 & 2 & 3 \end{vmatrix} - \begin{vmatrix} \psi_\alpha & \psi_\beta & \psi_\beta & \psi_\alpha \\ 4 & 4 & 2 & 3 \end{vmatrix}
 \end{aligned}$$

The symbol  $\left| \begin{array}{cccc} \psi_l^\alpha & \psi_m^\beta & \psi_n^\alpha & \psi_p^\beta \end{array} \right|$  represents the determinantal

configuration  $\phi_i$ , where

$$\phi_i = \left| \begin{array}{cccc} \psi_l(1) \alpha(1) & \psi_m(1) \beta(1) & \psi_n(1) \alpha(1) & \psi_p(1) \beta(1) \\ \psi_l(2) \alpha(2) & \psi_m(2) \beta(2) & \psi_n(2) \alpha(2) & \psi_p(2) \beta(2) \\ \psi_l(3) \alpha(3) & \psi_m(3) \beta(3) & \psi_n(3) \alpha(3) & \psi_p(3) \beta(3) \\ \psi_l(4) \alpha(4) & \psi_m(4) \beta(4) & \psi_n(4) \alpha(4) & \psi_p(4) \beta(4) \end{array} \right|$$

and  $\psi_l$ , for example, is a symmetry adapted molecular orbital and  $\alpha$  and  $\beta$  are spin functions.

### 3.5 Construction of the Matrix Elements

The analytical form of the total wave function was known, therefore, the secular equations  $(\mathbb{H} - \lambda \mathbb{S})\mathbb{C} = 0$  could be constructed. Because spin-orbit interaction had been neglected the Hamiltonian was spin independent. In other words, the space and spin parts of the matrix elements were independent and therefore could be integrated separately.

Each matrix element was comprised of one or more functions of the form

$$\iint \left| \psi_l^* \psi_m^* \psi_n^* \psi_p^* \right| F_{OP} \left| \psi_l' \psi_m' \psi_n' \psi_p' \right| d\tau_{SPACE} d\tau_{SPIN}$$

which were re-written<sup>(26)</sup> as

$$k \iint \psi_l^* \alpha(1) \psi_m^* \beta(2) \psi_n^* \alpha(3) \psi_p^* \beta(4) F_{OP} \left| \psi_l' \psi_m' \psi_n' \psi_p' \right| \quad (3.9)$$

$$\times d\tau_{SPACE} d\tau_{SPIN}$$

The constant k was, at this stage, absorbed into the coefficients  $C_{ki}$ . Because of the orthogonality of the spin eigenfunctions  $\alpha$  and  $\beta$  all the terms in equation (3.9) vanish except those for which the spins match exactly. For example, integration over spin in  $H_{11}$  and  $S_{11}$  gave the results:

$$H_{11} = \int \psi_1^{(1)*} \psi_1^{(2)*} \psi_2^{(3)*} \psi_2^{(4)*} E_{OP} \left[ \begin{array}{cccc} \psi_1^{(1)} & \psi_1^{(2)} & \psi_2^{(3)} & \psi_2^{(4)} \\ \psi_2^{(1)} & \psi_2^{(2)} & \psi_1^{(3)} & \psi_1^{(4)} \end{array} - 2 \psi_1^{(1)} \psi_2^{(2)} \psi_2^{(3)} \psi_1^{(4)} \right] d\tau_{SPACE} \quad (3.10)$$

$$S_{11} = \int \psi_1^{(1)*} \psi_1^{(2)*} \psi_2^{(3)*} \psi_2^{(4)*} \left[ \begin{array}{cccc} \psi_1^{(1)} & \psi_1^{(2)} & \psi_2^{(3)} & \psi_2^{(4)} \\ \psi_2^{(1)} & \psi_2^{(2)} & \psi_1^{(3)} & \psi_1^{(4)} \end{array} - 2 \psi_1^{(1)} \psi_2^{(2)} \psi_2^{(3)} \psi_1^{(4)} \right] d\tau_{SPACE} \quad (3.11)$$

Each determinantal function, equation (3.9), was reduced to a linear combination of four terms. In some cases two of the terms were identical, this occurred in  $H_{11}$  and  $S_{11}$ .

Both the  $\underline{H}$  and  $\underline{S}$  matrices were symmetrical about the leading diagonal; therefore only terms in the upper triangle were evaluated. Symmetry adapted molecular orbitals belonging to different irreducible representations are orthogonal. Thus, for certain matrix elements, integration over space was greatly simplified since some of their constituent terms were zero. To describe the consequences of the orthogonality conditions Figure 303 is used. The matrices are split into four blocks and each one is considered separately.

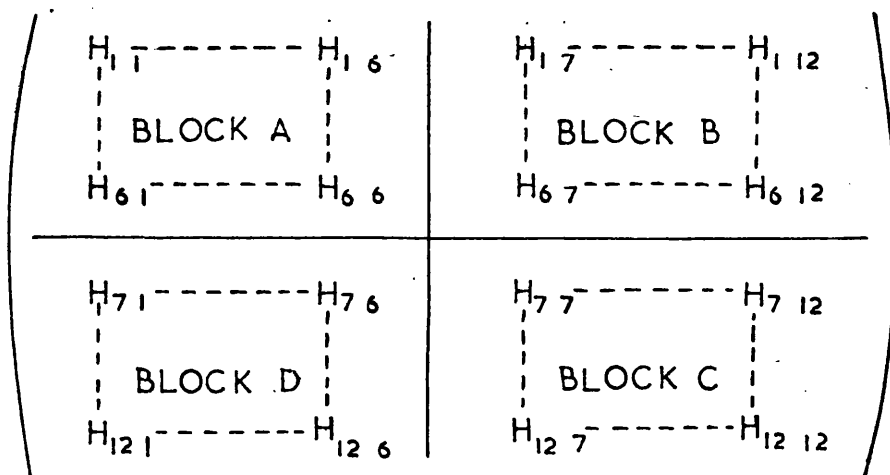


Figure 303. Sub-divisions of the Matrix Elements

The  $\mathbb{S}$  matrix is sub-divided and labelled in exactly the same manner as in Figure 303. All the symmetry adapted molecular orbitals contained in block A are of  $A_1$  symmetry; therefore, there was no reduction of terms due to orthogonality conditions. ( $\phi_1$  to  $\phi_6$  were constructed from  $\psi_1$ ,  $\psi_2$  and  $\psi_3$  only).

Configurations  $\phi_7$  to  $\phi_{12}$  were constructed from two molecular orbitals of  $A_1$  symmetry and two of  $B_2$  symmetry. Therefore all the one-electron terms in block B were zero. Only the two electron terms of the form

$$\iint \psi_{A_1}^*(1) \psi_{B_2}(1) \frac{1}{r_{12}} \psi_{A_1}^*(2) \psi_{B_2}(2) d\tau_1 d\tau_2 \int \psi_{A_1}^*(3) \psi_{A_1}(3) d\tau_3 \int \psi_{A_1}^*(4) \psi_{A_1}(4) d\tau_4 \quad (3.12)$$

remained, where  $d\tau_i$  denotes integration over the coordinates of electron  $i$ . All the configurations contained in block C were constructed from two orbitals of  $A_1$  symmetry and two of  $B_2$  symmetry. Only when the  $B_2$  orbitals matched exactly were the one electron terms not zero. The two electron terms of the type

$$\begin{aligned} & \iint \psi_{B_2}^*(1) \psi_{B_2}(1) \frac{1}{r_{12}} \psi_{B_2}^*(2) \psi_{B_2}(2) d\tau_1 d\tau_2 \int \psi_{A_1}^*(3) \psi_{A_1}(3) d\tau_3 \int \psi_{A_1}^*(4) \psi_{A_1}(4) d\tau_4 \\ & \iint \psi_{B_2}^*(1) \psi_{B_2}(1) \frac{1}{r_{12}} \psi_{A_1}^*(2) \psi_{A_1}(2) d\tau_1 d\tau_2 \int \psi_{B_2}^*(3) \psi_{B_2}(3) d\tau_3 \int \psi_{A_1}^*(4) \psi_{A_1}(4) d\tau_4 \\ & \iint \psi_{A_1}^*(1) \psi_{B_2}(1) \frac{1}{r_{12}} \psi_{B_2}^*(2) \psi_{A_1}(2) d\tau_1 d\tau_2 \int \psi_{B_2}^*(3) \psi_{B_2}(3) d\tau_3 \int \psi_{A_1}^*(4) \psi_{A_1}(4) d\tau_4 \end{aligned} \quad (3.13)$$

were also non-zero.

The consequences of the orthogonality conditions are summarized below.

For the  $\underline{S}$  matrix - block A was unaffected, blocks B and D were everywhere zero and the terms in block C were reduced in number.

For the  $\underline{H}$  matrix - block A was unaffected, blocks B and D contained only two electron terms and block C was again reduced.

The next stage in the work was the integration of the remaining terms. To perform this operation, computer programmes obtained from the "Quantum Chemistry Programme Exchange" were adapted for use on the S.R.C.Chilton "Atlas",<sup>(27)</sup>. Several sections of the programmes had to be re-written; these details and a description of each routine appear in Appendix I.

### 3.6 Evaluation of the Secular Equation

To determine the energy eigenvalues of the matrix equation  $(\underline{H} - \lambda \underline{S})\underline{C} = 0$ , a two part computer programme was written. The function of the first part was to calculate the numerical values of the individual matrix elements. This was accomplished by giving a code name to each integral, specifying the matrix elements in terms of the code, then reading into the programme the values of the integrals. The second section of the programme transformed the equation

$$(\underline{H} - \lambda \underline{S})\underline{C} = 0$$

into the form

$$(\underline{H}^1 - \lambda \underline{I})\underline{C}^1 = 0 \tag{3.14}$$

where  $\underline{I}$  represents a unit matrix,  $\underline{H}^1$  represents the  $\underline{H}$  matrix when transformed in the same manner as the  $\underline{S}$  matrix and  $\underline{C}^1$  denotes the column eigenvector corresponding to the transformed matrices. The Jacobi method was used to diagonalize the  $\underline{S}$  matrix and also to solve equation (3.14). The details of the programme are described in Appendix II.

The results were printed out so that underneath each energy eigenvalue were the corresponding twelve eigenvectors. Of the twelve sets of results, the lowest eigenvalue represented the ground state energy and the elements of the appropriate column vector gave the detailed form of the ground state wave function.

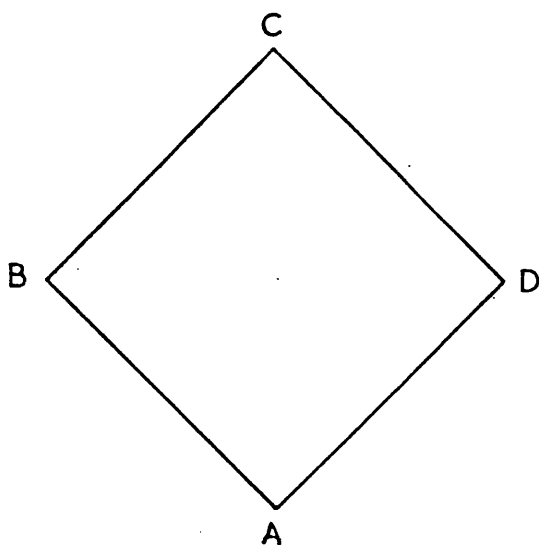
CHAPTER 4

TESTING THE PROGRAMME

The programme can be divided into two main sections (I) the evaluation of integrals and (II) the setting up and solution of the secular equations.

Section(I) was reasonably easy to check: each integral routine was used to compute known results<sup>(28)</sup>. The routines were considered correct when there was correspondence to six places of decimals. Testing Section (II) of the programme proved to be much more difficult since there was no "absolute" against which to check our work. Consequently several tests were employed.

The initial check was designed to give a guide to the accuracy and correctness of the methods used in Section (II) of the programme. For this purpose the energy of four hydrogen atoms at relatively large separations was calculated.



Distances  $AB = BC = CD = AD$   
Nuclear Charges  $Z_A = Z_B = Z_C = Z_D$   
Angle  $ABC = 90^\circ$

Figure 401. Geometrical Arrangement of Four Hydrogen Atoms

The bond length AB was set, in turn, at 5,7 and 9 au. In the limit of infinite separation the energy of the system should be - 2 au. The results were just slightly more positive than the limiting value and progressed towards it in the order expected.

The nearness of these results to - 2 au was very encouraging since, at the separations considered, the overlaps were very small and thus very little interaction was expected. Furthermore, the increase in energy with increased bond length indicated that the routine was at least predicting physically reasonable results. To complete this check, energies for bond lengths at which relatively large interaction took place were calculated. For this purpose, it was convenient to choose separations of 1.4 au and 1.66 au. The results of all five calculations are shown in Table 401.

Table 401. Energy of Four Hydrogen Atoms

Bond Length AB	Energy
1.4 au	- 1.55110 au
1.66 au	- 1.74591 au
5 au	- 1.99708 au
7 au	- 1.99987 au
9 au	- 1.99999 au

Each energy result recorded in Table 401 was optimised with respect to all orbital exponents. This simplicity of the calculations was the virtue of the above test. The results being as expected, moving on to more detailed and time consuming tests was therefore justifiable.



those of Maccias and are shown in Table 402.

It must be mentioned that some of the matrix elements in our four-centre programme were identically zero in both calculations for the  $H_3^-$  system. This was an unfortunate consequence of suppressing a centre. Obviously the matrix elements not mentioned in Table 402 had to be checked by an alternative method. Nevertheless, the test did prove that the method of solving the matrix equation  $(\underline{H} - \lambda \underline{S}) \underline{\zeta} = 0^*$  was correct. In addition many of the matrix elements were proved to be properly constructed, which in turn proved that the configurations  $\phi_2, \phi_3, \phi_7, \phi_8, \phi_9, \phi_{11}$  and  $\phi_{12}$  were correctly formulated. Therefore, in principle, sections (I) and (II) of the programme were checked out successfully.

\* See Appendix II.

Table 402. Comparison of Results for the  $H_3^-$  Ion

	Centre D Suppressed	Centre B Suppressed	Maccias
<b>Matrix Elements</b>			
H(2,2)	-2.482868	0	-2.482868
H(2,7)=H(7,2)	0.668613	0	0.668613
H(2,9)=H(9,2)	1.679077	0	1.679078
H(2,11)=H(11,2)	1.640730	0	1.640730
H(7,7)	-0.964537	0	-0.964537
H(7,9)=H(9,7)	-1.732925	0	-1.732923
H(7,11)=H(11,7)	-2.653028	0	-2.653028
H(9,9)	-19.766161	-19.766161	-19.766159
H(9,11)=H(11,9)	-10.737523	0	-10.737521
H(11,11)	-11.915733	0	-11.915732
H(3,3)	0	-2.482868	-2.482868
H(3,8)=H(8,3)	0	0.668613	0.668613
H(3,9)=H(9,3)	0	1.679077	1.679078
H(3,12)=H(12,3)	0	1.640730	1.640730
H(8,8)	0	-0.964537	-0.964537
H(8,9)=H(9,8)	0	-1.732925	-1.732923
H(8,12)=H(12,8)	0	-2.653028	-2.653028
H(9,9)	-19.766161	-19.766161	-19.766159
H(9,12)=H(12,9)	0	-10.737523	-10.737521
H(12,12)	0	-11.915733	-11.915732
<b>Ground State Energy (au)</b>	-1.581077	-1.581077	-1.581076
<b>Eigenvectors</b>			
$c_2$	0.111006	0	0.111006
$c_7$	-0.041780	0	-0.041781
$c_9$	-0.307091	-0.307091	-0.307091
$c_{11}$	-0.598073	0	-0.598073
$c_3$	0	0.111006	0.111006
$c_8$	0	-0.041780	-0.041781
$c_9$	-0.307091	-0.307091	-0.307091
$c_{12}$	0	-0.598073	-0.598073

The third major test of the programme was aimed at checking the matrix elements not covered by the previous work. The symmetry of the following type of system provided some useful information.

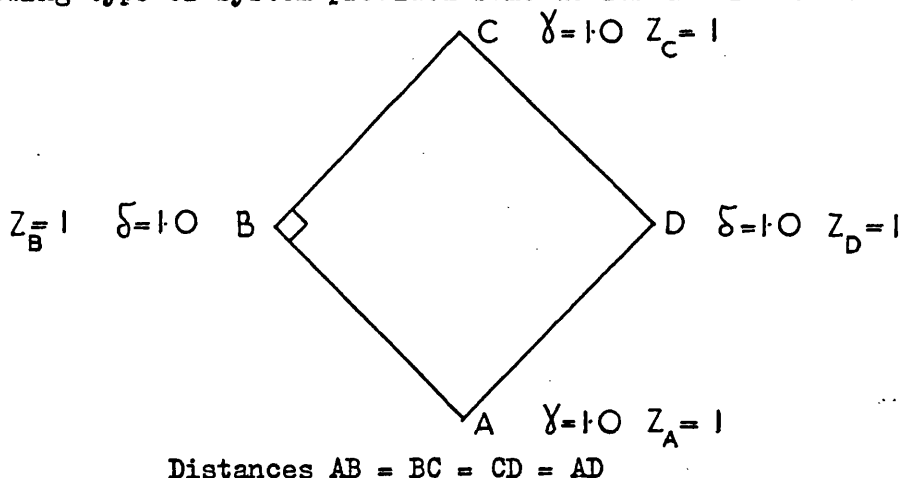


Figure 403. Geometry Used in the Symmetry Test

Both the nuclear charges and orbital exponents ( $\gamma$  and  $\delta$ ) were set equal to unity. The symmetry of this system in  $D_{4h}$  which is much higher than the minimum required by the programme. This implies that many of the matrix elements should have identical values. For example, the values of the matrix elements  $H(1,2)$  and  $H(1,3)$  should be equal. The reason for this equality can be best understood when the analytical forms are examined.<sup>(D)</sup>

$$H(1,2) = \int \phi_1^* H \phi_2 d\tau = \int \left| \begin{matrix} b & b & d & d \\ \alpha & \beta & \alpha & \beta \end{matrix} \right|^* H \left| \begin{matrix} b & b & (a+c) & (a+c) \\ \alpha & \beta & \alpha & \beta \end{matrix} \right| d\tau \quad (4.1)$$

$$H(1,3) = \int \phi_1^* H \phi_3 d\tau = \int \left| \begin{matrix} b & b & d & d \\ \alpha & \beta & \alpha & \beta \end{matrix} \right|^* H \left| \begin{matrix} d & d & (a+c) & (a+c) \\ \alpha & \beta & \alpha & \beta \end{matrix} \right| d\tau$$

Alternatively  $H(1,3)$  can be written as -

$$H(1,3) = \int \phi_1^* H \phi_3 d\tau = \int \left| \begin{matrix} d & d & b & b \\ \alpha & \beta & \alpha & \beta \end{matrix} \right|^* H \left| \begin{matrix} d & d & (a+c) & (a+c) \\ \alpha & \beta & \alpha & \beta \end{matrix} \right| d\tau \quad (4.2)$$

The  $C_2$  axis of symmetry through the centres A and C means that the atomic orbitals  $1sb$  and  $1sd$  will have identical roles in the wave

Footnote D. The symbol  $b_\alpha$ , for example, in equations (4.1), (4.2) and (4.3) denotes the spin-orbital  $1sb_\alpha$ .

function. The matrix element  $H(1,3)$  can be generated from  $H(1,2)$  by interchanging 1sb for 1sd and vice-versa; consequently  $H(1,2)$  and  $H(1,3)$  must have equal values. Many of the matrix elements were checked in this way since a large number of corresponding pairs existed. A complete list is shown below:

For all combinations of  $i$  and  $k$ :-

$H(i,k) = H(i,k+1)$

for  $i = 1,6,9,10$  and  $k = 2,4,7,11$ ;  
and  $H(i,k) = H(i+1, k-1)$   
for  $i = 2,4,7,11$  and  $k = 3,5,8,12$ ;  
and  $H(i,k) = H(i+1, k)$   
for  $i = 2,4,7,11$  and  $k = 6,9,10$ ;  
and  $H(i,k) = H(i+1, k+1)$   
for  $i = 2,4,7,11$  and  $k = 2,4,7,11$

The programme output contained a list of evaluated matrix elements. Thus, fulfillment of the conditions listed above was checked. For each pair of matrix elements the required equality existed.

A further consequence of the preceding discussion is that the configurations within each of the following pairs

$\phi_2$  and  $\phi_3$ ,  $\phi_4$  and  $\phi_5$ ,  $\phi_7$  and  $\phi_8$ ,  $\phi_{11}$  and  $\phi_{12}$

should carry equal weight in the total wave function  $\Psi$ . This consequence was apparent in the eigenvectors: for each eigenvalue the associated eigenvectors were such that  $C_2 = C_3$ ,  $C_4 = C_5$ ,  $C_7 = C_8$  and  $C_{11} = C_{12}$ .

A fourth test of the programme was again based on symmetry properties. The following systems, which had the same geometry as that shown in Figure 403 were examined.

- 1)  $Z_A = Z_B = Z_C = Z_D = 1$        $\gamma = 1.65$        $\delta = 1.7$
- 2)  $Z_A = Z_B = Z_C = Z_D = 1$        $\gamma = 1.7$        $\delta = 1.65$
- 3)  $Z_A = Z_C = 1, Z_B = Z_D = 1.4$        $\gamma = 1.65$        $\delta = 1.7$
- 4)  $Z_A = Z_C = 1.4, Z_B = Z_D = 1$        $\gamma = 1.7$        $\delta = 1.65$

Again the symmetry of the systems,  $D_{2h}$ , was much higher than the minimum required by the programme. For each individual system the inherent equalities of certain pairs of matrix elements and eigenvectors were again observed. However, the main reason for these calculations was to obtain comparisons for pairs of "identical systems" specified in different ways. The second system of each pair can be obtained by rotating the first through  $90^\circ$ . The ground state energies of systems 1 and 2 were equal; this was also true for the other pair. Further, after allowing for normalization constants,  $H(1,1)$  in system 1 was equal to  $H(9,9)$  in system 2. This calculation was performed to show that the roles of configurations  $\phi_1$  and  $\phi_9$  were interchanged in the two systems, thereby indicating a compatible and consistent formulation. Hence, only configurations  $\phi_6$  and  $\phi_{10}$  still needed to be investigated. To check these two remaining configurations the matrix elements  $H(6,6)$  and  $H(10,10)$  were considered in detail. The analytical expression for  $H(6,6)$  was expanded and then evaluated. Since

$$\phi_6 = \begin{vmatrix} (a+c) & (a+c) & bd \\ \alpha & \beta & \alpha\beta \end{vmatrix} - \begin{vmatrix} (a+c) & (a+c) & bd \\ \alpha & \beta & \beta\alpha \end{vmatrix} \quad (4.3)$$

and

$$\phi_{10} = \begin{vmatrix} (a-c) & (a-c) & bd \\ \alpha & \beta & \alpha\beta \end{vmatrix} - \begin{vmatrix} (a-c) & (a-c) & bd \\ \alpha & \beta & \beta\alpha \end{vmatrix}$$

a change of the sign of 1sc in the input data for H(6,6) should, and in fact did, generate the value obtained for H(10,10).

Summarizing, we can say of the tests described above:-

- (A) The reproduction of Maccias' results proved that the general formulation of the wave function and programme was correct.
- (B) A large number of the matrix elements were proved to be correctly constructed by the symmetry tests and also by Maccias' results.
- (C) The eigenvectors  $C_2, C_3, C_7, C_9, C_{11}$  and  $C_{12}$ , and the corresponding configurations  $\phi_2, \phi_3, \phi_7, \phi_8, \phi_9, \phi_{11}$  and  $\phi_{12}$  were shown to be correct by comparison with Maccias' results. The symmetry tests supported this evidence and also showed that  $C_4$  and  $C_5$ , and  $\phi_4$  and  $\phi_5$  were correct.
- (D) Configurations  $\phi_1, \phi_6, \phi_9$  and  $\phi_{10}$  were shown to be correctly constructed by comparing, under certain conditions, the matrix element H(1,1) with H(9,9) and H(6,6) with H(10,10).
- (E) The ground state energy was proved to be invariant with respect to rotation of the labelling.

In the light of the above evidence, it was considered that the programme was ready to be used in the calculations of interest.

CHAPTER 5

Results and Discussion

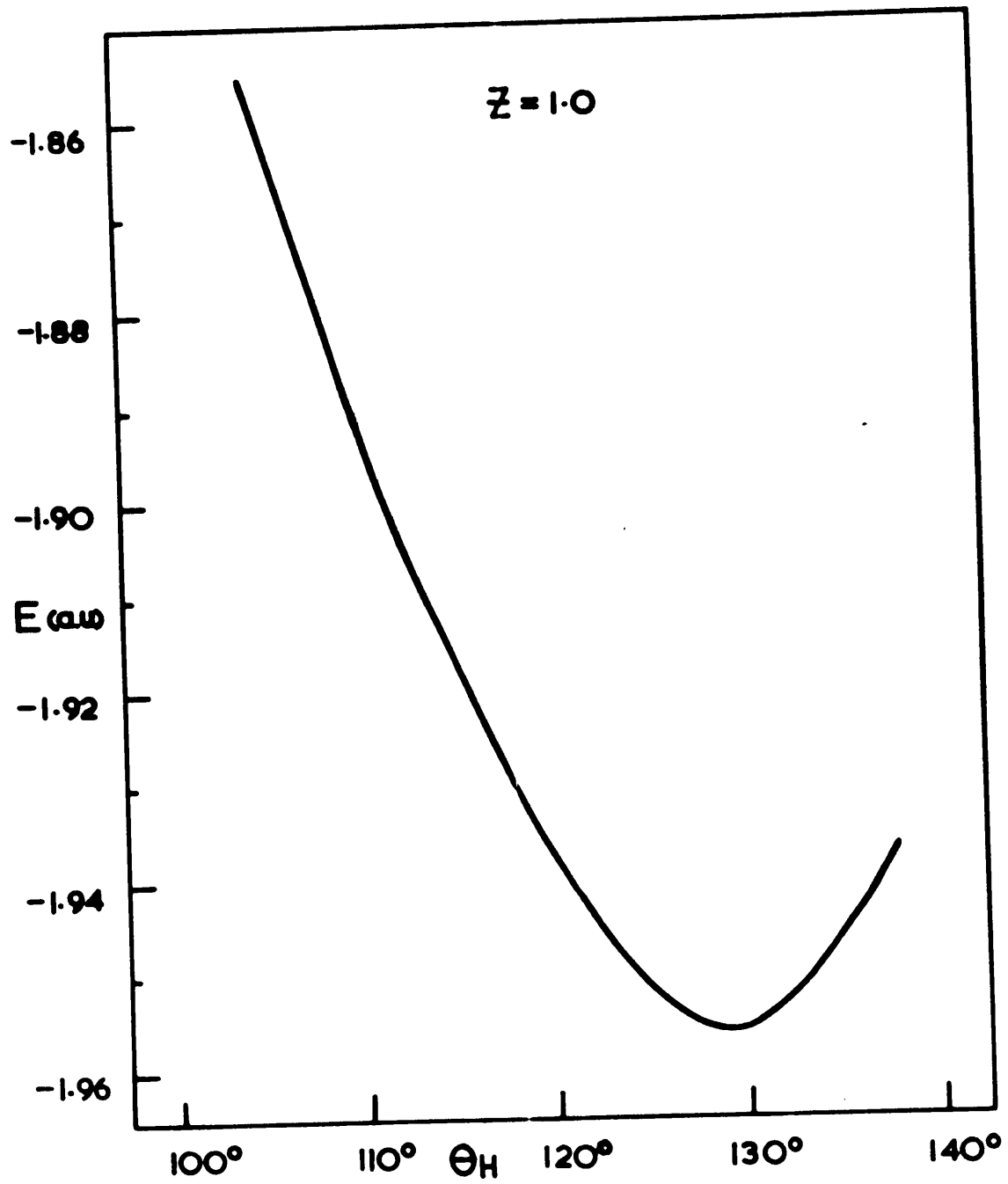
For ease of presentation and discussion the results have been split into two parts. In Part I the results for the double arbitrary Z ions,  $ZHZH^{+2Z-2}$ , are presented and Part II covers the Hamilton-like systems.

Part I - The double arbitrary Z ions,  $ZHZH^{+2Z-2}$ .

The geometry of the  $ZHZH^{+2Z-2}$  ions is shown in Figure 302. As previously mentioned the bond angle BCD was labelled  $\Theta_H$  and the 1s Slater-type orbitals centred on A and C had an exponent  $\gamma$ , and on B and D an exponent  $\delta$ . The nuclear charges at B and D were Z and at A and C unity. For preselected values of Z and  $\Theta_H$  the total molecular energy of the  $ZHZH^{+2Z-2}$  complexes was minimized with respect to  $\gamma$  and  $\delta$ . The values of the variational parameters ( $\gamma$  and  $\delta$ ) for minimum energy were obtained by an iterative trial and error technique. A range of  $\Theta_H$  values for Z = 1.0, 1.2, 1.4, 1.8 and 2.2 allowed the minimum molecular energy,  $E_M$ , for each system to be determined as a function of  $\gamma$ ,  $\delta$  and  $\Theta_H$ . The results for the whole range of these calculations are shown in Figures 501, 502 and 503, and Table 501. For the fully optimized systems the energy,  $E_M$ , orbital exponents  $\gamma$  and  $\delta$ , and optimum bond angle  $\Theta_H(\text{opt})$  are shown as a function of Z in Figure 504. These results are also presented in tabular form, Table 502. The total wave function,  $\Psi_k = \sum_i C_{ki} \phi_i$  describing these systems was normalized to unity, the eigenvectors  $C_{ki}$  of the wave functions corresponding to the energies  $E_M$  are given in Table 503.

Figure 501

The angular dependence of the molecular energy  $E$ ,  
after minimization with respect to the orbital exponents  
 $\gamma$  and  $\delta$ , for the systems  $ZH_2H^{+2Z-2}$  when  $Z = 1.0$ .



Figures 502

The angular dependence of the molecular energy  $E$ ,  
after minimization with respect to the orbital exponents  
 $\gamma$  and  $\delta$  for the systems  $ZHZH^{+2Z-2}$  when  $Z = 1.2, 1.4, 1.8$   
and  $2.2$ .

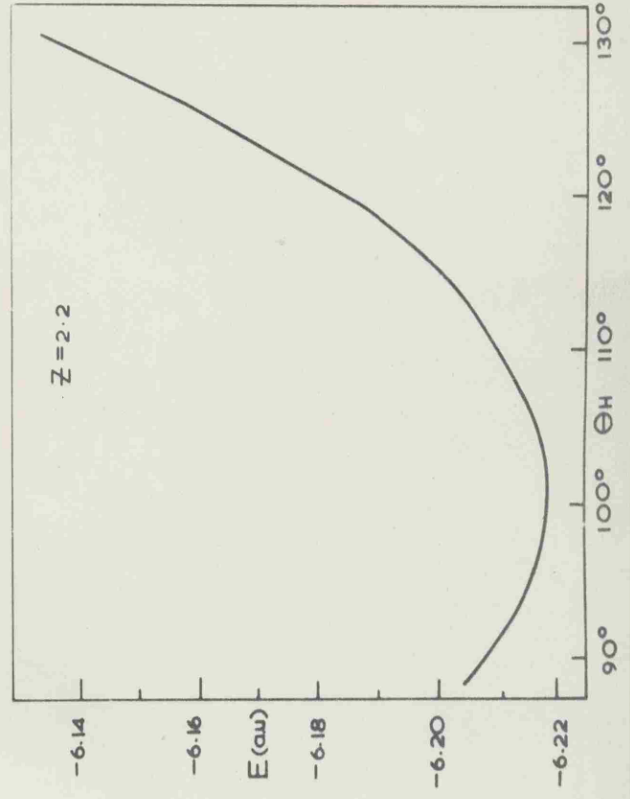
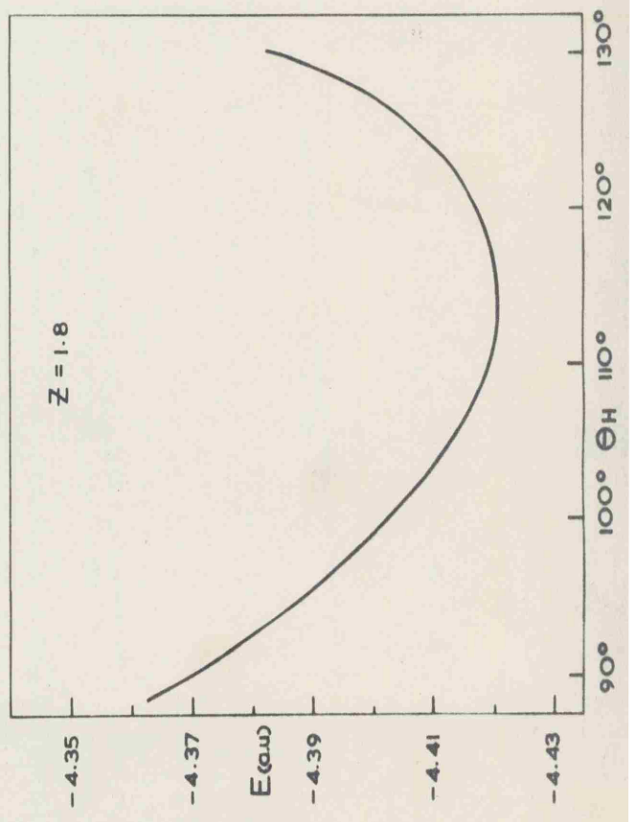
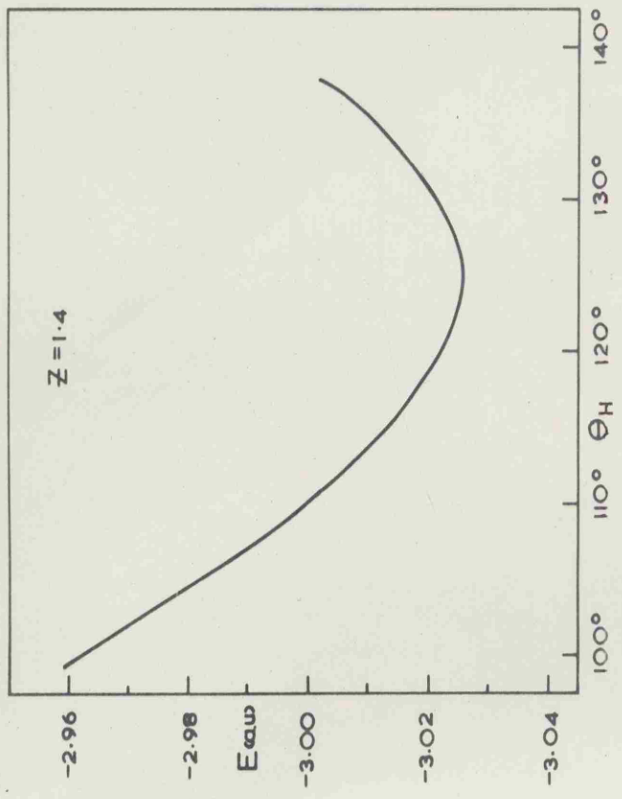
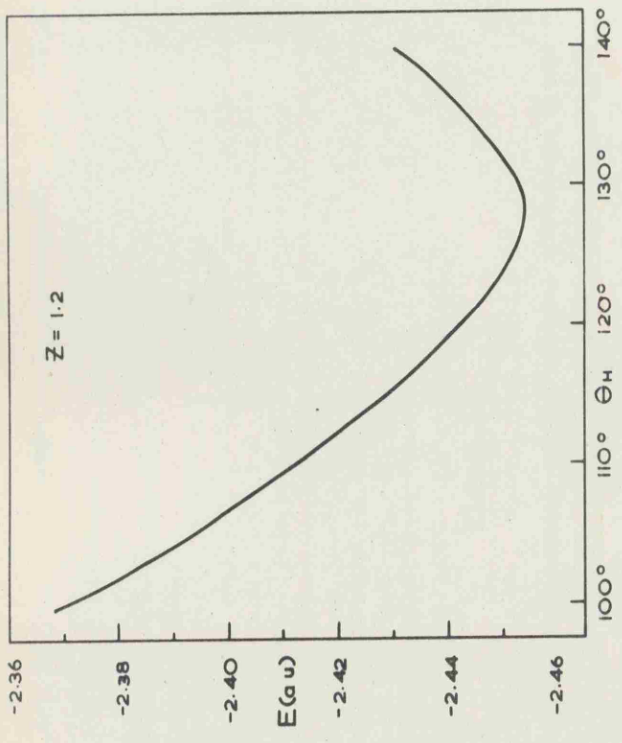


Figure 503

The optimum values of the orbital exponents  $\gamma$  and  $\delta$   
plotted as a function of  $\theta_H$  for fixed values of Z.

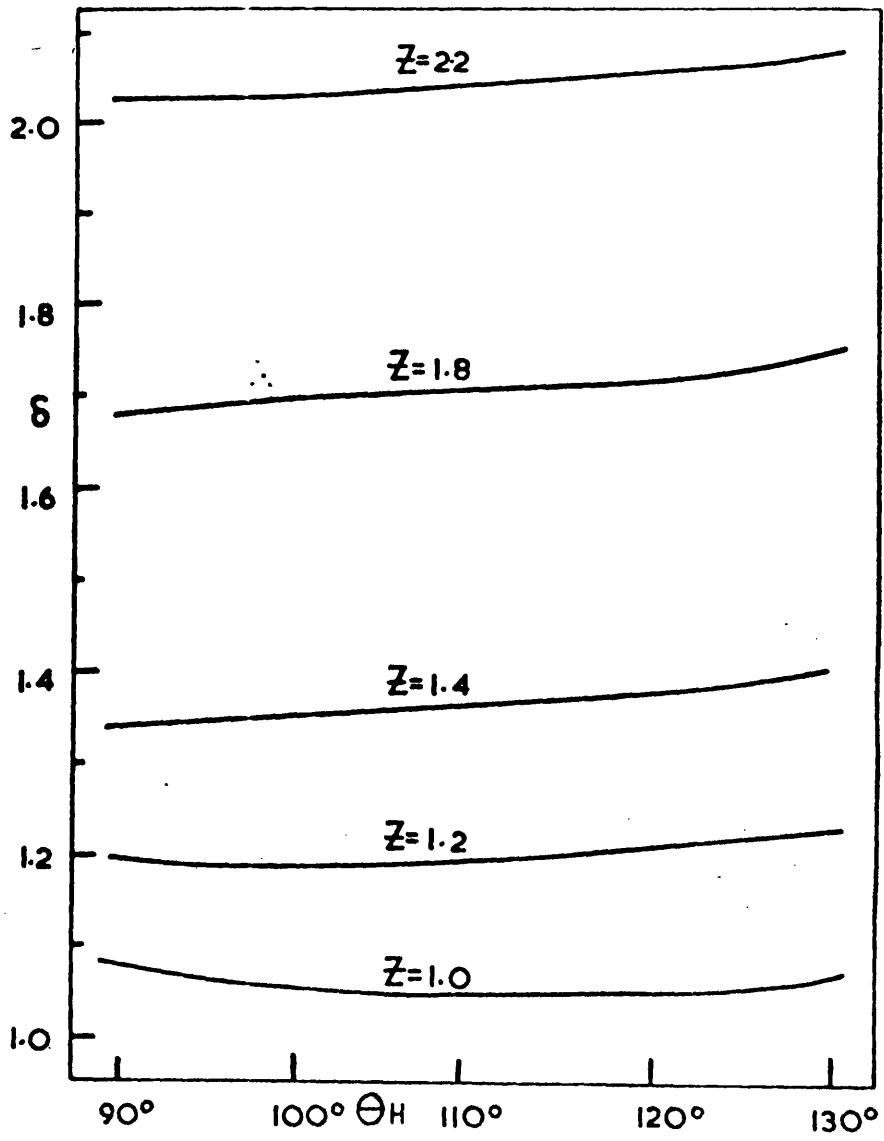
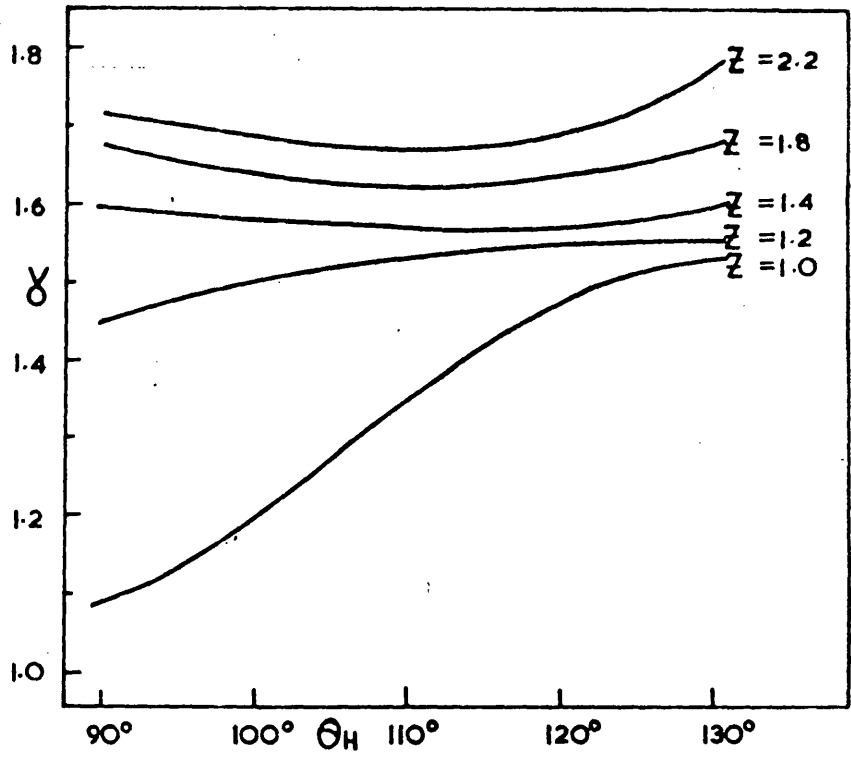


Figure 504

The optimum bond angle  $\theta_H(\text{opt})$ , molecular energy  $E_M$   
and the corresponding orbital exponents expressed as  
a function of  $Z$ .

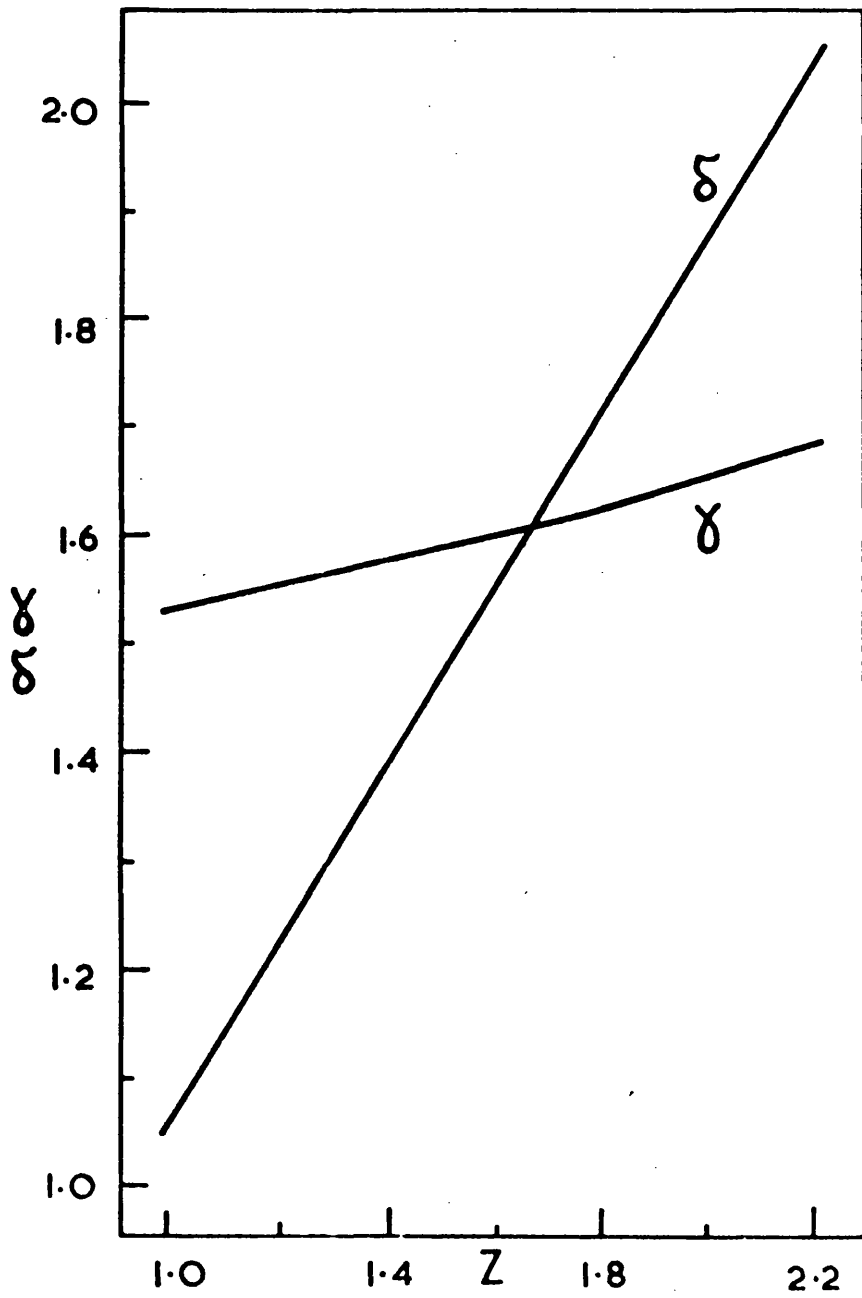
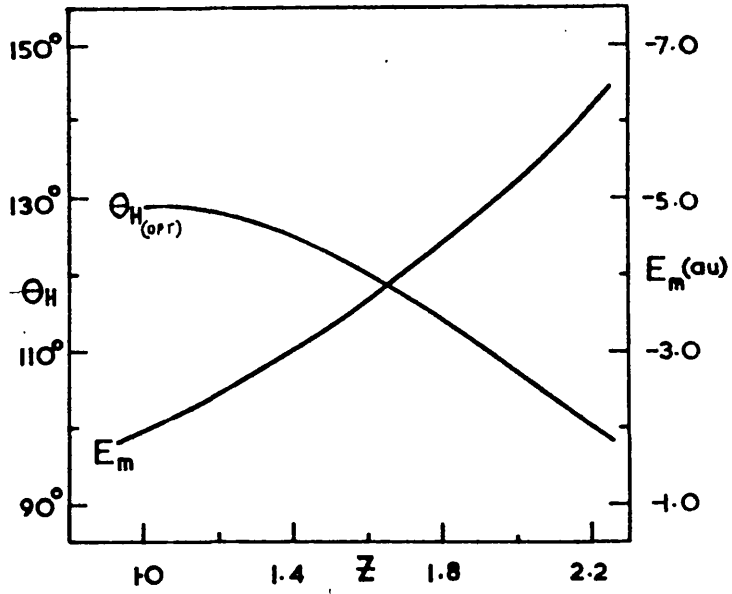


Table 501. Results for the optimized  $ZHZH^{+2Z-2}$  systems.

Z	$e_H^\circ$	E (au)	$\gamma$	$\delta$
1.0	90	- 1.74591	1.088	1.088
	100	- 1.80310	1.195	1.055
	110	- 1.89246	1.344	1.045
	120	- 1.93731	1.475	1.053
	130	- 1.95613	1.530	1.070
	135	- 1.94593	1.536	1.081
1.2	90	- 2.31989	1.446	1.196
	100	- 2.37018	1.497	1.190
	110	- 2.41212	1.533	1.195
	120	- 2.44220	1.548	1.210
	130	- 2.45353	1.559	1.231
	135	- 2.44396	1.561	1.240
1.4	90	- 2.90849	1.594	1.340
	100	- 2.96186	1.580	1.351
	110	- 2.99900	1.571	1.365
	120	- 3.02152	1.570	1.380
	130	- 3.02113	1.589	1.402
1.8	90	- 4.36901	1.675	1.680
	100	- 4.40250	1.638	1.698
	110	- 4.41870	1.621	1.710
	120	- 4.41732	1.637	1.720
	130	- 4.38397	1.675	1.742
2.2	90	- 6.20818	1.715	2.025
	100	- 6.21870	1.684	2.031
	110	- 6.21086	1.670	2.040
	120	- 6.18431	1.689	2.054
	130	- 6.13750	1.774	2.074

Table 502. Results for the  $ZHZH^{+2Z-2}$  systems optimized with respect to  $\gamma$ ,  $\delta$  and  $\theta_H$

Z	$\theta_H^*$ (opt)	$E_M$ (au)	$\gamma$	$\delta$
1.0	129	- 1.95651	1.527	1.069
1.2	128	- 2.45418	1.555	1.226
1.4	125	- 3.02555	1.576	1.390
1.8	114	- 4.42020	1.623	1.712
2.2	101	- 6.21871	1.684	2.031

Table 503. The eigenvectors  $C_{ki}$ , of the wave functions corresponding to the energies  $E_M$ , for the  $ZHZH^{+2Z-2}$  systems

	Z = 1.0	Z = 1.2	Z = 1.4	Z = 1.8	Z = 2.2
$C_{k1}$	0.0567112	0.0770042	0.1227676	0.2223854	0.3413128
$C_{k2}$	0.0768374	0.0503600	0.0267652	0.0023283	-0.0070364
$C_{k3}$	0.0768374	0.0503600	0.0267652	0.0023283	-0.0070364
$C_{k4}$	0.1545528	0.1445333	0.1392078	0.1215760	0.0871157
$C_{k5}$	0.1545528	0.1445333	0.1392078	0.1215760	0.0871157
$C_{k6}$	-0.1640399	-0.1424194	-0.1092606	-0.0594450	-0.0216080
$C_{k7}$	-0.0199632	-0.0151766	-0.0127637	-0.0083194	-0.0047103
$C_{k8}$	-0.0199632	-0.0151766	-0.0127637	-0.0083194	-0.0047103
$C_{k9}$	0.0011360	0.0010520	0.0008732	0.0004823	0.0002098
$C_{k10}$	0.0303583	0.0259311	0.0232537	0.0163160	0.0083477
$C_{k11}$	-0.0031687	-0.0030692	-0.0026889	-0.0017167	-0.0007866
$C_{k12}$	-0.0031687	-0.0030692	-0.0026889	-0.0017167	-0.0007866
$E_M$	-1.95651	-2.45418	-3.02555	-4.42020	-6.21871

These energy calculations exhibit several interesting features especially when compared with the  $ZHZ^{+2Z-1}$  study. At  $\theta_H(\text{opt})$  the Z-dependence of the orbital exponents  $\gamma$  and  $\delta$  is almost linear and, as with the  $ZHZ^{+2Z-1}$  system,  $\delta$  increases more rapidly than  $\gamma$ . For very large Z we anticipate that the exponent  $\delta$  will have a value similar to that of a helium-like atom, that is  $\delta \rightarrow (Z - 5/16)$ . The electron density distribution along the inter-nuclear axes (which is reported later in this chapter) substantiates this

prediction since, as  $Z$  increases, the electron density in the vicinity of the  $Z$  nuclei increases and therefore the system is tending to behave as two helium atoms and two protons. Under the same conditions the value of  $\delta$  for the  $ZHZ^{+2Z-1}$  systems approached  $Z$ . However, as  $Z \rightarrow 0$  the  $\delta$ -curve extrapolates to give  $0.3 \rightarrow 0.4$ , a result similar in magnitude to that obtained when the  $ZHZ^{+2Z-1}$  system was reduced to  $H^-$ . When  $Z < 1.7$ , Figure 504 shows that  $\gamma > \delta$ , this is not unreasonable since the corresponding value for  $\theta_H(\text{opt})$  indicates that the H-H distance is considerably smaller than the  $Z - Z$  distance.

The  $Z$ -variation of  $\theta_H(\text{opt})$  is of particular interest. At  $Z = 1.0$  the value of  $\theta_H(\text{opt})$  is  $129^\circ$ , consequently the rhombic diagonals BD and AC are about 3.0 and 1.4 au in length - the smaller H-H distance being almost identical with the bond length in the hydrogen molecule  $H_2$ . Such a value for  $\theta_H(\text{opt})$  implies that the energy for  $H_4$  will increase when the bond angle is fixed at  $90^\circ$ : the results for this calculation gave an energy of  $-1.74591$  au and orbital exponents of  $\gamma = \delta = 1.088$ . When  $Z = 1.0$  the systems with  $\theta_H = X^\circ$  or  $(180 - X)^\circ$  are identical. Therefore, the  $E$  against  $\theta_H$  curve is symmetric about a potential barrier situated at  $\theta_H = 90^\circ$ . This curve has minima at  $51^\circ$  and  $129^\circ$  and, as  $\theta_H \rightarrow 0^\circ$  or  $180^\circ$ , the magnitude of  $E(\theta_H)$  increases sharply. Also, symmetry about  $\theta_H = 90^\circ$  is apparent in the orbital exponents. For example, at  $\theta_H = 90^\circ$  the exponents are identical, at  $\theta_H = 100^\circ$  we have  $\gamma = 1.195$  and  $\delta = 1.055$  and at  $\theta_H = 80^\circ$  the parameters were found to be interchanged, i.e.  $\gamma = 1.055$  and  $\delta = 1.195$ . The energetically unfavourable nature of the square nuclear framework for  $H_4$  is somewhat surprising - but already known (30, 31).

For values of  $Z$  greater than unity the symmetry of the  $E(\theta_H)$  curve is destroyed such that an absolute minimum will occur at  $90^\circ < \theta_H(\text{opt}) < 180^\circ$ .

The  $E(\theta_H)$  curves for  $Z = 1.2, 1.4, 1.8$  and  $2.2$ , and  $\theta_H$  ranging from  $90^\circ$  to  $130^\circ$  are given in Figures 502. These curves show that  $\theta_H(\text{opt})$  decreases when  $Z > 1.0$ ; consequently, the Z-Z distance decreases from its value of 3.0 au (at  $Z = 1.0$ ). Therefore the nuclear repulsion of the Z nuclei increases due to increasing Z and also due to  $\theta_H$  decreasing. As with the  $ZHZ^{+2Z-1}$  ions the increased charge cloud in the Z-Z region more than compensates for this effect. Evidence for this argument is provided by the distribution of electron density along the OZ axis - an increase in Z is accompanied by an even larger increase in the charge cloud in the vicinity of Z. As a result of keeping the Z-H distances fixed  $\theta_H(\text{opt})$  will ultimately pass through a minimum since, as Z increases the nuclear repulsion terms will cause  $\theta_H(\text{opt})$  to approach  $180^\circ$  asymptotically. A test calculation at  $Z = 10$  gave a value of  $\theta_H(\text{opt})$  of  $156^\circ$ . The orbital exponent  $\delta$  of this calculation had a value of 8.8 which is in keeping with  $Z \rightarrow Z-5/16$  when Z is large. At  $Z = 0$  the  $ZHZH^{+2Z-2}$  system becomes  $H_2^{--}$  with the molecular orbitals 1sb and 1sd now acting as 'floating orbitals',<sup>(32)</sup> located at specific points in space. Hence  $\theta_H(\text{opt})$  will approach zero in order to maximize the bond length within the constrained  $H_2^{--}$  system.

The  $E_M$  against Z curve in Figure 504, which is for a Z-H distance fixed at 1.66 au, shows that the  $ZHZH^{+2Z-2}$  is energetically stable with respect to a theoretical dissociation of the type  $2Z^{+(Z-1)} + 2H$ . for  $Z \geq 1.2$ . The dissociation to give 4H at  $Z = 1.0$  contrasts with the marginal stability of square  $H_4$  at  $R \sim 1.66$  au predicted by the considerably more elaborate - and presumably more accurate - calculation of Conroy and Malli. For both calculations,  $H_4$  is energetically unstable with respect to  $2H_2$ .

The electron density distribution along the three internuclear axes was examined for each system reported in Table 501. The results of

these calculations have already been used in the earlier discussion. Also, the electron density distribution allows us to examine the movement of charge as a function of  $Z$  and  $\theta_H$ . Reformulating the wave function for each system in terms of natural spin orbitals (NSO's) provided the most efficient method of calculating the electron density at various points in the system. A brief description of NSO's and a listing of the computer programmes used to evaluate the electron densities are presented in Appendix III. For completeness, the coefficients and occupation numbers of the NSO's for the systems optimized with respect to  $\gamma$ ,  $\delta$  and  $\theta_H$  are also given in Appendix III. The distribution of electron density along the internuclear axes of the  $ZHZH^{+2Z-2}$  systems is shown in Figures 505-530. The densities along axes OC and OD are symmetrical about  $X' = 0$  and  $Y = 0$  respectively, and the cusps in the densities coincide exactly with the nuclear sites. The electron density distribution of the fully optimized systems are shown in Figures 528, 529 and 530. It has been possible to compare the electron densities of the  $ZHZH^{+2Z-2}$  systems with those of the  $ZHZ^{+2Z-1}$  ions for  $\theta_H = 100^\circ$  and  $120^\circ$  when  $Z = 1.0, 1.4, 1.8$  and  $2.2$ . The densities of the two-electron systems are presented in the same diagrams as the corresponding four electron systems.

There is a general tendency when  $Z > 1.0$  for the electron density around the  $Z$  nuclei to decrease as  $\theta_H$  increases, this can be seen in Figures 510, 513, 518 and 523. This is reasonable since an increase in the  $Z$ - $Z$  distance causes the  $Z$ - $Z$  nuclear repulsion to decrease, hence less of the electron density is required to shield the  $Z$  nuclei. As a result the density along the  $H$ - $H$  direction increases as  $\theta_H$  increases (see Figures 511, 514, 519 and 524). As one would expect the electron density along  $H$ - $H$  and  $Z$ - $Z$  is dependent on the magnitude of  $Z$  - the greater the value of  $Z$  the smaller the density along  $H$ - $H$ . A particularly interesting feature is shown

in Figures 519 and 524, as  $y$  increases from zero the electron density for the systems with  $\theta_H = 90^\circ$  drops to a minimum at about  $y \approx 0.5$  au. This seemingly strange 'hump', at  $y = 0$  in this instance, is due to the internuclear charge cloud being concentrated along the Z-Z axis. A similar effect can be seen in the x-direction when  $Z$  is small and  $\theta_H = 130^\circ$ , the charge build-up in this case being along H-H. This can be seen in Figures 510, 513 and 518. The electron density along the ZH direction is given in Figures 512, 515, 520 and 525. As  $\theta_H$  increases there is a noticeable movement of charge from the vicinity of Z to regions near the H nucleus. Since the Z-H distance is fixed the density curves along Z-H are superimposed for all values of  $\theta_H$ ; for this reason only the curves for  $\theta_H = 90^\circ$  and  $130^\circ$  are given in Figures 507, 512, 515, 520 and 525.

For the  $Z = 1.0$  systems the electron density distribution as a function of  $\theta_H$  does not, in general, follow the pattern set by the systems when  $Z > 1.0$ . For example, when  $Z = 1.0$  the density at Z increases with increasing  $\theta_H$  whereas, when  $Z > 1.0$ , the reverse is true. As one would expect, when  $\theta_H = 90^\circ$ , the electron density is symmetrical about the mid-points of all the internuclear axes. In the central regions of H-H and Z-Z, at  $0 < x < 0.5$  au,  $0 < y < 0.5$  au, the electron density is much smaller when  $\theta_H = 90^\circ$  than when  $\theta_H = 130^\circ$ . The 'hump' in the density for  $\theta_H = 130^\circ$ ,  $x = 0$  in Figure 505 shows that the build up of charge in these central regions (as  $\theta_H$  increases) is primarily along the H-H direction. The electron density along the Z-H axis, Figure 507, shows that the charge in the vicinity of H decreases as  $\theta_H$  increases. This charge is redistributed along H-H and also in the proximity of Z ( $Z = 1.0$ ). This movement of charge towards Z does not occur when  $Z > 1.0$ . However, when  $Z = 1.0$  and  $\theta_H > 60^\circ$ , the ZH nuclear repulsion is greater than the ZZ nuclear repulsion; consequently, the movement of electron density from Z to H maintains a balance in the ZH internuclear shielding. These results for  $Z = 1.0$  fit

into a definite pattern; as  $\theta_H$  increases from  $90^\circ$  to  $130^\circ$  the system changes from four interacting hydrogen atoms to two hydrogen atoms interacting with a hydrogen molecule. Not surprisingly the latter system is the most stable energetically. In fact, the optimum energy occurs when  $\theta_H = 129^\circ$  which gives an H-H distance that is almost identical with the bond length in  $H_2$ .

The most unusual feature of this work is the decrease in  $\theta_H(\text{opt})$  as  $Z$  increases. To a great extent, the optimum geometry of the systems investigated here is dependent on the contribution to the total energy of the H-H 'bond'. For  $Z = 1.0$  and  $\theta_H = 129^\circ$  the charge build up along H-H provides a large negative contribution to the total energy of approximately  $(E_{\theta_H(\text{opt})} - E_{\theta_H = 90^\circ})$ , which is 10% of the total energy. When  $Z = 2.2$  the contribution of this bond is very small for two reasons, (a) the charge build-up along H-H is less and (b) the total energy of the system increases with increasing  $Z$ . The minimum energy of the  $Z = 2.2$  system will probably occur when the four nuclei are most effectively shielded from each other by the electron density. For the  $Z = 2.2$  system  $\theta_H(\text{opt})$  is  $101^\circ$ , and it can be seen from Figures 523 and 524 that for  $\theta_H = 100^\circ$  the internuclear density is flattest. Therefore, the electron density is concentrated in the proximity of the nuclear sites. It is reasonable, then, to assume that the electron density for  $\theta_H \approx 100^\circ$  affords the most effective shielding of the nuclei. The values of  $\theta_H(\text{opt})$  for the systems with  $Z = 1.2, 1.4$  and  $1.8$  are  $128^\circ, 125^\circ$  and  $114^\circ$  respectively. As  $Z$  increases the contribution of the H-H 'bond' to the total energy decreases and the nuclear-nuclear repulsions increase. Therefore, for these systems the most stable geometry is a function of both the H-H 'bond' and the nuclear shielding. It can be assumed, because of the magnitude of  $\theta_H(\text{opt})$ , that for  $Z = 1.2$  and  $1.4$

the H-H 'bond' contributes significantly to the optimum energy. The contribution it has when  $Z = 1.8$ ,  $\theta_H(\text{opt}) = 114^\circ$  is certainly much smaller. One must then ask why, if the nuclear-nuclear repulsions are dominant, is  $\theta_H(\text{opt})$  for  $Z = 1.8$  greater than that for  $Z = 2.2$ ? The probable answer to this point stems from the fact that as  $Z$  increases the electron density in the proximity of  $Z$  increases; consequently the density in the vicinity of H decreases. Therefore as  $Z$  increases from 1.8 to 2.2 the H-H nuclear repulsion increases, hence  $\theta_H(\text{opt})$  decreases. This argument assumes that the increased Z-H and Z-Z nuclear repulsions of the larger  $Z$  value are more than compensated for by the increased electron density in the proximity of  $Z$ . This assumption appears to be reasonable when the electron densities in the vicinity of  $Z$ , for  $Z = 1.8$  and 2.2, are compared in Figures 518 and 523.

There are two fundamental differences between the  $ZHZH^{+2Z-2}$  and  $ZHZ^{+2Z-1}$  systems -

- (a) The  $ZHZ^{+2Z-1}$  ion is constructed from three nuclei and two electrons whereas the  $ZHZH^{+2Z-2}$  complex contains two extra electrons and only one more nucleus - a proton.
- (b) The  $Z$  nuclei in the  $ZHZ^{+2Z-1}$  system are in terminal positions, but, in the  $ZHZH^{+2Z-2}$  complex, this characteristic is destroyed by the extra proton.

The electron density distributions of these two systems are compared for  $\theta_H = 100^\circ$  and  $120^\circ$ , when  $Z = 1.0, 1.4, 1.8$  and 2.2. For each value of  $Z$  the effects that (a) and (b) have on the density distributions are assessed.

When the value of the effective nuclear charge  $Z$  is unity the electron density along the Y-axis (O-H) is almost identical for both systems. The build up of charge that occurs along H-H in the four electron system is

just beginning to show when  $\theta_H = 120^\circ$ . Along the X-axis (Z-Z) the shapes of the density distributions are similar, but the magnitudes of the densities, especially in the vicinity of Z, are very different. Therefore, the addition of a proton and two electrons to the  $ZHZ^{+2Z-1}$  system ( $Z = 1.0$ ) conserves the density near the hydrogen nuclei and the remaining electron density is distributed in the vicinity of the Z nuclei. This charge movement is reasonable since  $Z = 1.0$  and therefore all four nuclei of the  $ZHZH^{+2Z-2}$  system will have local densities that are very similar to the density near H in the corresponding  $ZHZ^{+2Z-1}$  system ( $Z = 1.0$ ). In this context the corresponding  $ZHZ^{+2Z-1}$  system is one which has a bond angle  $\theta_H$  when the centres A and C of  $ZHZH^{+2Z-2}$  are being considered and  $(180^\circ - \theta_H)$  when centres B and D are considered. Clearly, the densities near H and Z in the  $ZHZH^{+2Z-2}$  ( $Z = 1.0$ ) systems are more alike when  $\theta_H = 100^\circ$  than when  $\theta_H = 120^\circ$ , see Figures 508 and 509.

When  $Z = 1.4$  the density distributions along OH, Figure 513, are similar for  $\theta_H = 120^\circ$ . However, at  $\theta_H = 100^\circ$  the density in the vicinity of H is greatest for the two-electron system. For the  $ZHZH^{+2Z-2}$  complex the density along OH is known to increase as  $\theta_H$  increases, the build up of the density in the centre of H-H is already showing in both diagrams. The addition of a proton and two electrons to the  $ZHZ^{+2Z-1}$  system causes a decrease in the density near the hydrogen nuclei and a marked increase in the density near Z. The density is certain to increase in the vicinity of Z since, as far as the Z nucleus is concerned, the system is changing from  $ZHZ^{+2Z-1}$  to something more like  $HZH^{+Z}$ .

For both the two and four electron systems an increase in Z from 1.4 to 1.8 results in an increase in the electron density along the X-axis. When  $\theta_H = 120^\circ$  the density along OH is greatest for the four electron system, but for  $\theta_H = 100^\circ$  the two density distributions are almost alike. This pattern is similar to that observed when  $Z = 1.4$  although the changes in density are

not so marked. This is to be expected since for both the two and four electron complexes most of the electron density is held in the vicinity of the Z nuclei. Consequently, destroying the terminal nature of the Z nuclei does not have as great an effect as when  $Z = 1.0$  or  $1.4$ . For  $Z = 2.2$  the characteristics of the electron density distributions are similar to those for  $Z = 1.8$ . Again the density is not greatly affected by the addition of a proton and the density of the extra two electrons is distributed throughout the system, see Figures 526 and 527.

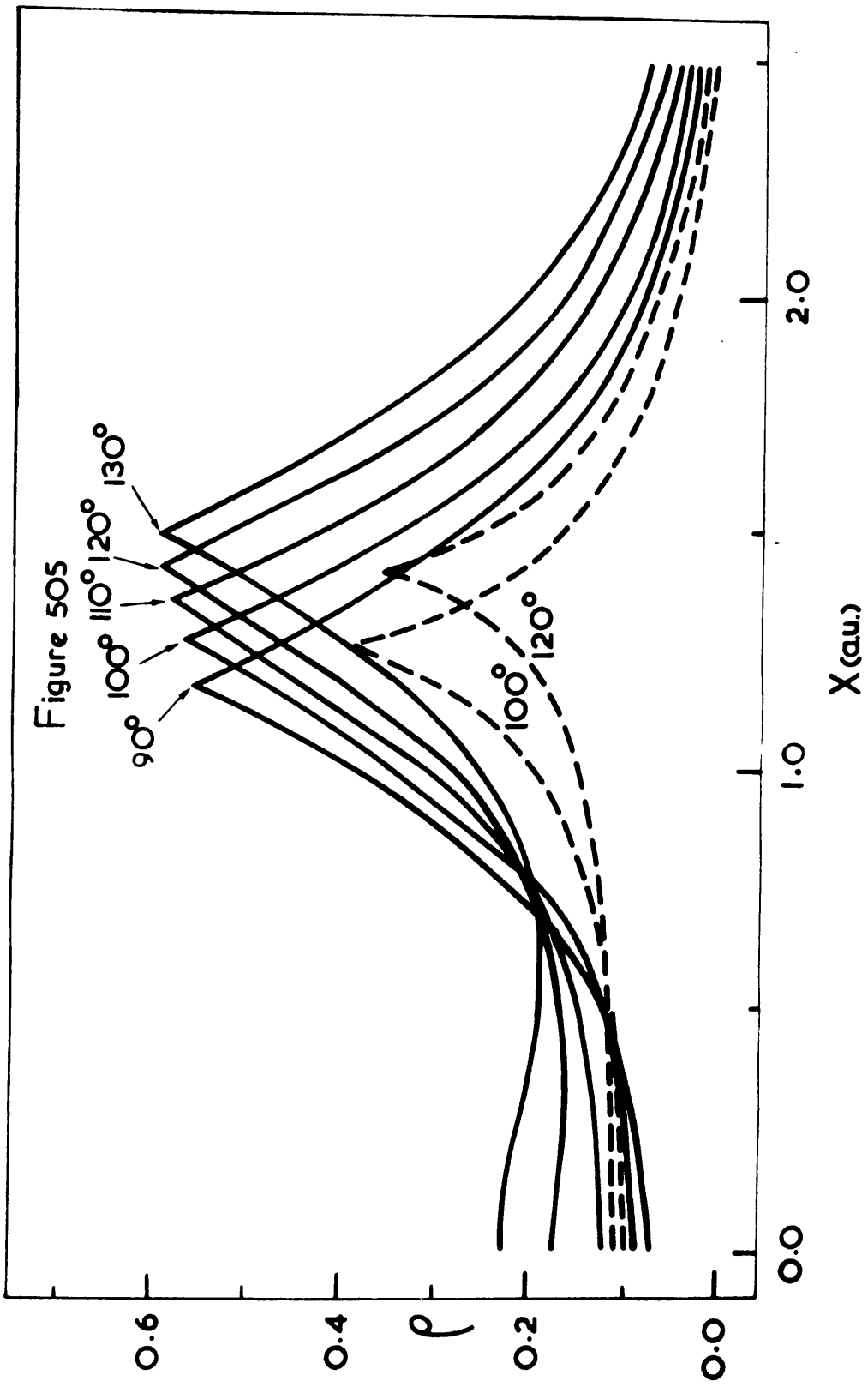
Figures 505 - 509

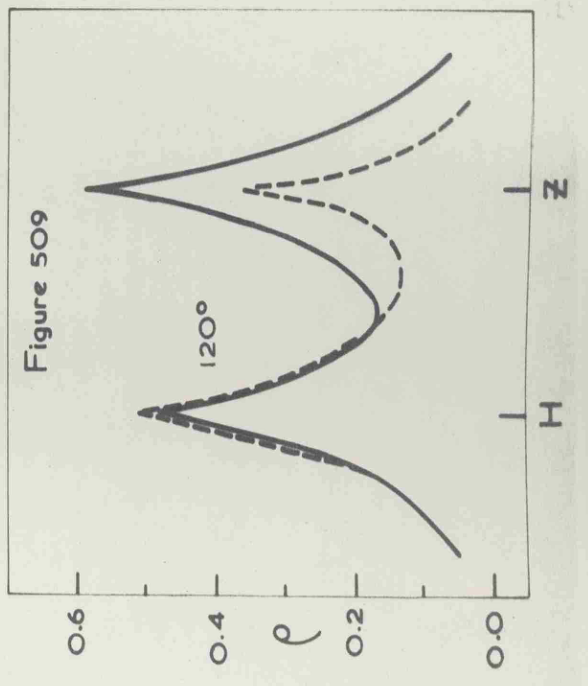
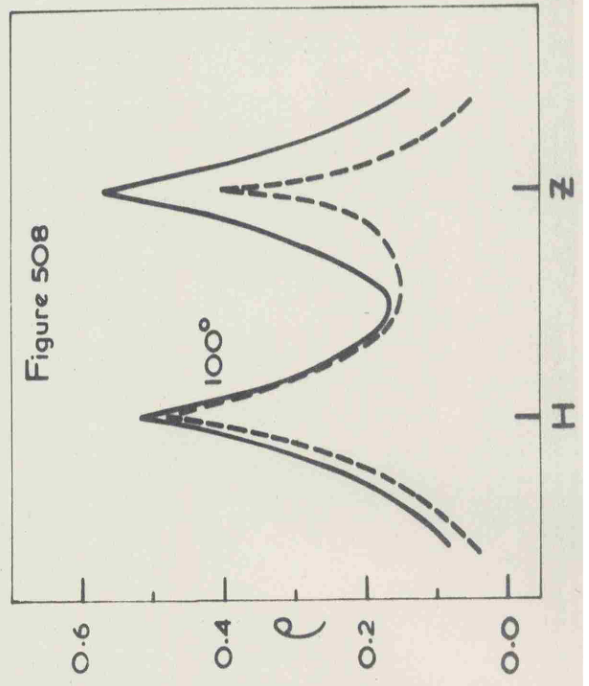
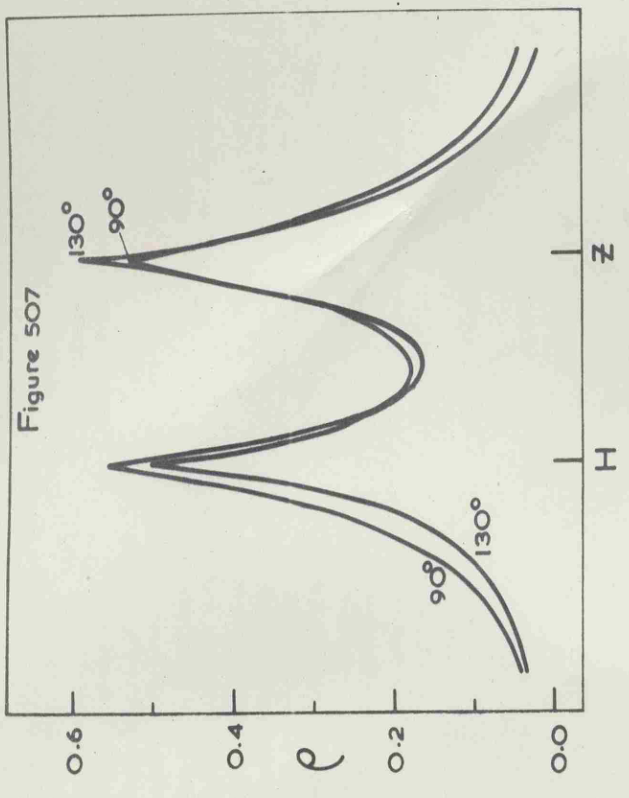
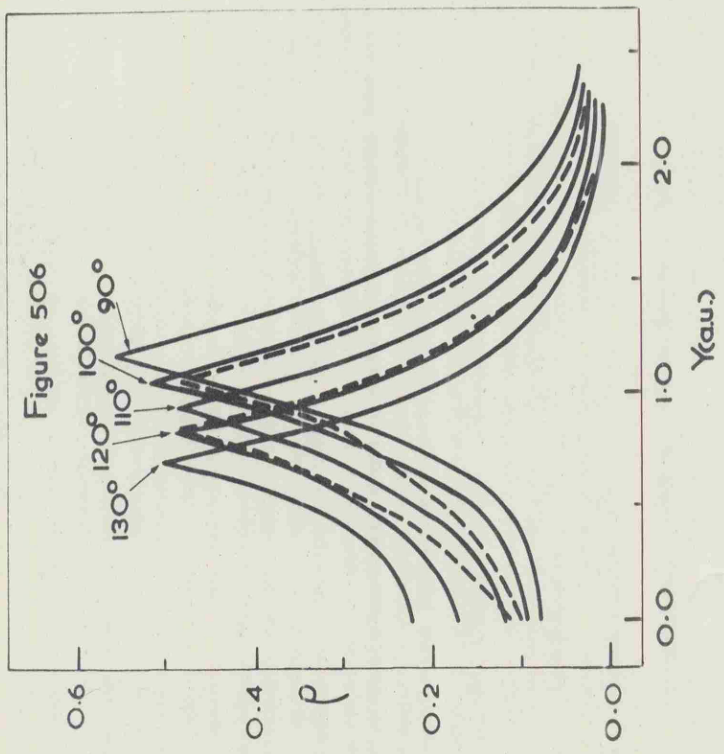
The electron density distributions along the three internuclear axes for the  $ZHZH^{+2Z-2}$  and  $ZHZ^{+2Z-1}$  systems when  $Z = 1.0$ . The densities of the two electron systems are distinguished by the dotted lines.

Figure 505 The electron density along  $O - Z$ .

Figure 506 The electron density along  $O - H$ .

Figures 507, 508 and 509 The electron density along  $Z - H$





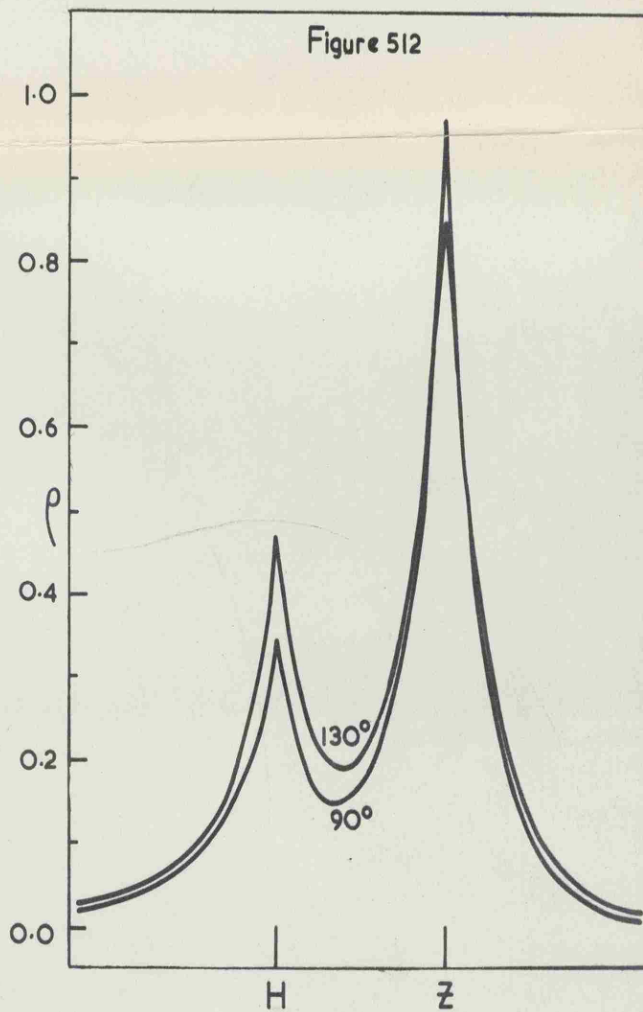
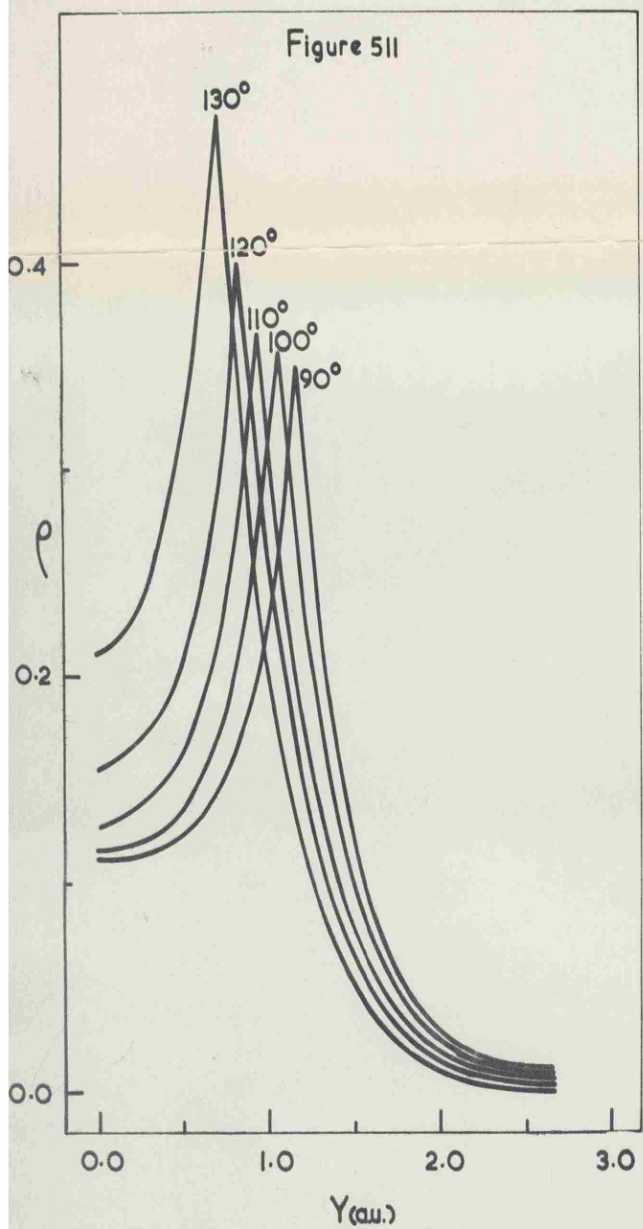
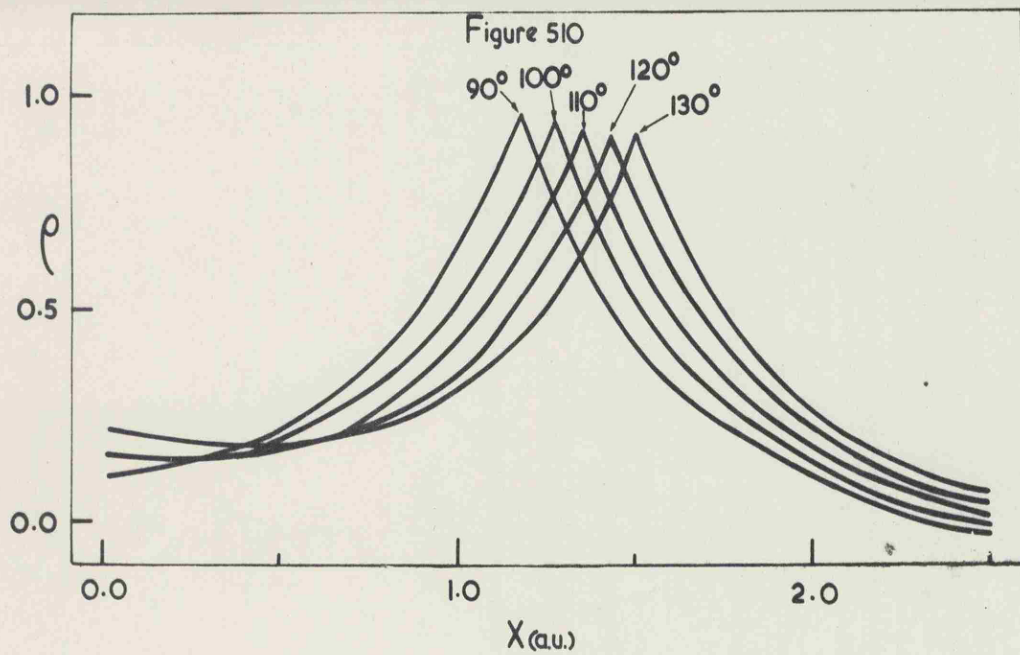
Figures 510 - 512

The electron density distribution along the three internuclear axes for the  $ZHZH^{+2Z-2}$  systems when  $Z = 1.2$

Figure 510 The electron density along O - Z.

Figure 511 The electron density along O - H.

Figure 512 The electron density along Z - H.



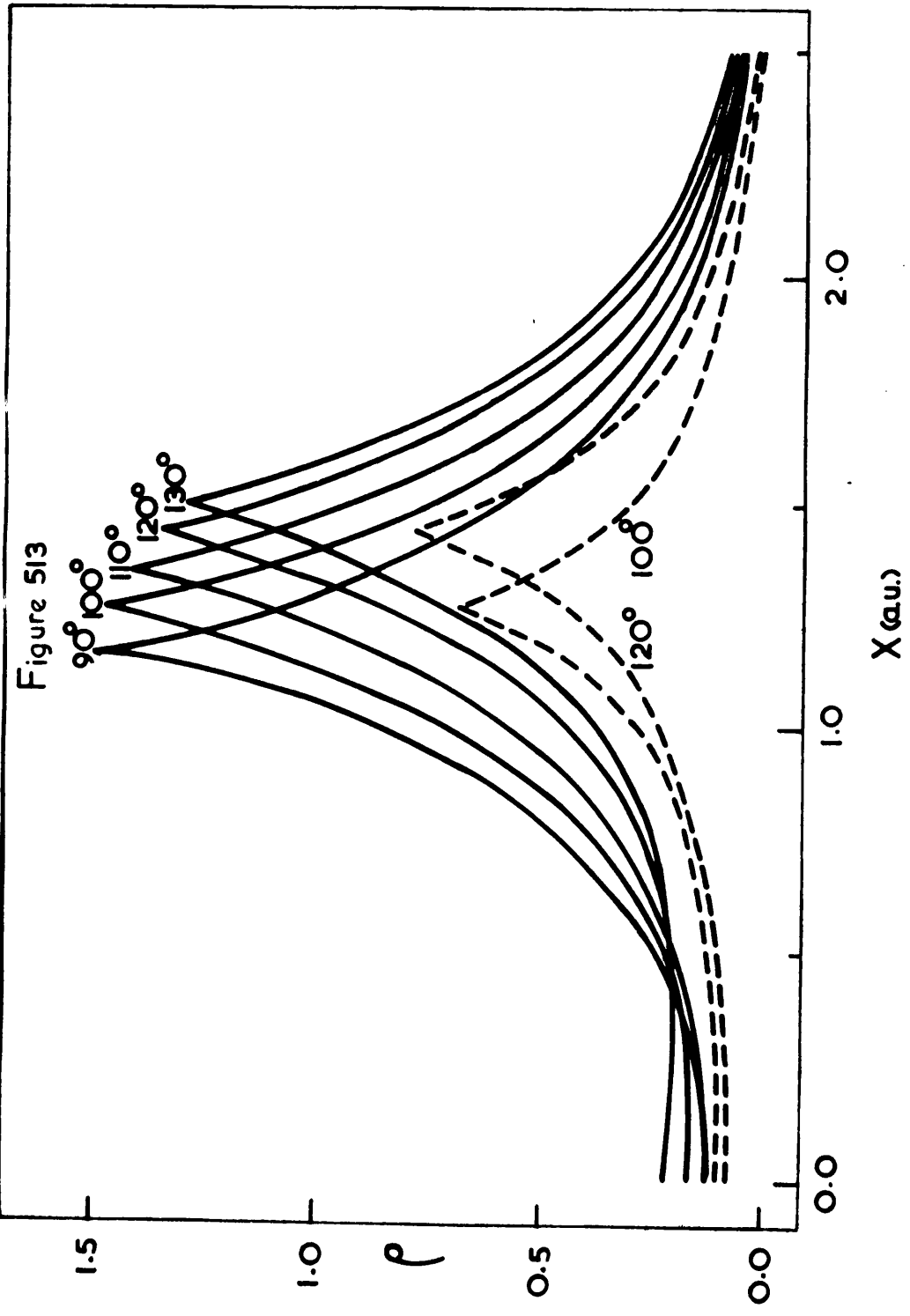
Figures 513 - 517

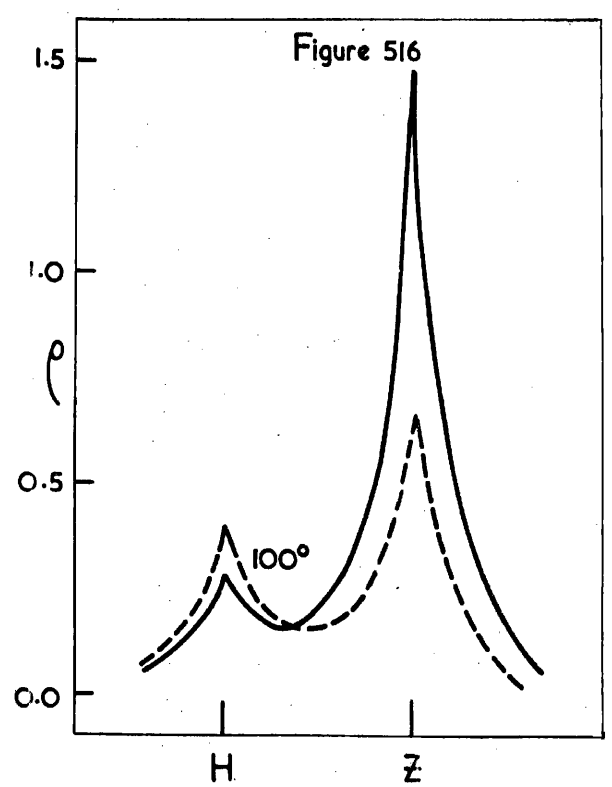
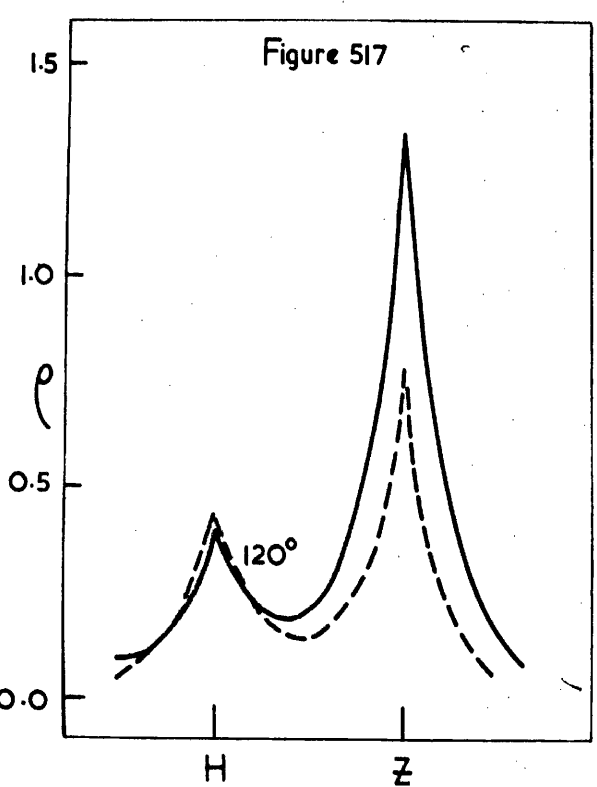
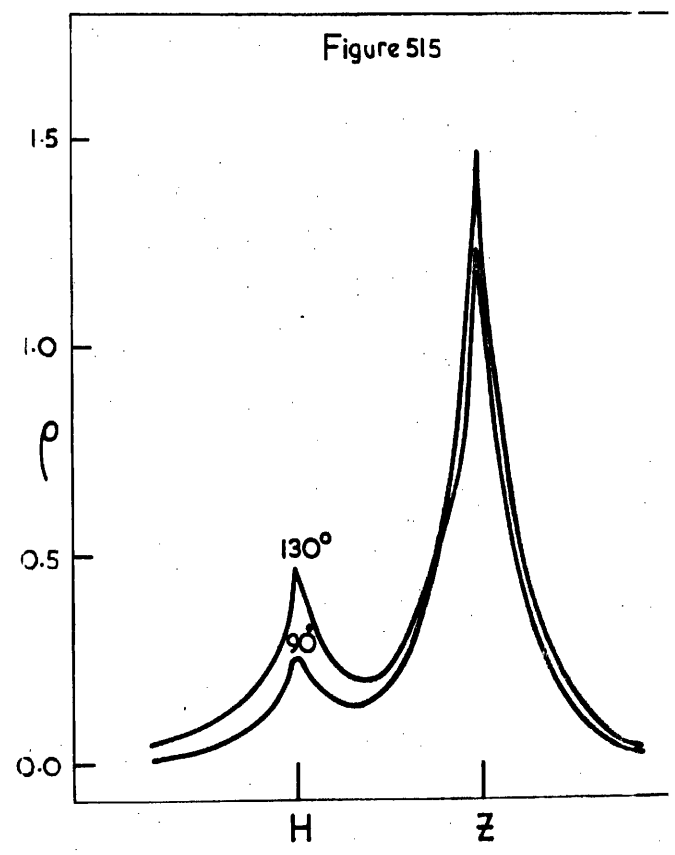
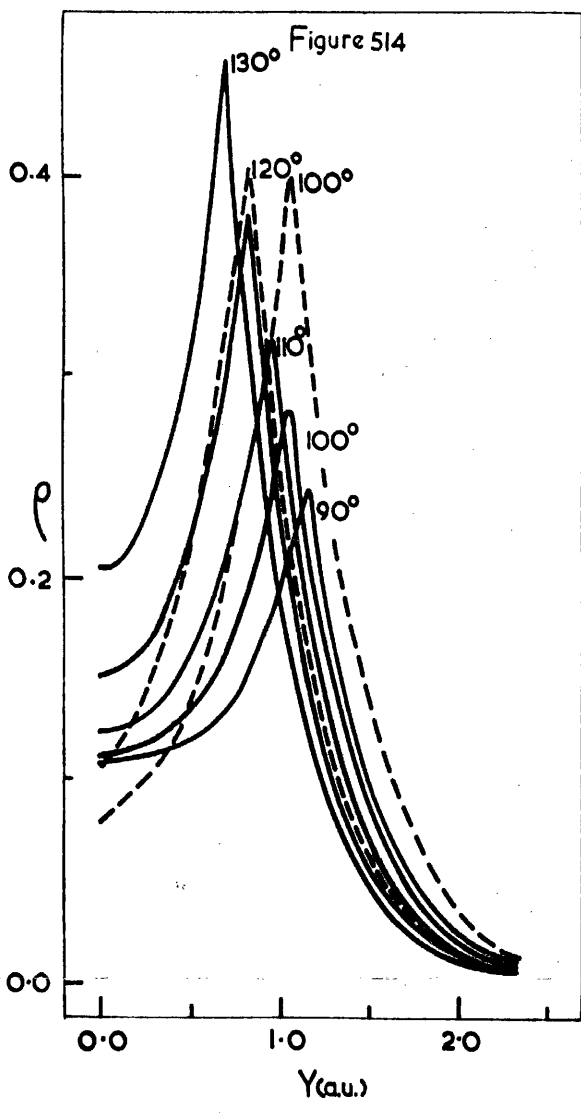
The electron density distributions along the three internuclear axes for the  $ZHZH^{+2Z-2}$  and  $ZHZ^{+2Z-1}$  systems when  $Z = 1.4$ . The densities of the two electron systems are distinguished by the dotted lines.

Figure 513 The electron density along O - Z.

Figure 514 The electron density along O - H.

Figures 515, 516 and 517 The electron density along Z - H.





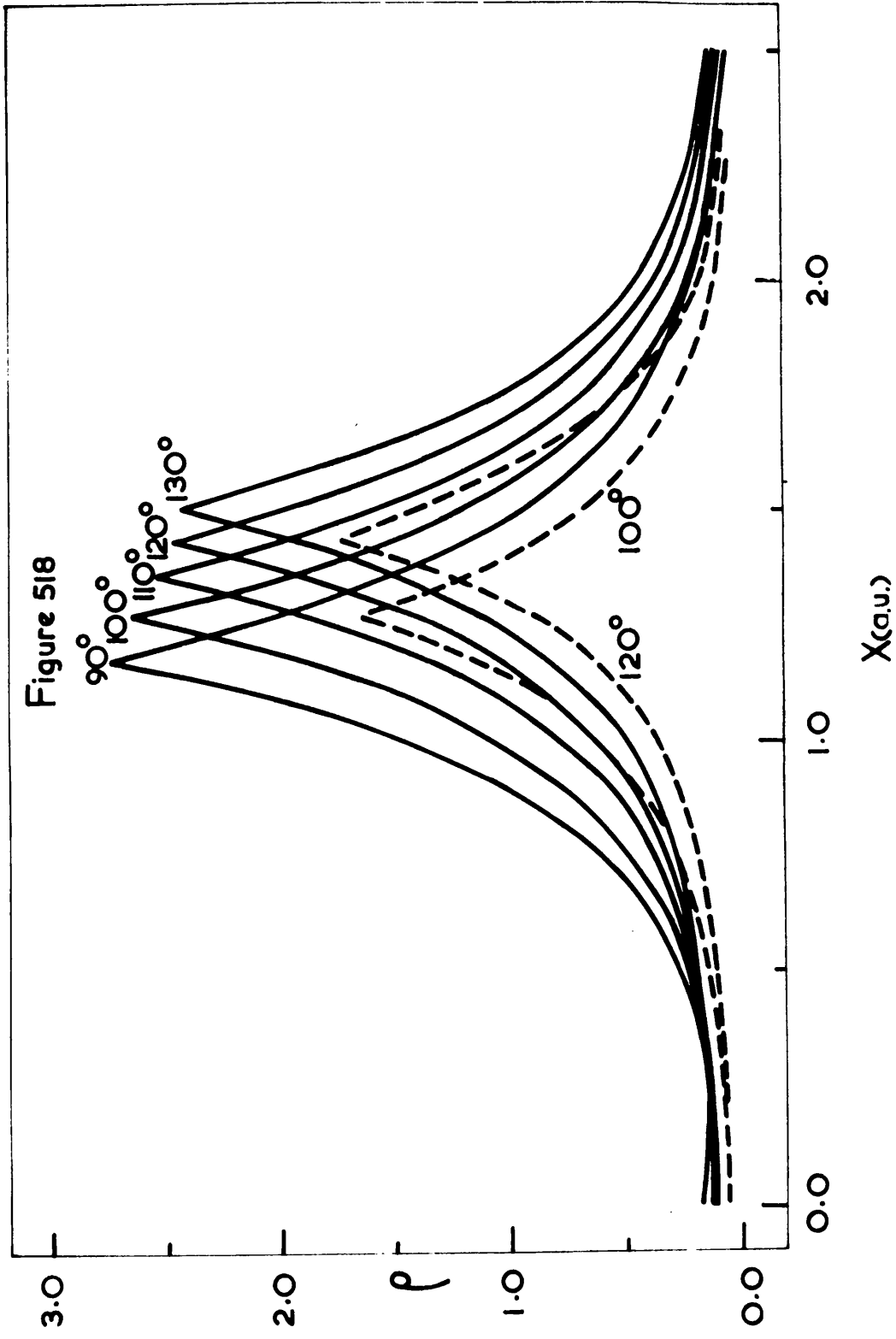
Figures 518 - 522

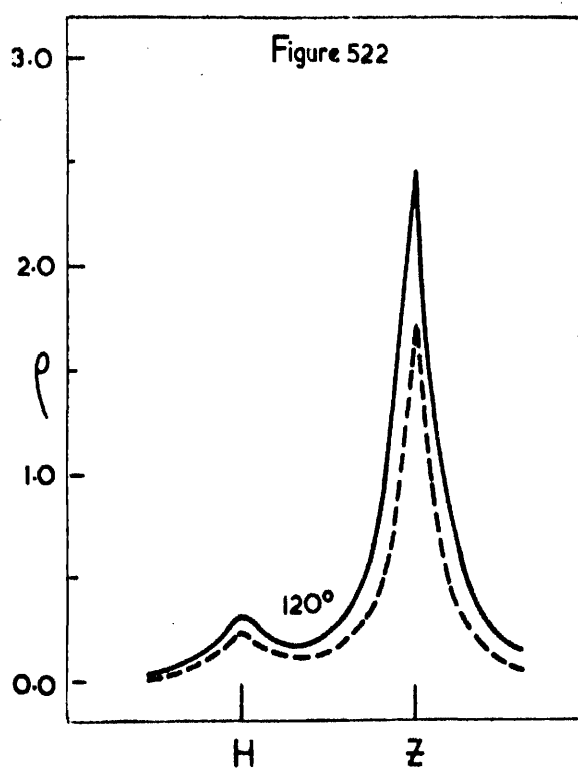
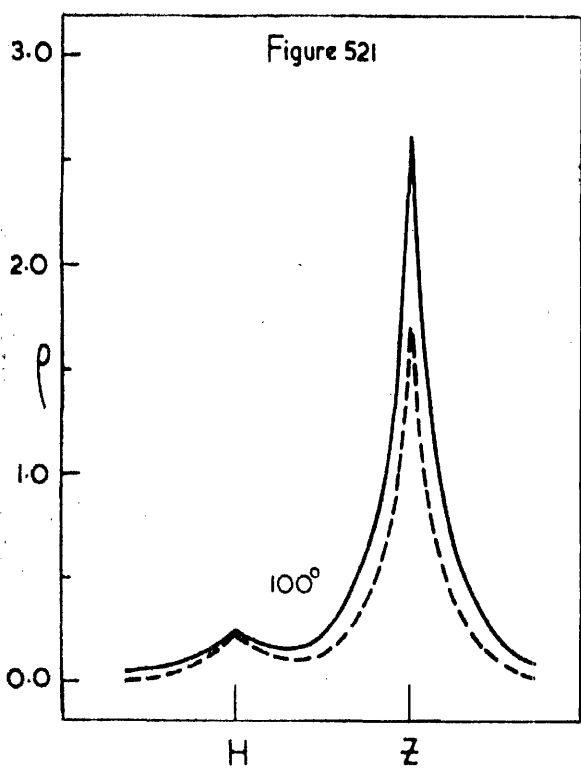
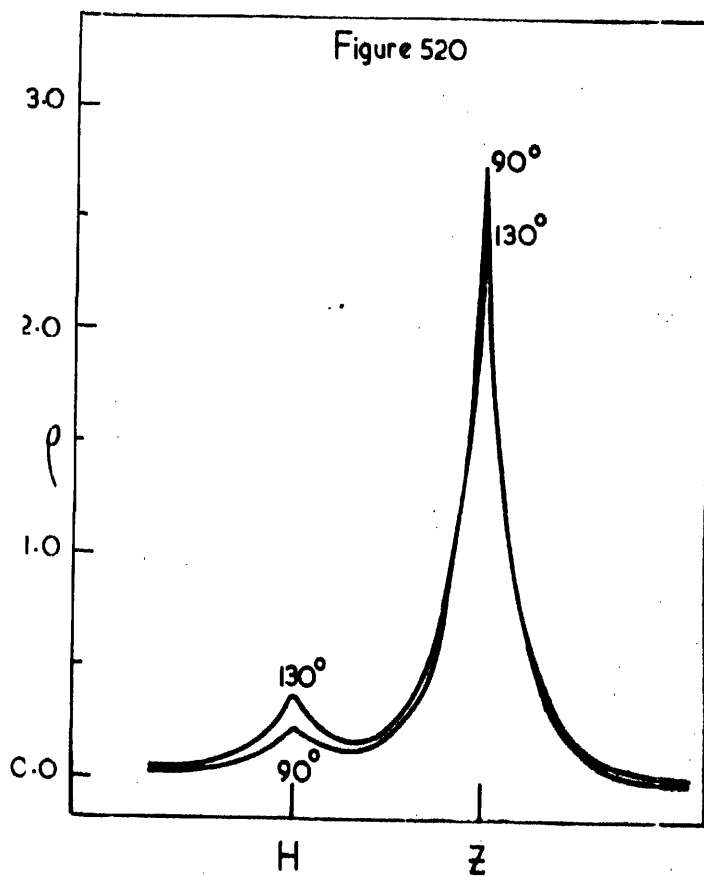
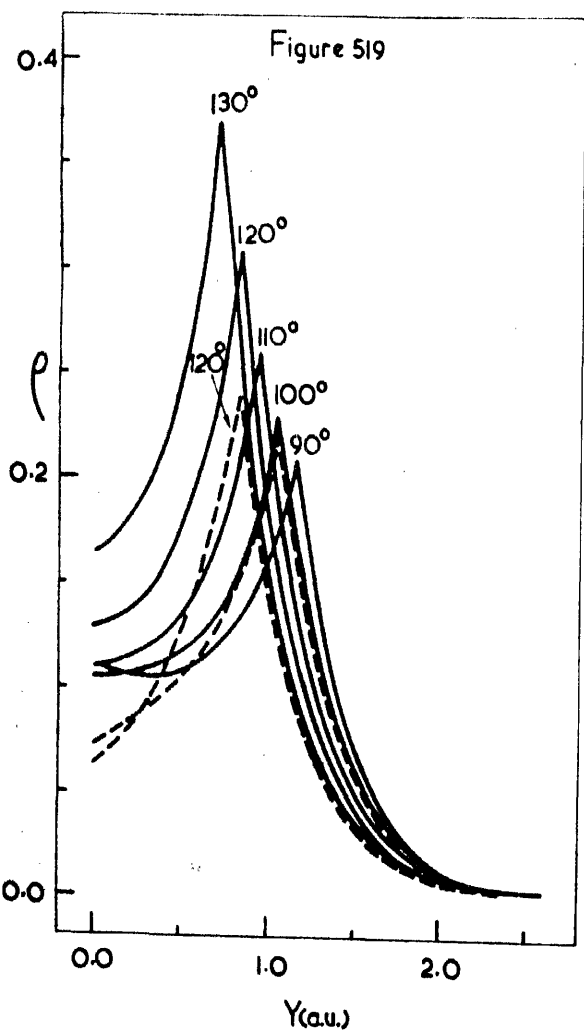
The electron density distributions along the three internuclear axes for the  $ZHZH^{+2Z-2}$  and  $ZHZ^{+2Z-1}$  systems when  $Z = 1.8$ . The densities of the two electron systems are distinguished by the dotted lines.

Figure 518 The electron density along  $O - Z$ .

Figure 519 The electron density along  $O - H$ .

Figures 520, 521 and 522 The electron density along  $Z - H$ .





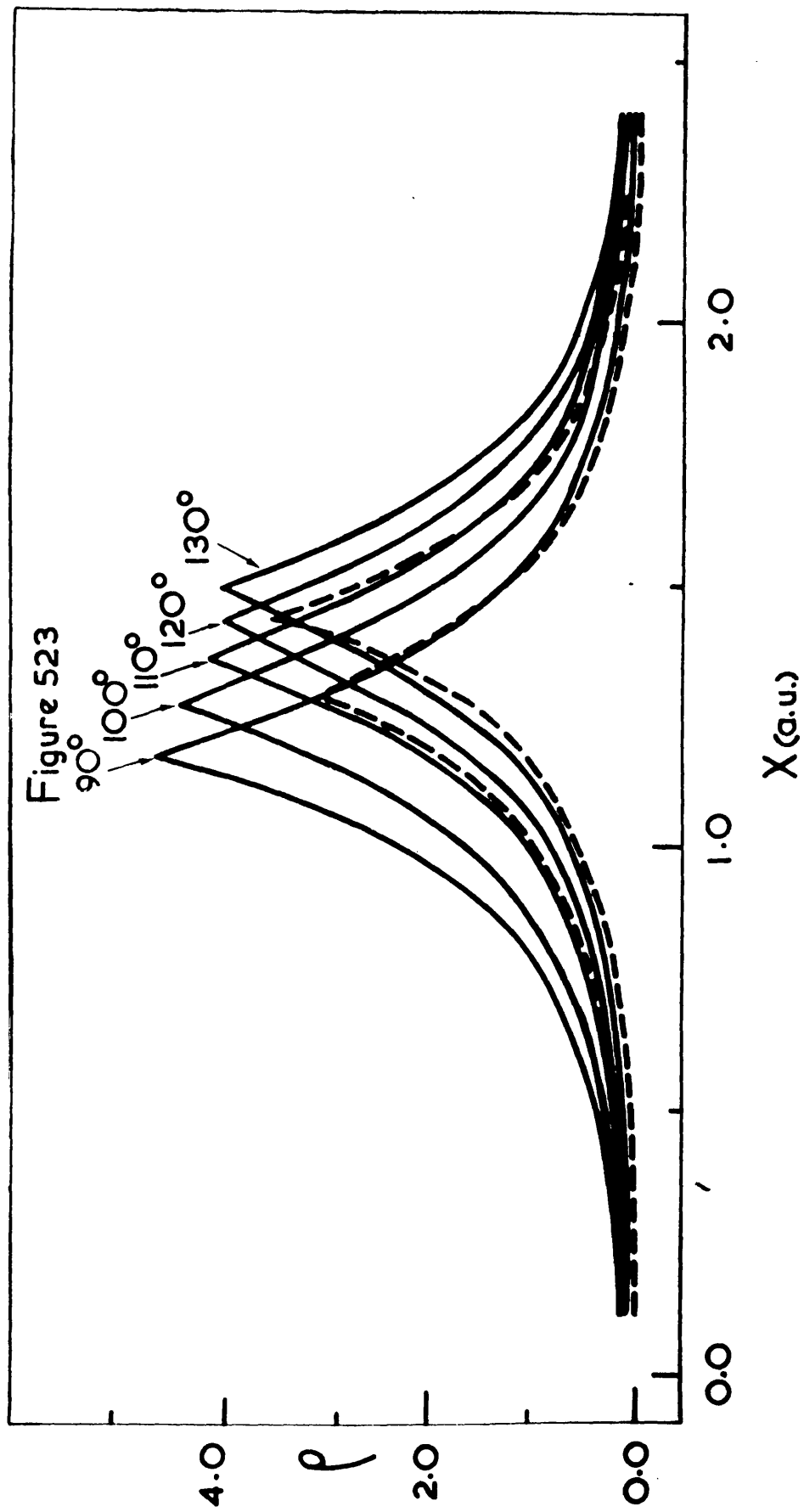
Figures 523 - 527

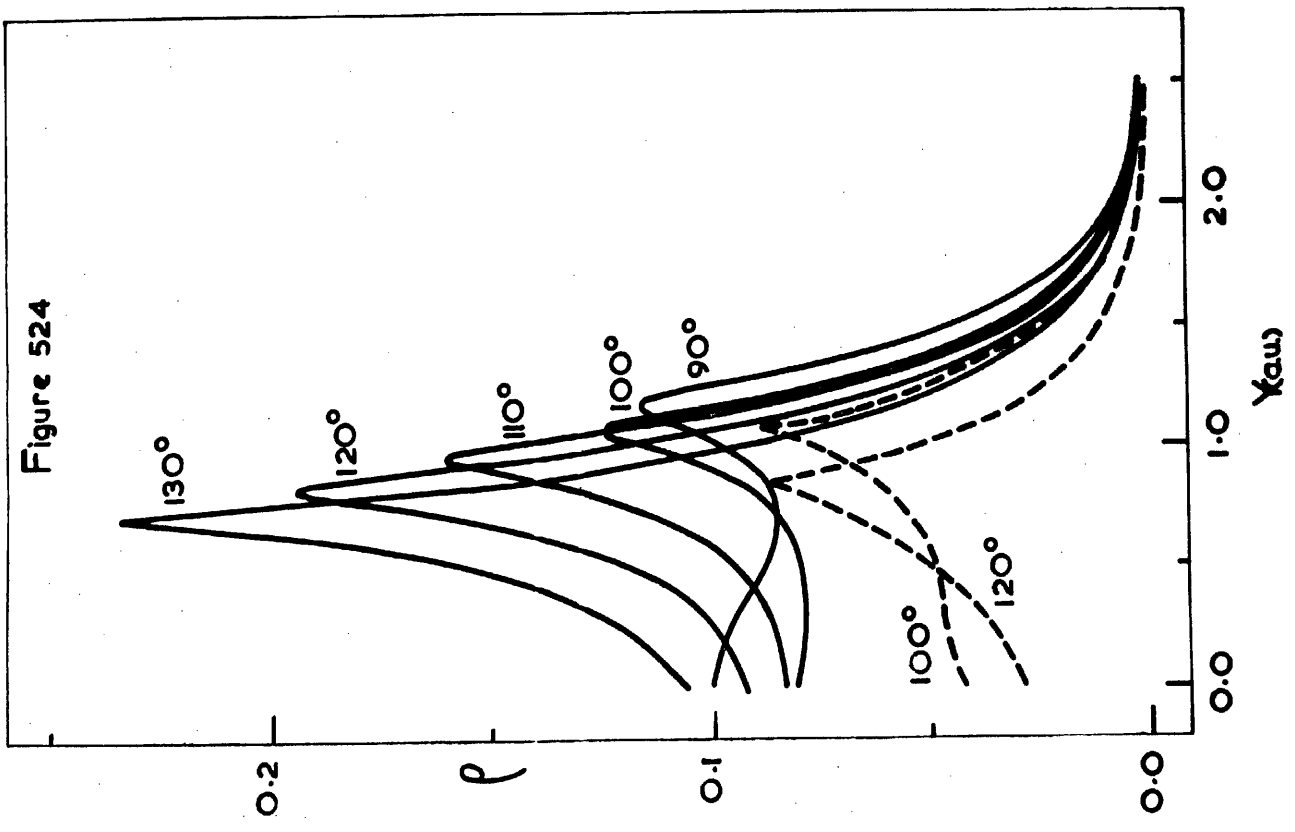
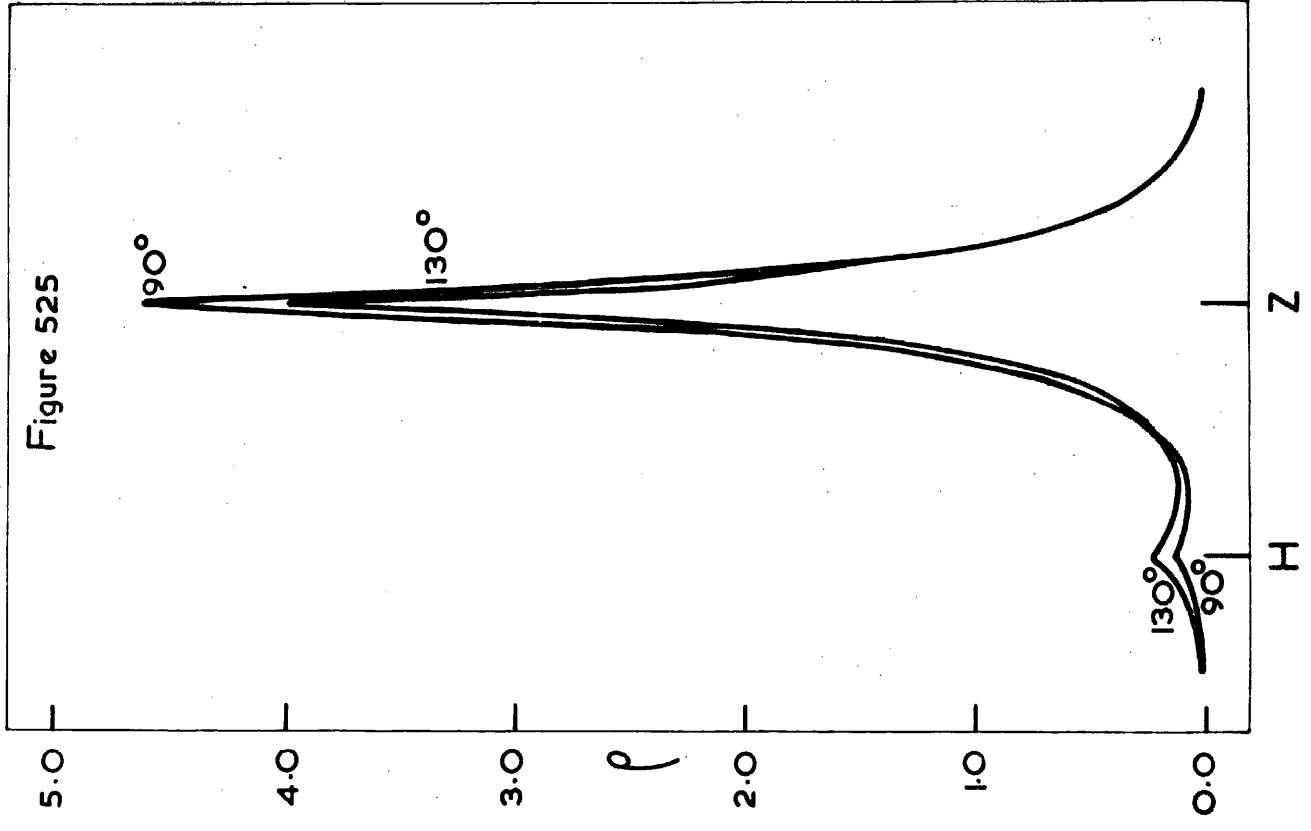
The electron density distributions along the three internuclear axes for the  $ZHZH^{+2Z-2}$  and  $ZHZ^{+2Z-1}$  systems when  $Z = 2.2$ . The densities of two electron systems are distinguished by the dotted lines.

Figure 523 The electron density along  $O - Z$ .

Figure 524 The electron density along  $O - H$ .

Figures 525, 526 and 527 The electron density along  $Z - H$ .





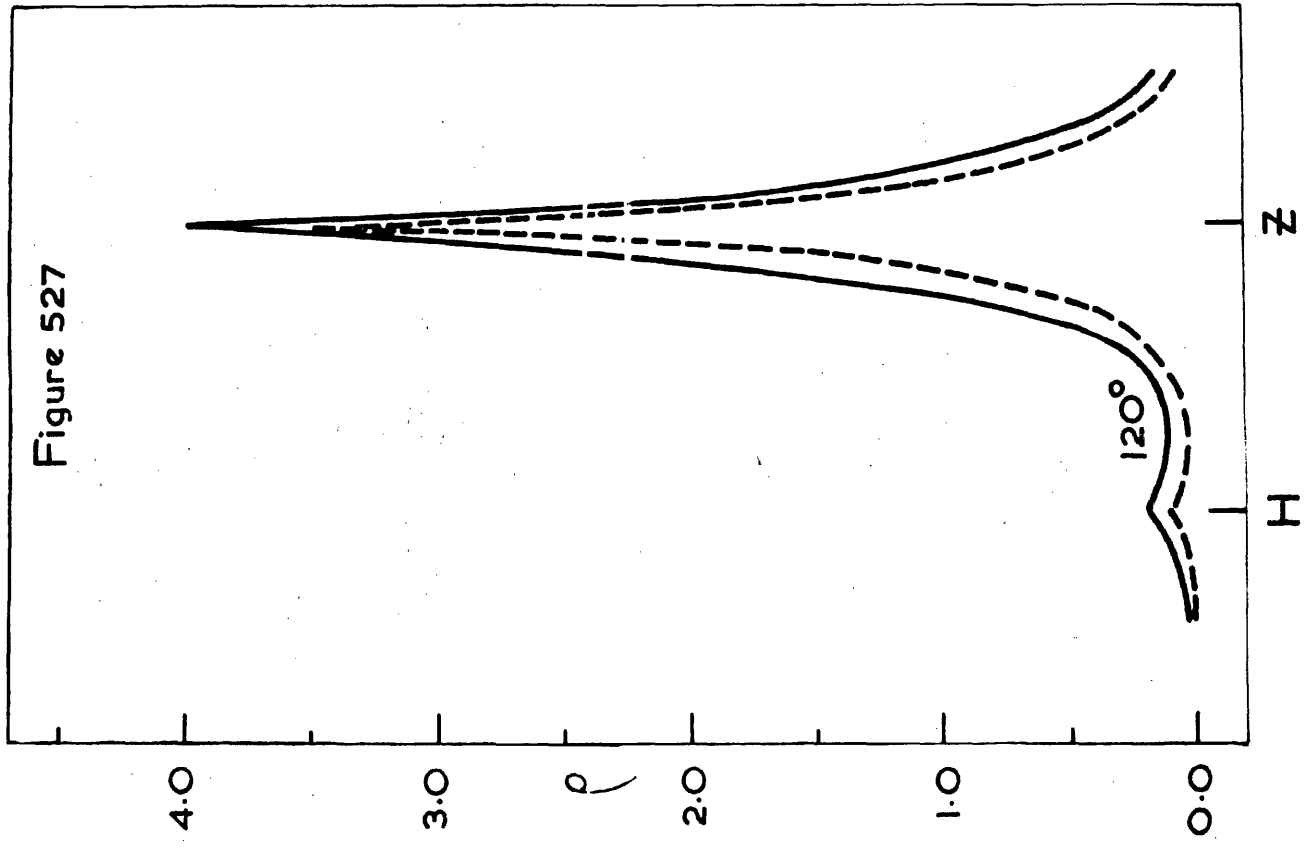
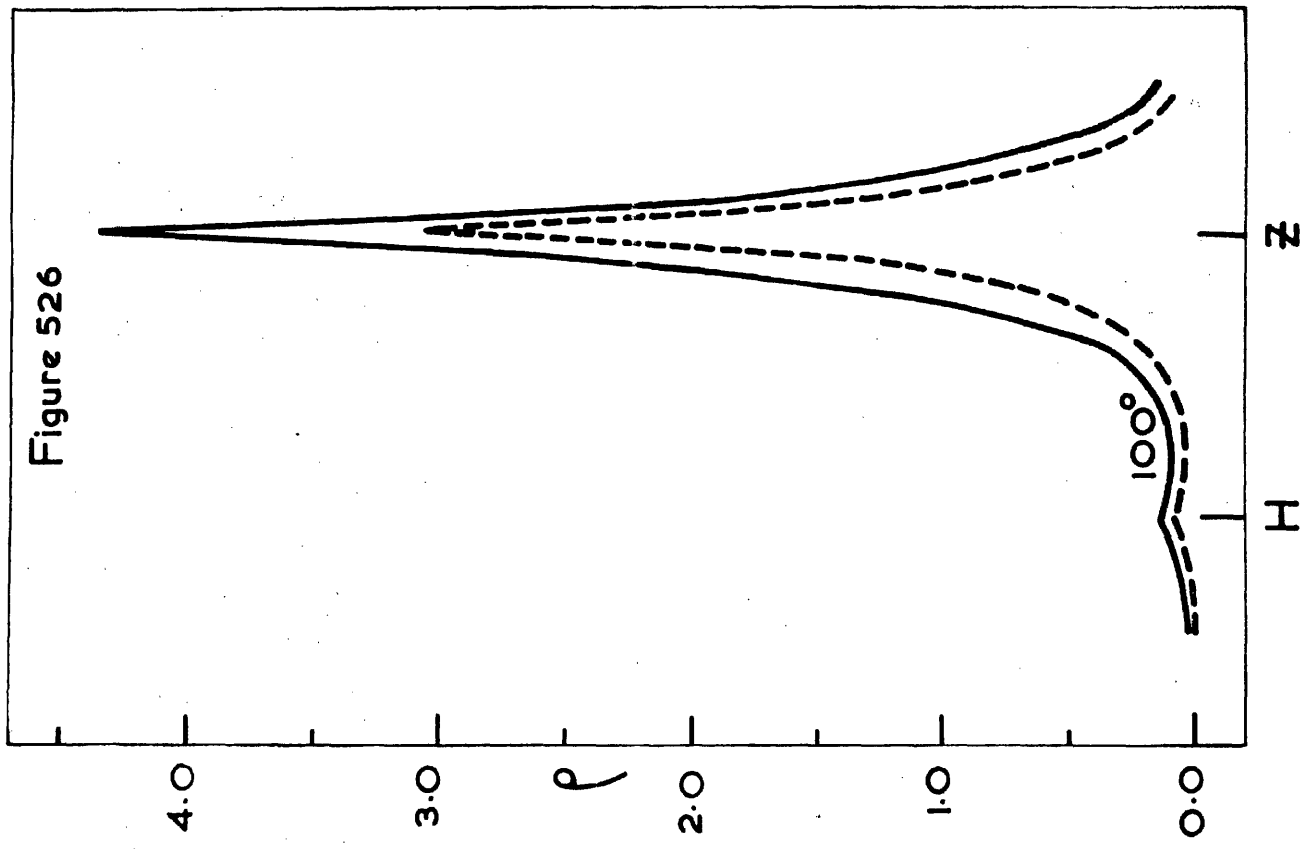


Figure 528

The electron density distribution along  
0 - Z for the fully optimized  $ZHZH^{+2Z-2}$   
systems.

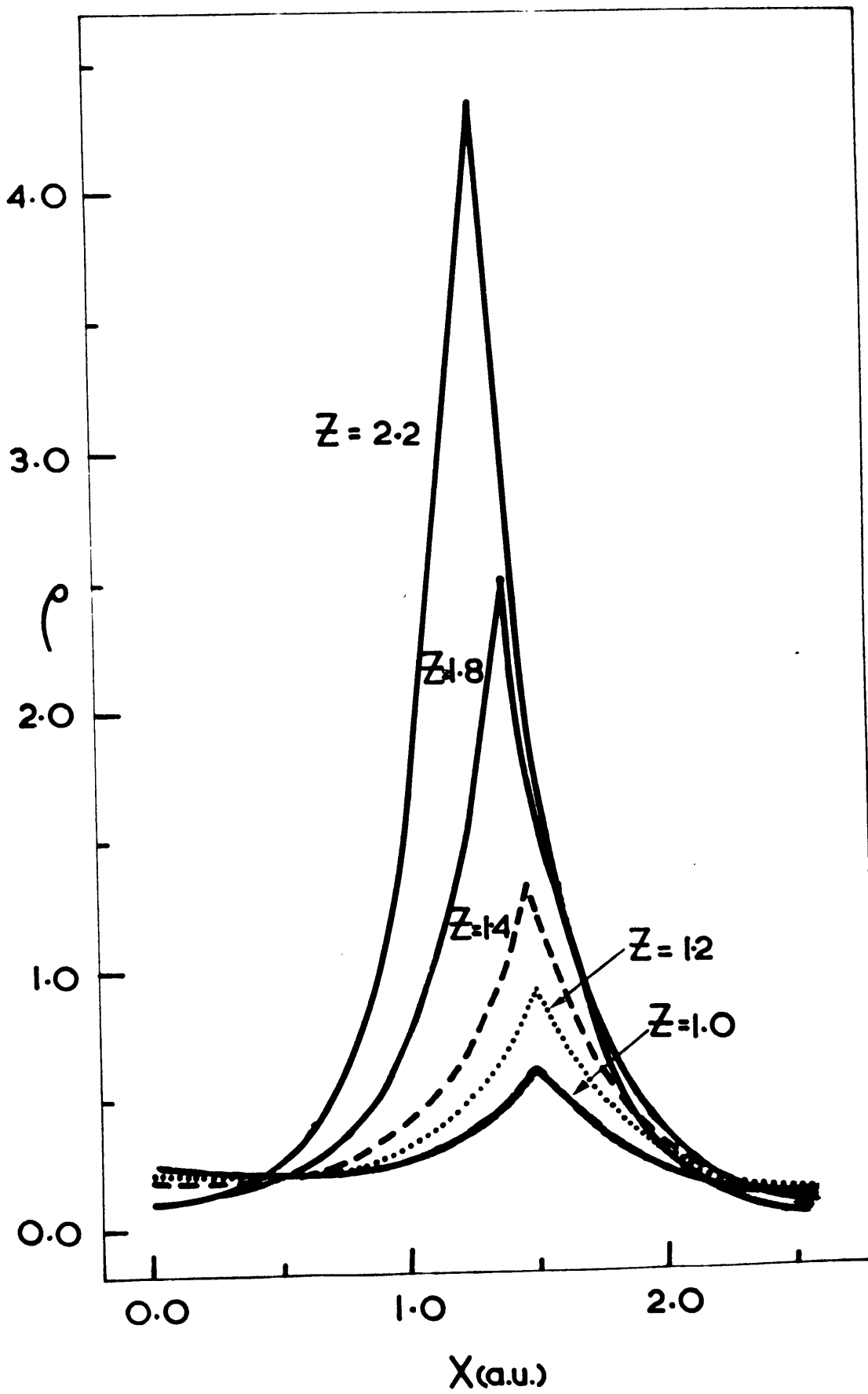


Figure 529

The electron density distribution along  
O-H for the fully optimized  $ZHZH^{+2Z-2}$   
systems.

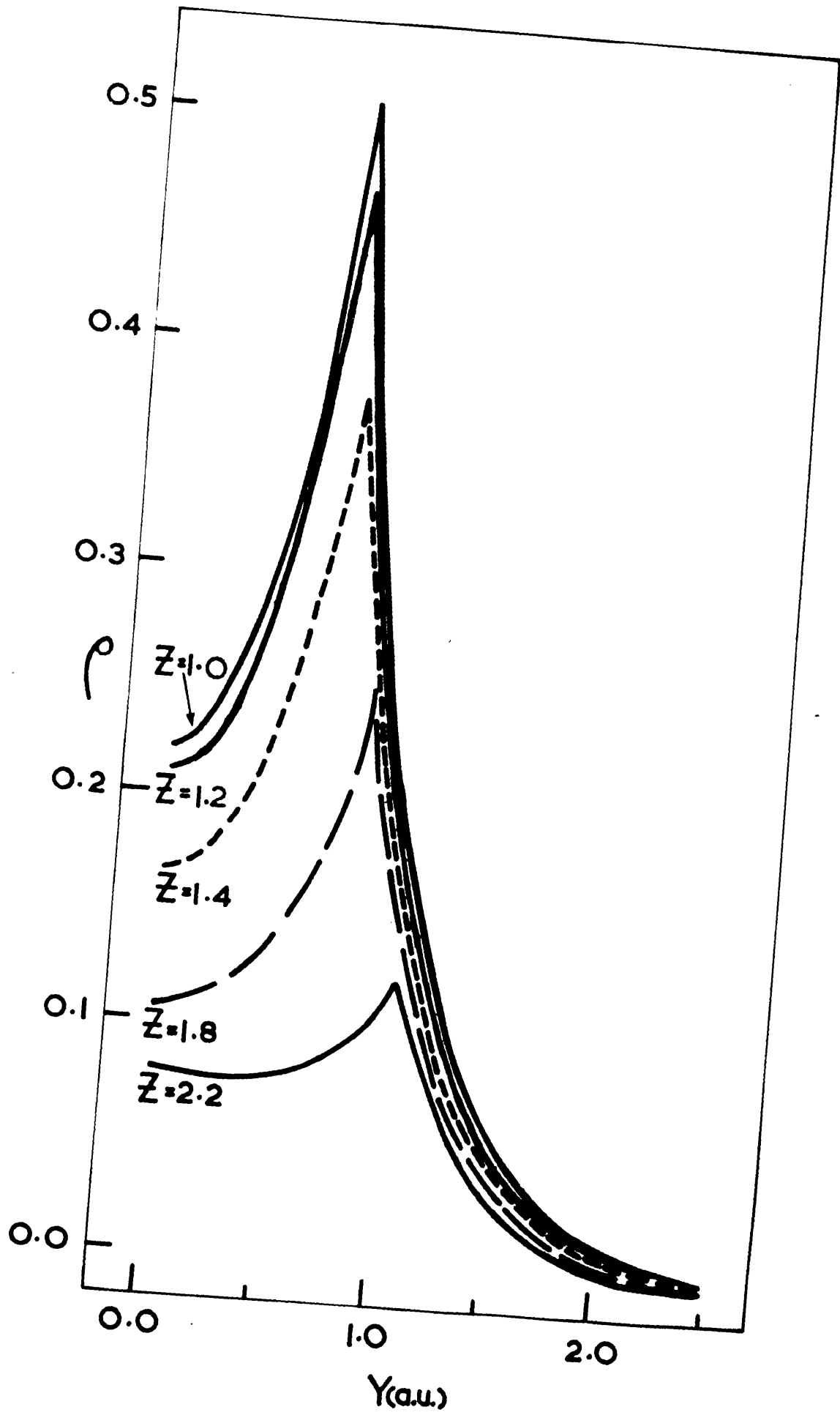
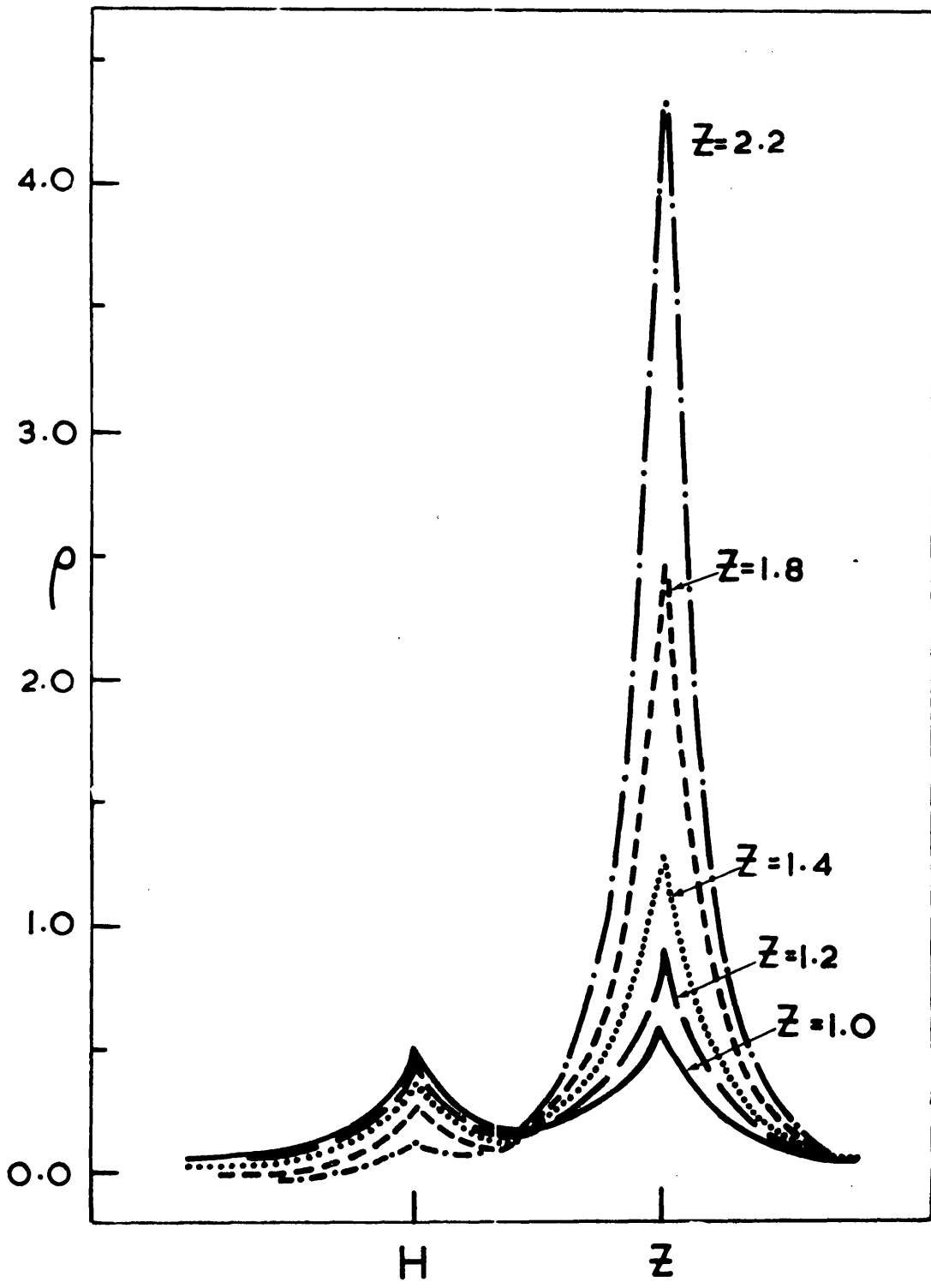


Figure 530

The electron density distribution along Z-H  
for the fully optimized ZHZH<sup>+2Z-2</sup> systems.



Part II - The Hamilton-like Systems

We recall that the  $ZHZH^{+2Z-2}$  study is an extension of the  $ZHZ^{+2Z-1}$  calculations rather than an attempt to represent the bridge in diborane. A more realistic representation of the bridge in diborane is provided by the Hamilton-like system given in Figure 301, since the true bridge geometry is used. With this system a 2s Slater-type orbital, with an exponent  $\beta$ , was centred on each boron nucleus and a 1s Slater-type orbital with an exponent  $\alpha$  was centred on each proton. The use of 2s rather than 1s orbitals was an attempt to provide a more realistic description of the outer boron electrons. Although we realised that a 2s orbital would not give an accurate description of the electron density near the boron nuclei, the integral routines available restricted us to s-type orbitals. Nevertheless these calculations, particularly the electron densities along the internuclear axes, provide interesting results when compared with  $ZHZ^{+2Z-1}$ ,  $ZHZH^{+2Z-2}$  and Hamiltons work.

The boron nucleus was given an effective nuclear charge,  $B_Z$ , of 2.0, 2.5 and 3.0 in an attempt to allow for the shielding of inner shell electrons. For each value of  $B_Z$  the molecular energy was minimised with respect to the orbital exponents. The results of these calculations are given in Table 504 and Figure 531. The total wave function,  $\Psi_k = \sum_i c_{ki} \phi_i$  was normalized to unity and the eigenvectors,  $c_{ki}$ , of the wave functions corresponding to minimum energy are given in Table 505. For each optimized system the electron density distribution along the three internuclear axes is shown in Figures 532, 533 and 534. The method used to evaluate the electron densities is given in Appendix III, along with the occupation numbers and transformation matrices that define the NSO's of the optimized Hamilton-like systems.

Table 504. The optimum molecular energy and orbital exponents of the Hamilton-like systems.

$B_Z$	$\alpha$	$\beta$	E (au)
2.0	1.040	2.795	-4.01235
2.5	0.964	3.401	-5.91719
3.0	0.883	4.071	-8.41555

Table 505. The eigenvectors of the wave functions which describe the optimized Hamilton-like systems.

$c_{ki}$ \ $B_Z$	2.0	2.5	3.0
$c_{k1}$	0.2094148	0.3284251	0.4100744
$c_{k2}$	0.0253939	0.0133735	0.0063996
$c_{k3}$	0.0253939	0.0133735	0.0063996
$c_{k4}$	0.1312437	0.1112413	0.0800614
$c_{k5}$	0.1312437	0.1112413	0.0800614
$c_{k6}$	-0.0927936	-0.0395411	-0.0160403
$c_{k7}$	-0.0078919	-0.0025653	-0.0007215
$c_{k8}$	-0.0078919	-0.0025653	-0.0007215
$c_{k9}$	0.0003991	-0.0000008	-0.0000027
$c_{k10}$	0.0297865	0.0066428	0.0014164
$c_{k11}$	-0.0008129	-0.0000455	-0.0000230
$c_{k12}$	0.0008129	-0.0000455	-0.0000230
$E$ (au)	-4.01235	-5.91719	-8.41555

Figure 531

The variational parameters and optimum energy plotted  
as a function of  $Z$  for the Hamilton-like systems.

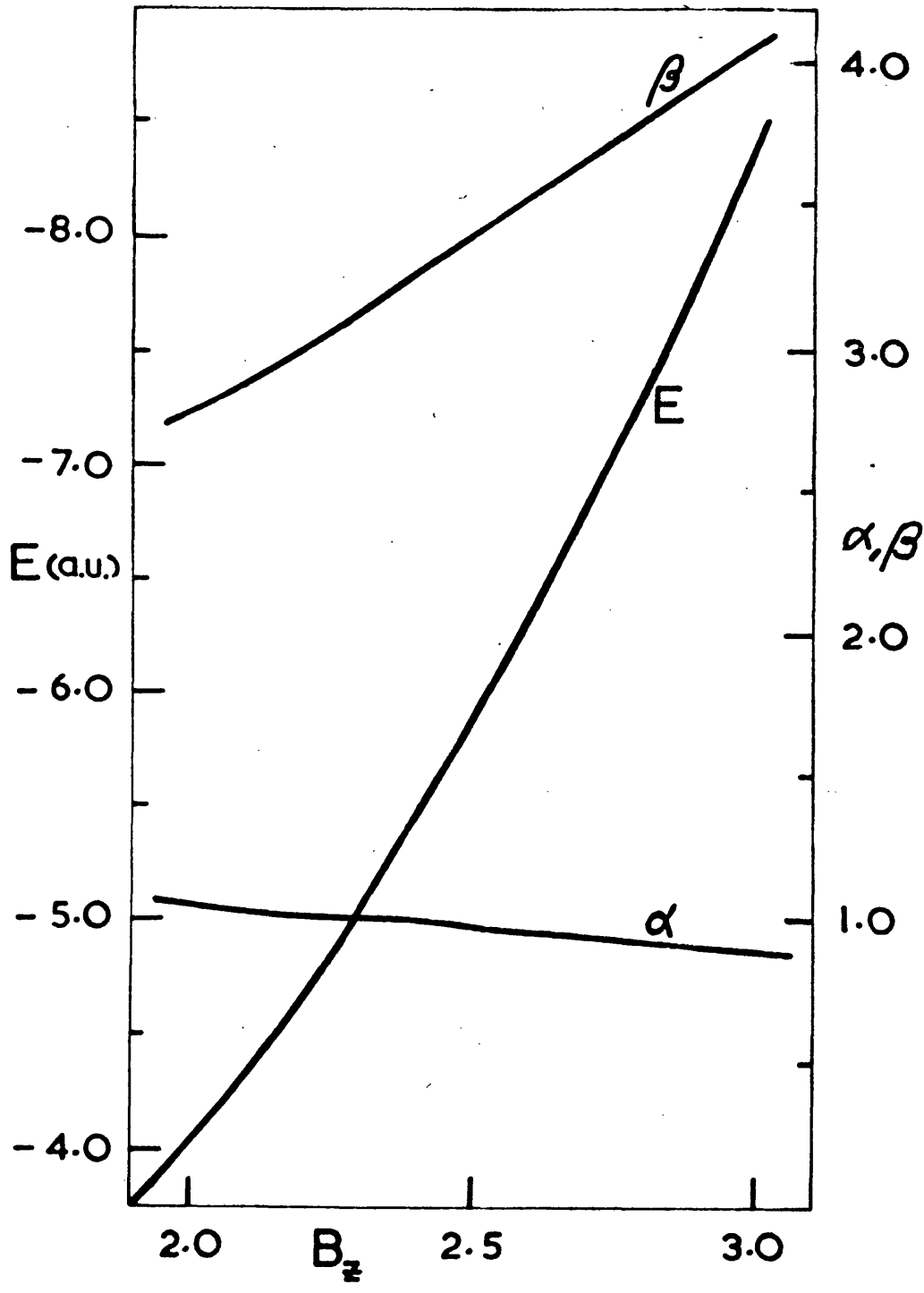


Figure 532

The electron density distribution along  
the O-B axis of the Hamilton-like systems.

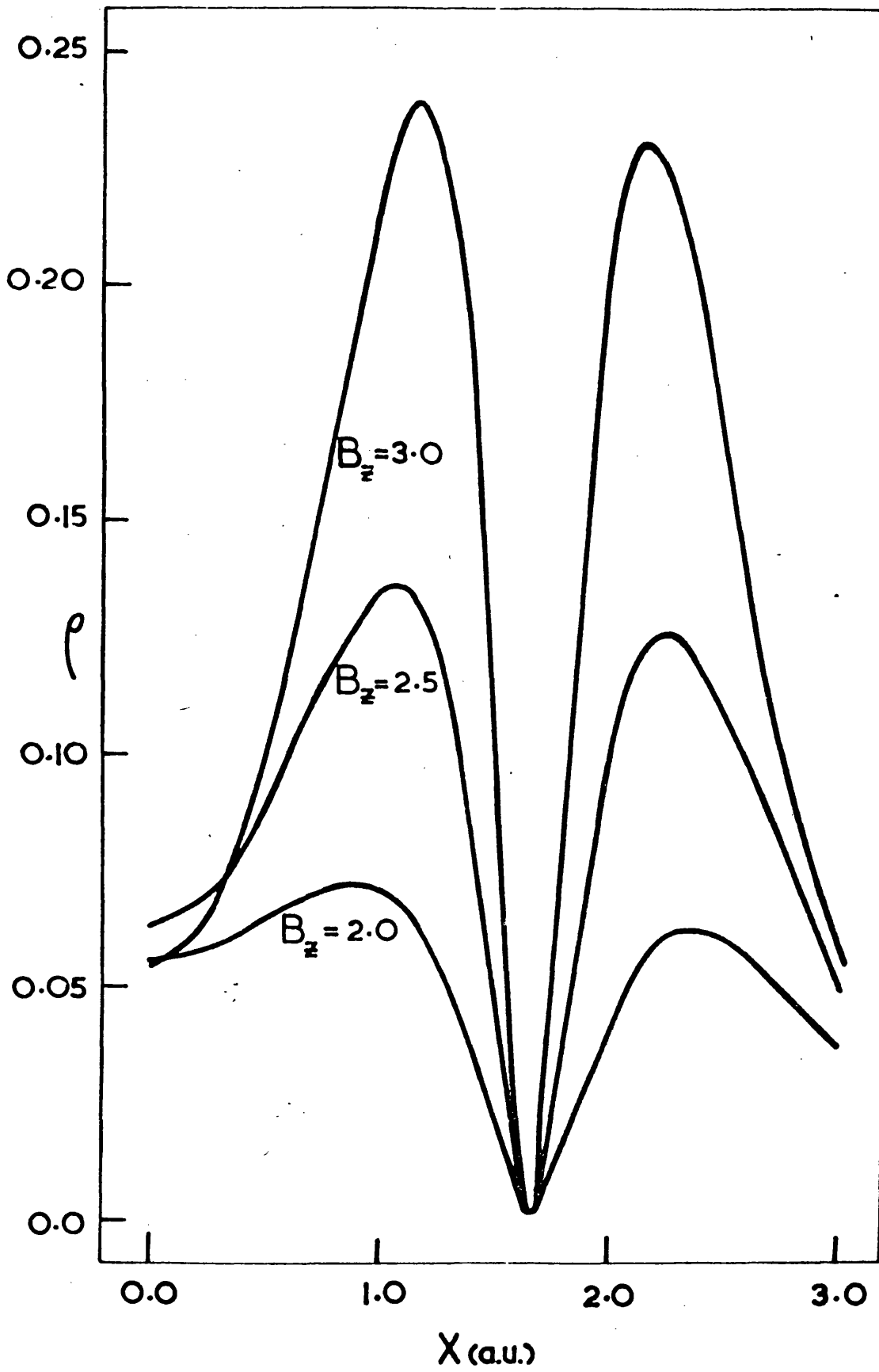


Figure 533

The electron density distribution along the  
O-H axis of the Hamilton-like systems.

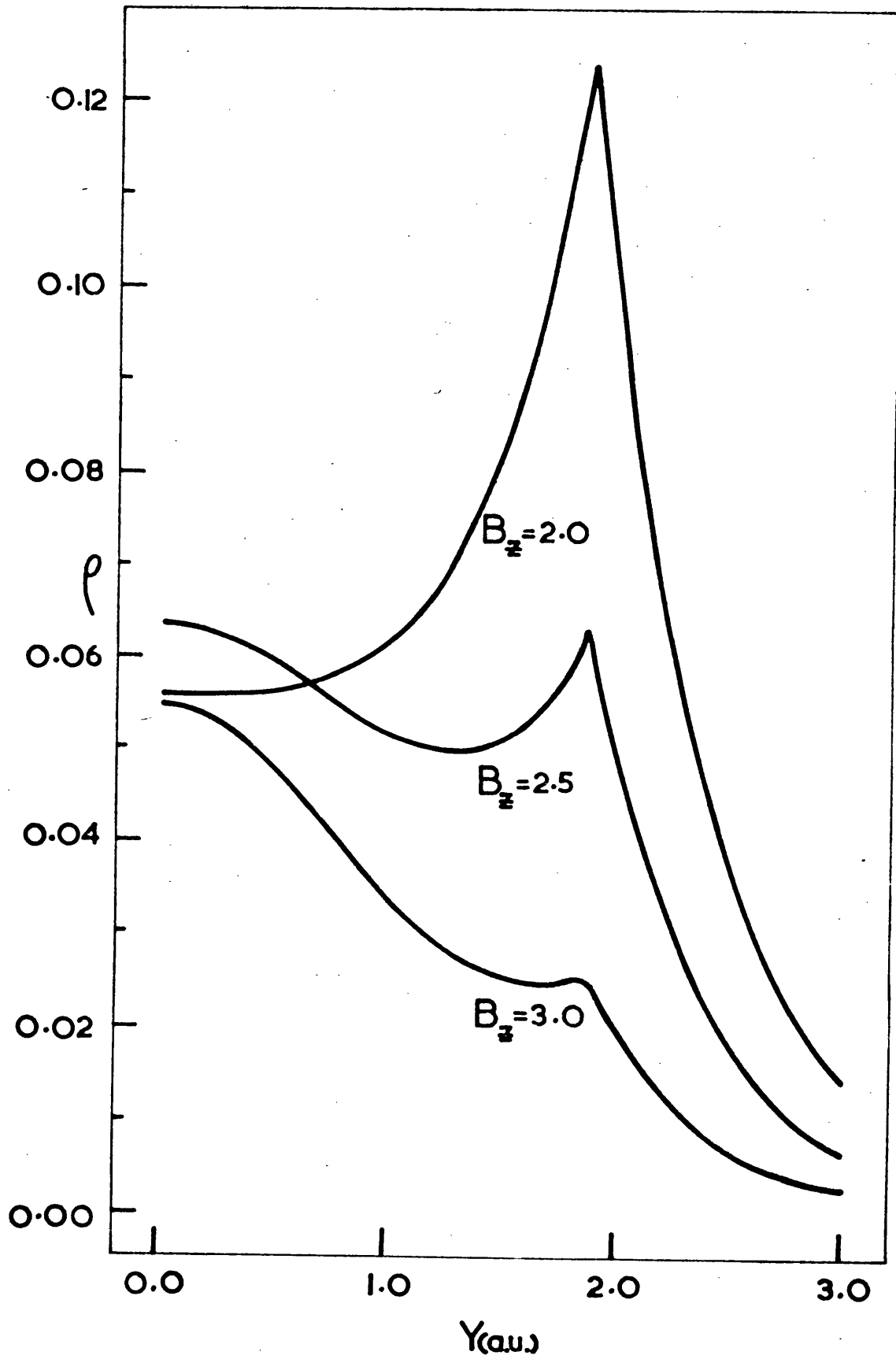
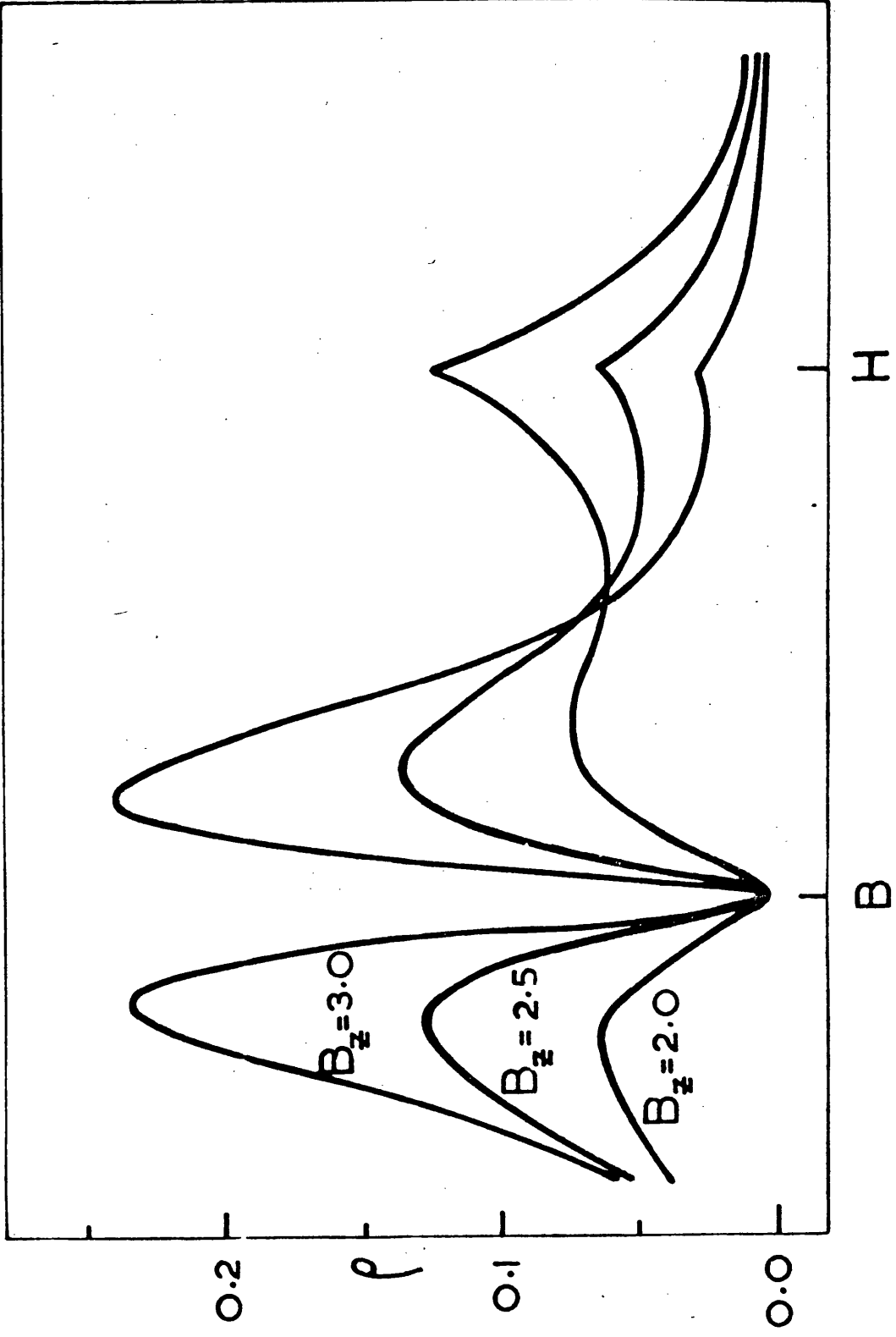


Figure 534

The electron density distribution along the  
Z-H axis of the Hamilton-like systems.



The energy and variational parameters of the Hamilton-like systems vary smoothly over the range of effective boron nuclear charge  $2.0 \leq B_Z \leq 3.0$  (see Figure 531). As expected, when  $B_Z$  is increased from 2.0 to 3.0 both the orbital exponent  $\beta$  and the electron density in the vicinity of the boron nucleus show a marked increase. These changes are accompanied by a decrease in  $\alpha$  and a decrease in the electron density near the protons. In fact, when  $B_Z = 3.0$  there is only a small cusp in the electron density at the H nucleus. A measure of the interaction of the 1s and 2s orbitals was obtained by comparing the electron density within a radius of 1 au of the boron nucleus with that of an isolated 2s orbital which has the same exponent. It can easily be shown that the peak density of an isolated 2s Slater-type orbital occurs at a distance  $r_M = \frac{2}{\beta}$  from the nucleus, where  $\beta$  is the orbital exponent. Table 506 gives the distances  $r_M$  and the equivalent distances in the Hamilton-like systems. These results, along with the density distributions, indicate that the system tends to have doubly occupied 2s orbitals and bare protons as  $B_Z$  increases. This comparison was taken a stage further by evaluating the peak densities of the isolated equivalent 2s orbitals. The expression

$$\rho_{2s} = \frac{\beta^5}{96\pi} r^2 e^{-\beta r}$$

gave peak densities of 0.0392, 0.0706 and 0.1211 for orbital exponents 2.795, 3.401 and 4.071 respectively. These peak density values are for orbitals containing a single electron, the density doubles when two electrons are present. For the Hamilton-like systems the peak densities near the boron nucleus are 0.0721, 0.1360 and 0.2400 for  $B_Z = 2.0, 2.5$

and 3.0 respectively. These results provide further evidence to support the prediction that the electrons populate the 2s orbitals to a greater extent as  $B_Z$  increases from 2.0 to 3.0.

The proton in the Hamilton-like system becomes more acidic as the effective nuclear charge  $B_Z$  is increased, see Figure 533. Even when  $B_Z = 2.0$  the electron density at proton sites is 0.1245, which is only 35.8% of the peak density of a corresponding isolated equivalent 1s Slater-type orbital. Obviously this percentage decreases as  $B_Z$  increases. Since the diborane bridge proton is known to be hydridic the density near the proton in the Hamilton-like system does not give an accurate description of the diborane bridge proton. In fact the charge distribution in the vicinity of the proton in the Hamilton-like system with  $B_Z = 2.0$  is similar to that near the hydrogen nucleus in the  $ZHZH^{+2Z-2}$  system with  $Z = 2.2$  and  $\theta_H = 90^\circ$ . Hamilton, in his study of the diborane bridge, used an effective boron nuclear charge of 3.0 and orbital exponents of 1.0 and 2.6 for the orbitals centred on the hydrogen and boron nuclei respectively. The protons in this system were slightly hydridic. This is not surprising since his hybridized molecular orbitals give a preferred direction, B-H, for the distribution of charge. In both Hamilton's work and the work described here the electron density in the vicinity of  $B_Z$  is not an accurate representation of the charge distribution near the boron nuclei in the diborane bridge.

The electron density distributions along the three internuclear axes were used to obtain approximate contour maps of the Hamilton-like systems. For the system with  $B_Z = 2.0$  the contours proved to be particularly interesting since there is evidence of a "bent bond" along

the B-H direction. The density line of maximum charge, i.e. minimum slope, as we move between centres B and D is curved inwards towards the centre of the nuclear framework. (This line is such that the density always decreases in magnitude when evaluated at adjacent positional co-ordinates along its normal, provided that the co-ordinates are in the same quadrant of the x, y axes). This effect was observed in the  $ZHZ^{+2Z-1}$  system and also in Christoffersen's study of  $H_3^+$ . The "bent bonds" would appear, therefore, to be characteristic of calculations on electron deficient systems which have s-type basis orbitals.

The total energy of Hamilton's best single configuration was -2.53 au and he estimated that configuration interaction would lower this value to about -2.55 au. The energies found for the systems investigated here are more negative. A direct comparison of energies is not particularly meaningful since Hamilton's calculation uses a different molecular orbital description. In fact, Hamilton's calculation was an attempt to provide firmer grounds for discrimination between several bonding descriptions that had been proposed for diborane and, due to the approximations involved, the energy results were only of secondary interest. The work described here provides accurate energies but, because of the limited set of basis orbitals, the electron density distributions are not good representations of the diborane bridge bond.

Table 506. The distance of peak density from the boron nucleus.

$B_Z$	$\beta$	$\tau_M$		
		isolated 2s orbital	inside the Hamilton nuclear framework.	outside
2.0	2.795	0.716	0.773	0.707
2.5	3.401	0.588	0.615	0.587
3.0	4.071	0.492	0.498	0.493

S U M M A R Y

The most interesting feature of the results for the  $ZHZH^{+2Z-2}$  systems is the decrease in  $\Theta_H(\text{opt})$  when the magnitude of the effective nuclear charge  $Z$  is increased from unity. This effect occurs throughout the range  $1.0 \leq Z \leq 2.2$ , although a calculation with  $Z = 10$  showed that  $\Theta_H(\text{opt})$  will ultimately pass through a minimum and then approach  $180^\circ$  when the value of  $Z$  is very large. A similar effect was found with the  $ZHZ^{+2Z-1}$  complexes for  $1.0 \leq Z \leq 1.7$ . The electron density distributions of both molecular systems indicate that the increased nuclear repulsion energy due to the decrease in  $\Theta_H$  is more than offset by the energy changes due to the increased charge cloud in the  $Z$ - $Z$  regions.

Each fully optimized  $ZHZH^{+2Z-2}$  system has a different geometry and, not surprisingly, individual characteristics. For example, when  $Z = 1.0$  the system behaves as a hydrogen molecule interacting with two hydrogen atoms. However, when  $Z \geq 2.2$  the molecular complex has the characteristics of two helium like atoms (which have a nuclear charge  $Z$ ) interacting with two protons. The systems with  $1.0 < Z < 2.2$  show the transition between the two limiting cases. For the range of  $Z$  used in the calculations the fully optimized systems with  $Z \geq 1.2$  are energetically stable with respect to a theoretical dissociation of the type  $2Z^{+Z-1} + 2H$ . The dissociation to give  $4H$  at  $Z = 1.0$  contrasts with the results of Conroy and Malli, but for both calculations  $H_4$  is unstable with respect to  $2H_2$ .

The electron density along the three internuclear axes of the  $ZHZH^{+2Z-2}$  systems show the movement of charge as a function of  $\Theta_H$  and  $Z$ . These results were used in conjunction with the energy calculations to determine the characteristics of the fully optimized systems. The comparison of electron density distributions in the  $ZHZH^{+2Z-2}$  and  $ZHZ^{+2Z-1}$  complexes shows that the most marked differences occur when  $Z \leq 1.4$ . The terminal nature of the  $Z$  nuclei in  $ZHZ^{+2Z-1}$  accounts for this effect. As

Z increases beyond 1.4 the charge builds up in the vicinity of the Z nuclei and the terminal nature of the Z nuclei in the two-electron systems becomes less important. Consequently, the electron density distribution of the corresponding two- and four-electron systems are more alike for the larger values of Z.

The study of the Hamilton-like system was restricted to a single nuclear geometry - the diborane bridge configuration. For the range of the effective boron nuclear charge, namely  $2.0 < B_Z < 3.0$ , the optimized systems have smoothly varying orbital exponents and molecular energy. The probability of finding an electron in the 2s orbitals centred on the boron nuclei increases as  $B_Z$  increases. By comparing these results with those of Hamilton it must be concluded that the bridge bonds representation of diborane cannot be described accurately by a wave function that is constructed from s-type orbitals only. A much more realistic representation is obtained by using molecular orbitals compounded of approximately tetrahedral hybrids at the two boron atoms and a 1s orbital at the appropriate hydrogen.

A P P E N D I X I

Evaluation of Integrals

The most serious technical difficulty in many calculations of molecular theory lies in the analytical complexity of the integrals which arise as soon as two or more centres of force become involved. Calculations of the properties of molecules containing four or more nuclei entails the evaluation of one-, two-, three- and four-centre integrals. All of the integrals involving one-electron operators over Slater-type orbitals can be written as closed form expressions with the exception of one of the nuclear attraction integrals. Thus, the molecular integral problem can be expressed quite simply as the evaluation of the electron repulsion integral of the form

$$\iint \Psi(C_1, A_1, 1) \Psi(C_2, A_2, 1) \frac{1}{r_{12}} \Psi(C_3, A_3, 2) \Psi(C_4, A_4, 2) d\tau_1 d\tau_2, \quad I(1)$$

and the three-centre nuclear attraction integral

$$\int \Psi(C_1, A_1, 1) \frac{1}{R_{A3}} \Psi(C_2, A_2, 1) d\tau_1 \quad I(2)$$

The symbol  $\Psi(C, X, i)$  denotes a one-electron atomic orbital for an electron  $i$ , referred to an atomic nucleus  $X$  as origin, and with an analytical form that is specified by the label  $C$ . The distance between electrons labelled 1 and 2 is  $r_{12}$ , and integration is over the space of these two electrons;  $d\tau_1$  and  $d\tau_2$  denote the volume elements.  $R_{xi}$  represents the distance between electron  $i$  and nucleus  $X$ . If  $(r_{xi}, \theta_{xi}, \phi_{xi})$  are the polar co-ordinates of electron  $i$ , measured from nucleus  $X$  as origin, each Slater type orbital is of the form

$$N(n, \ell, m) r_{xi}^{n-1} e^{-kr_{xi}} P_{\ell}^m(\cos \theta_{xi}) \sin^m \phi_{xi}, \quad I(3)$$

where  $N(n, \ell, m)$  represents a normalizing factor and the Legendre functions  $P_{\ell}^m(\cos \theta)$  are those defined by Hobson<sup>(33)</sup>. In the notation  $\Psi(c, X, i)$ , the label  $c$  summarizes the quantum numbers  $n, \ell$  and  $m$  and the screening parameter  $k$ . In equation I(1), the nuclei  $A_1$  to  $A_4$  may be distinct, or may coincide in different combinations. When all four nuclei are coincident a one-centre or mononuclear integral results. When  $A_1$  and  $A_2$  coincide, and  $A_3$  and  $A_4$  also coincide equation I(1) is termed a two-centre Coulomb integral. Coincidence between  $A_1$  and  $A_3$  and also between  $A_2$  and  $A_4$  results in a two-centre exchange integral, whereas when  $A_1, A_2$  and  $A_3$  are a common centre and  $A_4$  is distinct, equation I(1) then gives rise to a hybrid integral. When  $A_1$  and  $A_2$  coincide, but  $A_1, A_3$  and  $A_4$  are all distinct we obtain a three-centre Coulomb integral. If  $A_1$  and  $A_3$  coincide, but  $A_1, A_2$  and  $A_4$  are all distinct, I(1) is called a three-centre exchange integral. The case in which the nuclei  $A_1$  to  $A_4$  are all distinct defines the four-centre integral.

The technique that was employed to evaluate the "non-closed form integrals" was first formulated by Coulson<sup>(34)</sup> to obtain values for three-centre nuclear attraction integrals. The general technique, usually called the zeta-function method, was developed by Barnett and Coulson<sup>(35)</sup> in such a manner that it is applicable to all multicentre integrals. The essence of the zeta-function method is that the entire integrand can be expressed as a function of the polar co-ordinates of one of the atoms, say atom A. To this end the zeta-function series is introduced; the portion of the integral which involves orbitals centred on nucleus B can be written:

$$t_b^{m-1} e^{-\beta t_b} = \sum_{q=0}^{\infty} \left( \frac{2q+1}{\sqrt{t_a R_{AB}}} \right) P_q(\cos \theta_a) \mathcal{I}_{m,q}(\beta, t_a; R_{AB})$$

I (4)

$$= \beta^{-m+1} \sum_{q=0}^{\infty} \left( \frac{2q+1}{\sqrt{t \tau_b}} \right) P_q(\cos \theta_a) \mathcal{I}_{m,q}(1, t; \tau_b)$$

where  $t = \beta r_a$  and  $\tau_b = \beta R_{AB}$ .

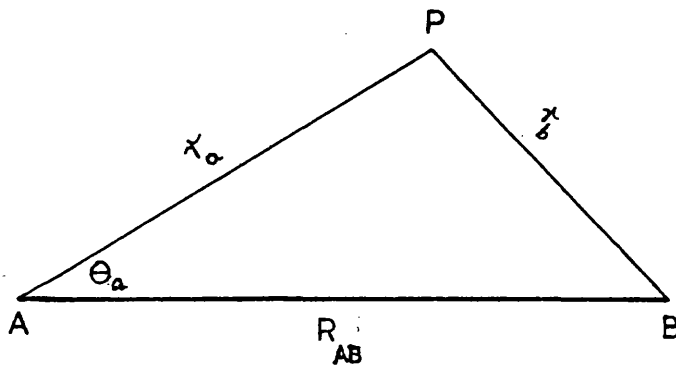


Figure I(1) Co-ordinates used in the Zeta-Function Expansion

In the case that  $m = 0$ , the expansion takes on a particularly simple form

$$\mathcal{I}_{0,q}(\beta, t_a; R_{AB}) = I_{q+\frac{1}{2}}(\tau_b) K_{q+\frac{1}{2}}(t) \quad (t_a \gg R_{AB}) \quad \text{I (5)}$$

where  $I_{q+\frac{1}{2}}$  and  $K_{q+\frac{1}{2}}$  are Bessel functions of purely imaginary argument.

If  $r_a \ll R_{AB}$  the roles of  $\tau_b$  and  $t$  in equation I(5) are interchanged.

The zeta-functions of higher  $m$  values can be computed by means of simple recurrence formulas.

The one- and two-electron, one- and two-centre integrals appearing in the calculation were evaluated using MIDIAT, a programme supplied by the Atlas Computer Laboratory. This programme uses formulae based on the zeta-function expansion in the evaluation of

the Coulomb, exchange and hybrid integrals, and closed form expressions for all the other integrals.

The three and four centre integrals appearing in the calculation were evaluated using programmes<sup>(36)</sup> supplied by the "Quantum Chemistry Programme Exchange"<sup>(37)</sup>. Each programme was based on the zeta-function method for evaluating molecular integrals. One programme per integral-type was necessary, namely:

- (a) Q.C.P.E.: 22A for the evaluation of three-centre Coulomb integrals.
- (b) Q.C.P.E.: 22B for the evaluation of three-centre one-electron nuclear attraction integrals.
- (c) Q.C.P.E.: 23 for the evaluation of three-centre exchange integrals.
- (d) Q.C.P.E.: 24 for the evaluation of four-centre integrals.

Most sections of the programmes listed above were coded in Fortran II, the remainder coded in F.A.P.(Fortran Assembly Programme). Access to an I.B.M.Computer was not readily available, therefore the programmes were adapted for use on the Atlas computer. The "dialect" of the Fortran accepted by the Atlas compiler is derived from Fortran II and known as Hartran. The Fortran II sections of the programmes, therefore, required very little alteration. The F.A.P. sections had to be completely re-written in either Hartran or Atlas machine code. Hartran was chosen since we were more familiar with this code. Unfortunately other difficulties were encountered with Q.C.P.E.programmes 22A and 22B. Errors, which proved particularly difficult to locate, were present in some of the dimension statements. With the help of Mr.M.E.Claringbold of the Atlas Computer Laboratory, these errors were corrected.

A P P E N D I X II

The Eigenvalue Problem

After all the necessary integrals had been calculated and the matrix elements formulated, the problem remained of finding the eigenvalues  $\lambda$ , of the equation

$$(\underline{H} - \lambda \underline{S}) \underline{C} = 0 \quad \text{II (1)}$$

The formalism adopted for this purpose was as follows -

A matrix  $\underline{U}$  was calculated which was consistent with the equation

$$\underline{U}^\dagger \underline{S} \underline{U} = \underline{I} \quad \text{II (2)}$$

where  $\underline{I}$  denotes a unit matrix and  $\underline{U}^\dagger$  denotes the complex conjugate transpose of  $\underline{U}$ . In other words, the matrix transformation which diagonalized and normalized the overlap matrix was found. The transformation which had been applied to  $\underline{S}$  was then applied to the  $\underline{H}$  matrix. Equation II(1) was then of the form

$$(\underline{H1} - \lambda \underline{I}) \underline{C1} = 0 \quad \text{II (3)}$$

where  $\underline{H1} = \underline{U}^\dagger \underline{H} \underline{U}$ . For the convenience of the programme notation  $\underline{H1}$  and  $\underline{C1}$  were adopted such that, for example,  $\underline{C1}$  denotes the column eigenvector corresponding to the transformed matrices.

The system of homogeneous equations II(3), has non-trivial solutions, if, and only if

$$\det \left| \underline{H1} - \lambda \underline{I} \right| = \begin{vmatrix} H1_{1,1} - \lambda & H1_{1,2} & \dots & H1_{1,12} \\ H1_{2,1} & H1_{2,2} - \lambda & \dots & H1_{2,12} \\ \vdots & \vdots & \ddots & \vdots \\ H1_{12,1} & H1_{12,2} & \dots & H1_{12,12} - \lambda \end{vmatrix} = 0 \quad \text{II (4)}$$

The expansion of the determinant yields a polynomial  $\phi(\lambda)$  of degree 12. The equation  $\phi(\lambda) = 0$  is described as the characteristic equation of matrix  $\underline{H1}$  and its roots  $\lambda_1, \lambda_2, \dots, \lambda_{12}$  as the characteristic roots. Described more technically,  $\underline{H1}$  is a twelve-square Hermitian matrix with characteristic roots  $\lambda_1, \lambda_2, \dots, \lambda_{12}$ . A property of Hermitian matrices is that there exists a unitary matrix  $\underline{W}$ , such that

$$\underline{W}^\dagger \underline{H1} \underline{W} = \text{diag} (\lambda_1, \lambda_2, \dots, \lambda_{12}) \quad \text{II (5)}$$

where the  $i_{\text{th}}$  column of matrix  $\underline{W}$  is the column eigenvector of  $\underline{H1}$  corresponding to the eigenvalue  $\lambda_i$ . Therefore, the solution of equation II(3) was found from diagonalizing  $\underline{H1}$ . The energy eigenvalues (or characteristic roots)  $\lambda_i$  and their corresponding column vectors  $\underline{C1}$  were found from the single operation. The column eigenvectors  $\underline{C}$  of equation II(1) were also required; they were calculated using the relationship

$$\underline{U} \underline{C1} = \underline{C} \quad \text{II (6)}$$

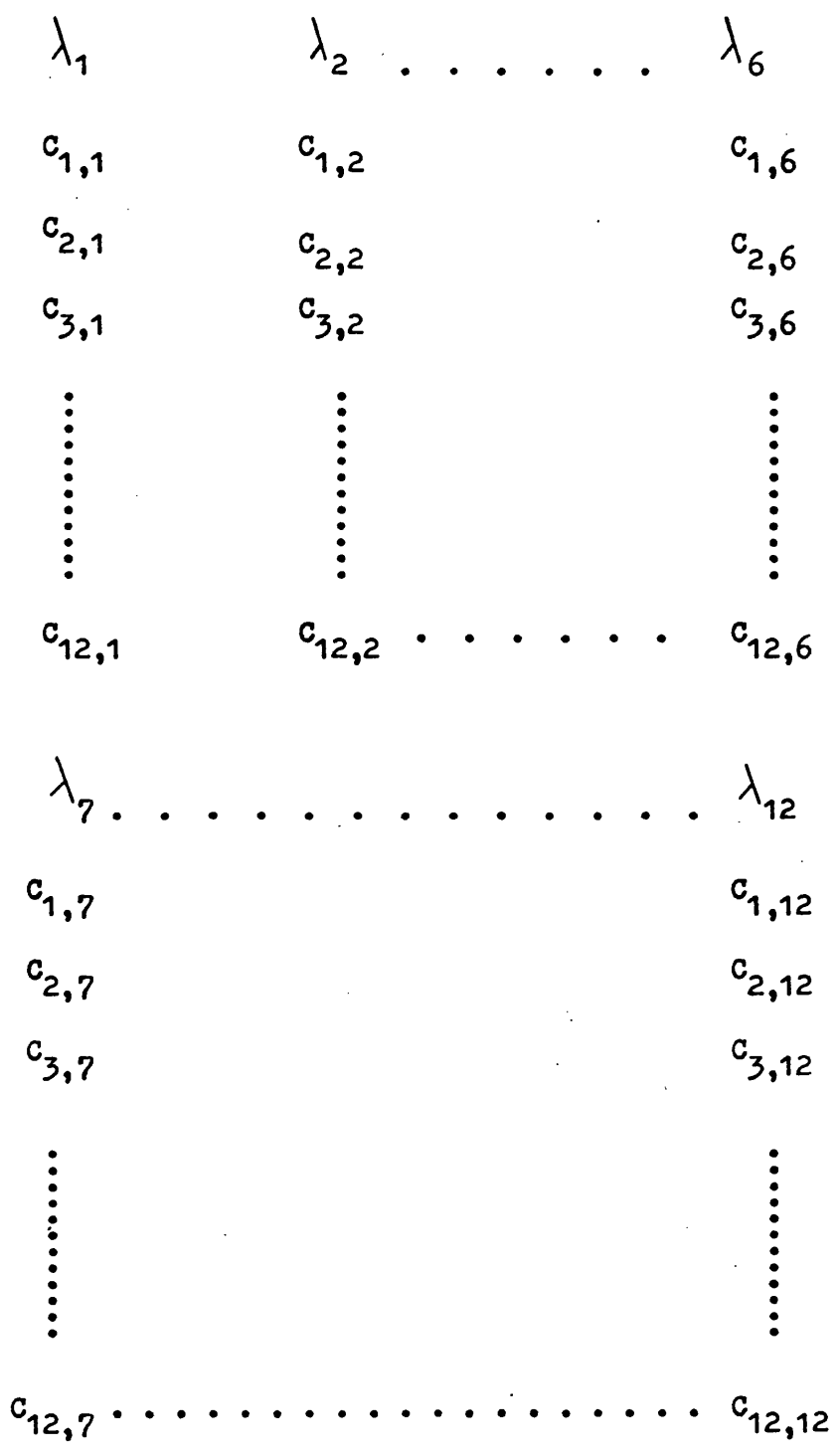
The column eigenvectors  $\underline{C1}$  and  $\underline{C}$  are comprised of twelve terms, for convenience the individual terms are described as eigenvectors and collectively as column eigenvectors.

A computer programme was written which set up and solved equation II(1). This programme is shown on page 97 and the function of each procedure called in the programme was as follows -

The procedure TRANS (A,B,M,N) transposes the matrix  $\underline{A}$  and stores the result in array B. The dimensions of matrix  $\underline{A}$  are M by N. SIGMA (TK, K,A,B) is a procedure which evaluates the sum over K, from A to B, of TK, with positive unit increments in K. The

procedure MXMULT (A,B,C,M,N,P) multiplies matrix  $\underline{A}$  by matrix  $\underline{B}$  and stores the result in array C. The dimensions of matrices  $\underline{A}$ ,  $\underline{B}$  and  $\underline{C}$  are M by N, N by P and M by P, respectively. The procedure JACOBI (A,B,N,RHO) computes the eigenvalues and eigenvectors of the matrix  $\underline{A}$ . After execution of the procedure, the eigenvalues are contained in  $\underline{A} [i, i]$  and the eigenvectors in  $\underline{B} [i, j]$ ,  $\underline{B} [i, j]$  being the  $i_{th}$  component of the column eigenvector which belongs to the  $j_{th}$  eigenvalue. Diagonalization is considered complete when the absolute value of the off diagonal terms is less than RHO. The value of RHO was set at  $10^{-8}$  because experimental tests showed the eigenvectors and eigenvalues were accurate to six decimal places if this value was used. The integer N denotes the dimension of the square matrix  $\underline{A}$ .

The method employed in solving equation II(1) has already been discussed and each stage in the solution can now be identified in the programme listing. The  $\underline{S}$  matrix is doubly stored in the arrays S and D, lines 1-3. If the matrix had been stored only once access to it in the later stages of the programme would have been lost. Line 4 diagonalizes the matrix D and lines 5-9 normalize it. The transformation  $\underline{U}^{\dagger} \underline{S} \underline{U} = \underline{I}$  is checked in lines 10-12. If this condition is violated the offending terms are printed out by lines 17-19. The matrix  $\underline{H1}$  is constructed by lines 13 and 14, and diagonalized by line 15. The eigenvectors  $C_{ik}$  are calculated from  $C1_{ik}$  in line 16. The remainder of the programme is comprised of print format statements which cause the results to be displayed in the following way -



```
"PROCEDURE" TRANS(A,B,M,N); "VALUE" M,N; "INTEGER" M,N;"ARRAY" A,B;
```

```
"BEGIN" "INTEGER" I,J;
```

```
  "FOR" I:=1 "STEP" 1 "UNTIL" M "DO"
```

```
  "FOR" J:=1 "STEP" 1 "UNTIL" N "DO"
```

```
  B [J,I] :=A [I,J] ;
```

```
"END" TRANS;
```

```
"REAL" "PROCEDURE" SIGMA(TK,K,A,B); "VALUE" A,B;"INTEGER" K,A,B;
```

```
"REAL" TK;
```

```
"COMMENT" ELLIOTT APPLICATIONS GROUP PROGRAM 138;
```

```
"BEGIN" "REAL" SUM;
```

```
  SUM:=0.0;
```

```
  "FOR" K:=A "STEP" 1 "UNTIL" B "DO"
```

```
SUM:=SUM+TK;
```

```
SIGMA:= SUM;
```

```
"END" SIGMA;
```

```
"PROCEDURE" MXMULT(A,B,C,M,N,P); "VALUE" M,N,P;
```

```
  "INTEGER" M,N,P; "ARRAY" A,B,C;
```

```
"COMMENT" C(1:M,1:P):=A(1:M,1:N)*B(1:N,1:P);
```

```
"BEGIN" "INTEGER" I,J,K;
```

```
  "FOR" I:=1 "STEP" 1 "UNTIL" M "DO"
```

```
  "FOR" J:=1 "STEP" 1 "UNTIL" P "DO"
```

```
  C [I,J] := SIGMA(A [I,K] *B [K,J] ,K,1,N);
```

```
"END" MXMULT;
```

```
"PROCEDURE" JACOBI(A,S,N,RHO);  
    "VALUE" N,RHO;"INTEGER" N; "REAL" RHO; "ARRAY" A,S;  
"BEGIN" "REAL" NORM1,NORM2,THR,MU,OMEGA,SINT,COST,INT1,V1,V2,V3;  
    "INTEGER" I,J,P,Q,IND;  
    "SWITCH" SS:=MAIN,MAIN1;  
    "FOR" I:= 1 "STEP" 1 "UNTIL" N "DO"  
    "FOR" J:= 1 "STEP" 1 "UNTIL" I "DO"  
    "IF" I=J "THEN" S [I,J] :=1.0 "ELSE" S [I,J] :=0;  
    INT1:= 0;  
    "FOR" I:= 2 "STEP" 1 "UNTIL" N "DO"  
    "FOR" J:= 1 "STEP" 1 "UNTIL" I-1 "DO"  
    INT1:= INT1+2*A [I,J] 2;  
    NORM1:=SQRT(INT1);  
    NORM2:= (RHO/N)*NORM1;  
    THR:= NORM1;  
    IND:= 0;  
    MAIN:THR:= THR/N;  
    MAIN1:"FOR" Q:= 2 "STEP" 1 "UNTIL" N "DO"  
        "FOR" P:= 1 "STEP" 1 "UNTIL" Q-1 "DO"  
            "IF" ABS(A [P,Q] ) "GE" THR "THEN"  
"BEGIN" IND:= 1;  
    V1:= A [P,P] ; V2:= A [P,Q] ; V3:= A [Q,Q] ;  
    MU:= 0.5*(V1-V3);  
    OMEGA:= "IF" MU=0.0 "THEN" -1.0  
        "ELSE -SIGN(MU)*V2/SQRT(V2*V2+MU*MU);  
    SINT:= OMEGA/SQRT(2*(1+SQRT(1 - OMEGA*OMEGA)));  
    COST:= SQRT(1-SINT*SINT);  
    "FOR" I:= 1 "STEP" 1 "UNTIL" N "DO"
```

```
"BEGIN" INT1 := A[I,P]*COST - A[I,Q]*SINT;  
      A[I,Q] := A[I,P]*SINT + A[I,Q]*COST;  
      A[I,P] := INT1;  
      INT1 := S[I,P]*COST - S[I,Q]*SINT;  
      S[I,Q] := S[I,P]*SINT + S[I,Q]*COST;  
      S[I,P] := INT1;  
"END";  
      "FOR" I := 1 "STEP" 1 "UNTIL" N "DO"  
"BEGIN" A[P,I] := A[I,P]; A[Q,I] := A[I,Q];  
"END";  
      A[P,P] := V1*COST*COST + V3*SINT*SINT - 2*V2*SINT*COST;  
      A[Q,Q] := V1*SINT*SINT + V3*COST*COST + 2*V2*SINT*COST;  
      A[P,Q] := A[Q,P] := (V1 - V3)*SINT*COST + V2*(COST*COST - SINT*SINT);  
"END";  
      "IF" IND = 1 "THEN"  
"BEGIN" IND := 0;  
      "GO TO" MAIN1  
"END";  
      "ELSE" "IF" THR > NORM2 "THEN" "GO TO" MAIN  
"END" "JACOBI";
```

Solution of equation II(1)

```
"FOR" I:=1 "STEP" 1 "UNTIL" 12 "DO"
"FOR" J:=1"STEP" 1 "UNTIL" 12 "DO"
D[I,J] :=S[I,J];
JACOBI(D,W,12,1.010-08);
"FOR" I:=1 "STEP" 1 "UNTIL" 12 "DO"
"FOR" J:=1 "STEP" 1 "UNTIL" 12 "DO"
"BEGIN" SYM:=CHECKR(D[J,J] );
      U[I,J]:=W[I,J]/SQRT(D[J,J] );
"END";
TRANS(U,UT,12,12);
MXMULT(UT,S,US,12,12,12);
MXMULT(US,U,II,12,12,12);
MXMULT(UT,H,UH, 12,12,12);
MXMULT(UH,U,H1,12,12,12);
JACOBI(H1,C1,12,1,010-08);
MXMULT(U,C1,C, 12,12,12);
"FOR"J:=1 "STEP" 1 "UNTIL" 12 "DO"
"IF" ABS(II[J,J]-1.0)>1.010-07 "THEN"
"PRINT" 'L'DIGITS(2),J,SAMELINE,'S3',SCALED(9), II[J,J];
"PRINT" 'L4',SAMELINE,SCALED(9),H1[1,1] ,'S3',H1[2,2] ,'S3',
      H1[3,3] ,'S3',H1[4,4] ,'S3',H1[5,5] ,'S3',H1[6,6] ,'L2';
"FOR" I:=1 "STEP" 1 "UNTIL" 12 "DO"
"PRINT" 'L', SAMELINE,SCALED(9),C[I,1] ,'S3',C[I,2] ,'S3',
      C[I,3] ,'S3',C[I,4] ,'S3',C[I,5] ,'S3',C[I,6];
"PRINT" 'L4',SAMELINE,SCALED(9), H1[7,7] ,'S3',H1[8,8] ,'S3'
      H1[9,9] ,'S3'H1[10,10] ,'S3',H1[11,11] ,'S3',
      H1[12,12] ,'L2';
"FOR" I:=1 "STEP" 1 "UNTIL" 12 "DO"
"PRINT" 'L', SAMELINE,SCALED(9),C[I,7] ,'S3',C[I,8] ,'S3',C[I,9],
      'S3',C[I,10] ,'S3',C[I,11] ,'S3',C[I,12];
"END";
```

A P P E N D I X III

N.S.O's and Electron Density Distribution

Natural spin orbitals are defined<sup>(14)</sup> as forming a basis set which diagonalizes the generalized first-order density matrix. Further, if a many-particle wave function  $\Psi$ , expressed as a superposition of configurations over some arbitrary basis set, is formulated in terms of configurations built up from natural spin orbitals, then this natural expansion of  $\Psi$  is distinguished as the superposition of configurations of most rapid convergence<sup>(24)</sup>. This definition can be described mathematically by writing the first-order reduced density matrix  $\gamma(x'_1|x_1)$  of an N-electron system in terms of the configuration interaction wave function and its natural expansion,

$$\gamma(x'_1|x_1) = N \int \Psi^*(x'_1, x_2, \dots, x_N) \Psi(x_1, x_2, \dots, x_N) (dx'_1) \quad \text{III(1)}$$

and

$$\gamma(x'_1|x_1) = \sum_k n_k \chi_k^*(x'_1) \chi_k(x_1) \quad \text{III(2)}$$

where  $\Psi(x_1, x_2, \dots, x_N)$  represents the normalized (to unity) configuration interaction wave function of a system of N electrons and  $X_i$  is the space-spin co-ordinates of electron i. The notation  $(dx'_1)$  indicates that the integration takes place over all co-ordinates except  $X_1$ . The prime on the  $X_1$  co-ordinate indicates that, when calculating the expectation value of some operator,  $X'_1$  is put equal to  $X_1$  after the operation has been performed. Thus the operator works simply on the unprimed co-ordinates.

The symbol  $\chi_k$  denotes the  $k^{\text{th}}$  NSO and  $n_k$  its occupation number. The occupation numbers satisfy the relation

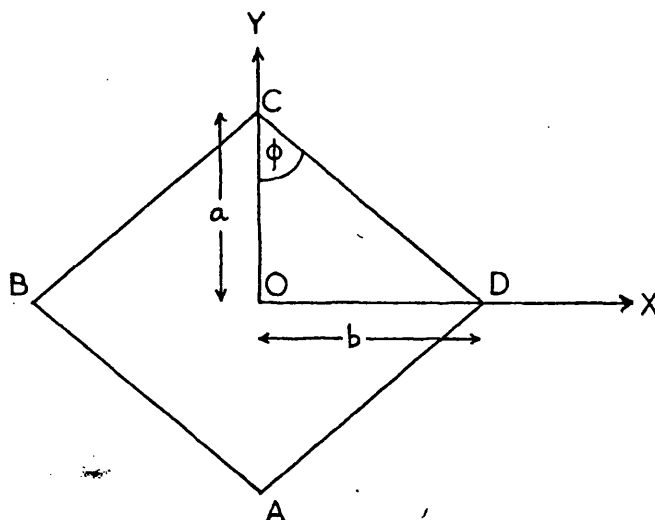
$$\sum_k n_k = N \quad \text{III(3)}$$

The absence of cross terms in equation III(2) is due to the fact that the NSO's form an orthonormal set, i.e.

$$\int \chi_k^*(x_i) \chi_l(x_i) dx_i = \delta_{kl} \quad \text{III (4)}$$

Consequently, the calculation of the electron density at any point in a system is greatly simplified when the wave function is expressed in terms of NSO's.

The procedure used in this work for evaluating the electron density at points along the internuclear axes was as follows. The molecular framework and basis orbitals were expressed in terms of a common co-ordinate system. Both the Hamilton-like and  $ZHZH^{+2Z-2}$  systems were specified by the co-ordinates shown in Figure III(1).



Distance  $OC = OA = a$

Distance  $OB = OD = b$

The orbitals centred on B and D are identical as are the ones centred on A and C.

Figure III(1) A representation of the systems in x,y co-ordinates

In all the calculations described here the molecular orbitals were constructed from 1s or 2s Slater-type functions. The analytical expressions for these orbitals in terms of x,y co-ordinates are given in equation III(5)

$$\begin{aligned}
 1sb &= \sqrt{\frac{\delta^3}{\pi}} \text{EXP} -\delta r_b = \sqrt{\frac{\delta^3}{\pi}} \text{EXP} -\delta \sqrt{(x+b)^2 + y^2} \\
 1sd &= \sqrt{\frac{\delta^3}{\pi}} \text{EXP} -\delta r_d = \sqrt{\frac{\delta^3}{\pi}} \text{EXP} -\delta \sqrt{(x-b)^2 + y^2} \\
 1sa &= \sqrt{\frac{\gamma^3}{\pi}} \text{EXP} -\gamma r_a = \sqrt{\frac{\gamma^3}{\pi}} \text{EXP} -\gamma \sqrt{x^2 + (y+a)^2} \\
 1sc &= \sqrt{\frac{\gamma^3}{\pi}} \text{EXP} -\gamma r_c = \sqrt{\frac{\gamma^3}{\pi}} \text{EXP} -\gamma \sqrt{x^2 + (y-a)^2} \\
 2sb &= \sqrt{\frac{\beta^5}{3\pi}} \text{EXP} -\beta r_b = \sqrt{\frac{\beta^5}{3\pi}} \sqrt{(b+x)^2 + y^2} \text{EXP} -\beta \sqrt{(b+x)^2 + y^2} \\
 2sd &= \sqrt{\frac{\beta^5}{3\pi}} \text{EXP} -\beta r_d = \sqrt{\frac{\beta^5}{3\pi}} \sqrt{(b-x)^2 + y^2} \text{EXP} -\beta \sqrt{(b-x)^2 + y^2}
 \end{aligned}
 \tag{III(5)}$$

where  $\gamma, \delta$  and  $\beta$  are the orbital exponents and  $r_b$ , for example, is the scalar distance of centre B from the point (x,y).

The basis spin molecular orbitals describing each system were then set up and evaluated at chosen points along the internuclear axes. NSO's were then constructed from the evaluated spin molecular orbitals by using the relationship

$$\psi_j(x,y) = \sum_i \psi_i^s(x,y) A_{ij}
 \tag{III(6)}$$

The normalized basis spin molecular orbitals of the  $ZHZH^{+2Z-2}$  systems are given in equation III(7) and the elements  $A_{ij}$  of the transformation matrix  $\underline{A}$  are presented at the end of this appendix.

$$\begin{array}{ll}
 \psi_1 = 1sb\alpha & \psi_2 = 1sb\beta \\
 \psi_3 = 1sd\alpha & \psi_4 = 1sd\beta \\
 \psi_5 = N_1(1sa + 1sc)\alpha & \psi_6 = N_1(1sa + 1sc)\beta \\
 \psi_7 = N_2(1sa - 1sc)\alpha & \psi_8 = N_2(1sa - 1sc)\beta
 \end{array}
 \tag{III(7)}$$

$N_1$  and  $N_2$  are normalization constants whose values are given by

$$N_1 = \frac{1}{\sqrt{2(1+ac)}} \quad N_2 = \frac{1}{\sqrt{2(1-ac)}} \quad , \tag{III(8)}$$

where  $ac$  represents the overlap between atomic orbitals  $1sa$  and  $1sc$ .

The electron density at the point  $(x,y)$ , denoted by  $\rho(x,y)$  was then evaluated quite simply since,

$$\rho(x,y) = \sum_j n_j \left| \chi_j(x,y) \right|^2 \tag{III(9)}$$

$n_j$  being the occupation number of the  $j^{\text{th}}$  NSO.

The computer programmes used in this part of the work are listed below. Also, the code names used in the programmes are identified in order to clarify each step in the calculation. The programme "ELECTRON DENSITY ALONG THE X AND Y AXES" calculates the density along the OD and OC directions at the points  $x = 0.0(0.1)3.0$  au,  $y=0.0$  and  $x=0.0$ ,  $y=0.0(0.1)3.0$  au. Along these axes the expressions for the normalized basis molecular orbitals are simplified since one or other of the  $x,y$

co-ordinates are zero. The second programme "ELECTRON DENSITY ALONG THE CD DIRECTION" calculates the electron density at the points  $x=(a-y)\tan \phi$ ,  $y$  for  $y=-1.0(0.1)3.0$  au. Both programme listings refer to the calculation of the  $ZHZH^{+2Z-2}$  densities; when the Hamilton-like systems were considered the expressions for Slater-type 2s orbitals replaced the 1s functions centred on B and D.

Programme code names

- LOOP - the number of calculations in the batch.
- ALPHA - the exponent of the orbitals centred on A and C.
- BETA - the exponent of the orbitals centred on B and D.
- AC - the overlap of the orbitals 1sa and 1sc.
- A - the distance OC (a).
- B - the distance OD (b).
- X,Y - the co-ordinates of the point at which the density is calculated.
- OSB - the analytical expression of the orbital centred on B.
- OSD - the analytical expression of the orbital centred on D.
- OSAP - the analytical expression of the normalized molecular orbital  
(1sa + 1sc).
- OSAM - the analytical expression of the normalized molecular orbital  
(1sa - 1sc).
- KI[J] - the  $j^{\text{th}}$  NSO
- A[I,J] - the elements of the transformation matrix  $\underline{A}$ .
- N[J] - the occupation number of the  $j^{\text{th}}$  NSO.
- RHO - the electron density at the point x,y.
- PHI - the angle  $\phi$

```
1. ELECTRON DENSITY ALONG THE X AND Y AXES;
2. "BEGIN" "INTEGER" K, LOOP;
3. "READ" LOOP;
4. "FOR" K:=1 "STEP" 1 "UNTIL" LOOP "DO"
5. "BEGIN" "INTEGER" I,J;
6. "REAL" ALPHA, BETA, AC,A,B,X,Y,OSB,OSD,OSAP,OSAM,RHO,PI;
7. "ARRAY" AA[1:8,1:8],N,KI,RO[1:8];
8. "READ" ALPHA,BETA,AC,A,B;
9. "FOR" I:=1 "STEP" 1 "UNTIL" 8 "DO"
10. "FOR" J:=1 "STEP" 1 "UNTIL" 8 "DO"
11. "READ" AA[I,J];
12. "FOR" J:=1 "STEP" 1 "UNTIL" 8 "DO"
13. "READ" N[J];
14. "PRINT" ' 'F' ';
15. PI:= 3.14159265;
16. "FOR" X:=0 "STEP" 0.1 "UNTIL" 3.0 "DO"
17. "BEGIN"
18. OSB:= SQRT(BETA↑3/PI)*EXP(-BETA*(B+X));
19. OSD:= SQRT(BETA↑3/PI)*EXP(-BETA*ABS(X-B));
20. OSAP:= SQRT(ALPHA↑3/(PI*2*(1+AC)))*2*EXP(-ALPHA*SQRT(A*A+X*X));
21. OSAM:= 0;
22. RHO:= 0;
23. "FOR" J:=1 "STEP" 1 "UNTIL" 8 "DO"
24. "BEGIN"
25. KI[J]:= OSB*AA[1,J]+OSB*AA[2,J]+OSD*AA[3,J]+OSD*AA[4,J]
26. + OASP*AA[5,J]+ OASP*AA[6,J]+ OSAM*AA[7,J]+OSAM*AA[8,J];
27. RO[J]:= N[J]*KI[J]*KI[J];
28. RHO:= RHO+RO[J];
29. "END";
30. "PRINT" ' 'L'RHO',SAMELINE,' 'S2'',SCALED(9),'X=',X,' 'S5'',RHO;
```

```

31. "END";
32. "FOR" Y:=0 "STEP" 0.1 "UNTIL" 3.0 "DO"
33. "BEGIN"
34. OSB:= SQRT(BETA↑3/PI)*EXP(-BETA*SQRT(B*B+Y*Y));
35. OSD:= OSB;
36. OSAP:= SQRT(ALPHA↑3/(PI*2*(1+AC)))*(EXP(-ALPHA*(A+Y))+
37.     EXP(-ALPHA*ABS(Y-A)));
38. OSAM:= SQRT(ALPHA↑3/(PI*2*(1-AC)))*(EXP(-ALPHA*(A+Y)) -
39.     EXP(-ALPHA*ABS(Y-A)));
40. RHO:=0.0;
41. "FOR" J:=1 "STEP" 1 "UNTIL" 8 "DO"
42. "BEGIN"
43. KI [J] := OSB*AA [1,J] + OSB*AA [2,J] + OSD*AA [3,J] + OSD*AA [4,J]
44. + OSAP*AA [5,J] + OSAP*AA [6,J] + OSAM*AA [7,J] + OSAM*AA [8,J];
45. RO [J] := N [J] * KI [J] * KI [J];
46. RHO := RHO + RO [J];
47. "END";
48. "PRINT" 'L'RHO', SAMELINE, SCALED(9), 'S3', 'Y = ', Y, 'S5', RHO;
49. "END";
50. "END";
51. "END";

```

The programme for evaluating the electron densities along the x and y axes of the Hamilton-like systems require lines 18, 19 and 34 to be replaced by:-

```

18. OSB:= SQRT(BETA↑5/(3*PI))*(B+X)*EXP(-BETA*(B+X));
19. OSD:= SQRT(BETA↑5/(3*PI))*ABS(B-X)*EXP(-BETA*ABS(B-X));
34. OSB:= SQRT(BETA↑5/3*PI)*SQRT(B*B+Y*Y)*EXP(-BETA*SQRT(B*B+Y*Y));

```

```
1. ELECTRON DENSITY ALONG THE CD DIRECTION;
2. "BEGIN" "INTEGER" K,LOOP;
3. "READ" LOOP;
4. "FOR" K:=1 "STEP" 1 "UNTIL" LOOP "DO"
5. "BEGIN" "INTEGER" I,J;
6. "REAL" ALPHA,BETA,AC,A,B,X,Y,OSB,OSD,OSAP,OSAM,RHO,PHI,PI;
7. "ARRAY" AA [1:8,1:8],N,KI,RO [1:8];
8. "READ" ALPHA,BETA,AC,A,B,PHI;
9. "FOR" I:= 1 "STEP" 1 "UNTIL" 8 "DO"
10. "FOR" J:= 1 "STEP" 1 "UNTIL" 8 "DO"
11. "READ" AA [I,J];
12. "FOR" J:= 1 "STEP" 1 "UNTIL" 8 "DO"
13. "READ" N [J];
14. "PRINT" 'F';
15. PI:= 3.14159265;
16. "FOR" Y:= -1.0 "STEP" 0.1 "UNTIL" 3.0 "DO"
17. "BEGIN"
18. X:= (A-Y)*SIN(PHI)/COS(PHI);
19. OSB:= SQRT(BETA↑3/PI)*EXP(-BETA*SQRT((X+B)↑2 +Y*Y));
20. OSD:= SQRT(BETA↑3/PI)*EXP(-BETA*SQRT((B-X)↑2 +Y*Y));
21. OSAP:= SQRT(ALPHA↑3/(PI*2*(1+AC)))*(EXP(-ALPHA*SQRT(X*X+(A+Y)↑2))
22.      +EXP(-ALPHA*SQRT(X*X+(A-Y)↑2)));
23. OSAM:= SQRT(ALPHA↑3/(PI*2*(1-AC)))*(EXP(-ALPHA*SQRT(X*X+(A+Y)↑2))
24.      -EXP(-ALPHA*SQRT(X*X+(A-Y)↑2)));
25. RHO:= 0.0;
26. "FOR" J:=1 "STEP" 1 "UNTIL" 8 "DO"
27. "BEGIN"
```

```
28. KI [J] := OSB*AA [1,J] + OSB*AA [2,J] + OSD*AA [3,J] + OSD*AA [4,J]
29. + OSAP*AA [5,J] + OASP*AA [6,J] + OSAM*AA [7,J] + OSAM*AA [8,J] ;
30. RO [J] := N [J] * KI [J] * KI [J] ;
31. RHO := RHO + RO [J] ;
32. "END" ;
33. "PRINT" 'L'RHO', SAMELINE, 'S2'', SCALED (9),
34. 'X = ', X, 'S2'', 'Y = ', Y, 'S5'', RHO;
35. "END"
36. "END" ;
37. "END" ;
```

The programme for evaluating the electron densities along the CD axis of the Hamilton-like systems required lines 19 and 20 to be replaced by:-

```
19. OSB := SQRT(BETA↑5/(3*PI)) * SQRT((X+B)↑2+Y*Y) * EXP(-BETA * SQRT((B+X)↑2+Y*Y));
20. OSD := SQRT(BETA↑5/(3*PI)) * SQRT((X-B)↑2+Y*Y) * EXP(-BETA * SQRT((X-B)↑2+Y*Y));
```

The occupation numbers  $n_j$  and elements  $A_{ij}$  of the transformation matrix  $\tilde{A}$  for the fully optimized systems are given in Tables III (i). Only the NSO's of  $\alpha$  spin are described in these tables since the spin eigenfunctions  $\alpha$  and  $\beta$  are degenerate. The transformation matrix is consistent with the relationship

$$\chi_j = \sum_i \psi_i A_{ij} \quad \text{III(10)}$$

where the basis spin molecular orbitals  $\psi_i$  (for the  $ZHZH^{+2Z-2}$  systems) are given in equation III(7). Each column of the tables is headed by  $n_j$  and followed by  $A_{ij}$ , where  $i = 1$  to 8. This NSO description represents a system of 4 electrons.

Table III(a) The  $ZHZH^{+2Z-2}$  system where  $Z = 1.0$ .

$n_j$	0.989504	0.993531	0.011858	0.005107
$A_{ij}$	0.849279	0.265199	-0.889221	0.0
	0.0	0.0	0.0	0.0
	-0.849279	0.265199	-0.889221	0.0
	0.0	0.0	0.0	0.0
	0.0	0.638708	1.357368	0.0
	0.0	0.0	0.0	0.0
	0.0	0.0	0.0	1.0
	0.0	0.0	0.0	0.0

Table III(b) The  $ZHZH^{+2Z-2}$  system where  $Z = 1.2$

$n_j$	0.988626	0.994473	0.012629	0.004272
$A_{ij}$	0.804791	0.298876	-0.855027	0.0
	0.0	0.0	0.0	0.0
	-0.804791	0.298876	-0.885027	0.0
	0.0	0.0	0.0	0.0
	0.0	0.605349	1.332928	0.0
	0.0	0.0	0.0	0.0
	0.0	0.0	0.0	1.0
	0.0	0.0	0.0	0.0

Table III(c) The  $ZHZH^{+2Z-2}$  system where  $Z = 1.4$

$n_j$	0.995155	0.990309	0.010796	0.003740
$A_{ij}$	0.356679	-0.780477	-0.849424	0.0
	0.0	0.0	0.0	0.0
	0.356679	0.780477	-0.849424	0.0
	0.0	0.0	0.0	0.0
	0.534537	0.0	1.309924	0.0
	0.0	0.0	0.0	0.0
	0.0	0.0	0.0	1.0
	0.0	0.0	0.0	0.0

Table III(d) The  $ZHZH^{+2Z-2}$  system where  $Z = 1.8$

$n_j$	0.996982	0.994306	0.006645	0.002067
$A_{ij}$	0.464909	-0.750915	-0.742651	0.0
	0.0	0.0	0.0	0.0
	0.464909	0.750915	-0.742651	0.0
	0.0	0.0	0.0	0.0
	0.400739	0.0	1.244456	0.0
	0.0	0.0	0.0	0.0
	0.0	0.0	0.0	1.0
	0.0	0.0	0.0	0.0

Table III(e) The  $ZHZH^{+2Z-2}$  system where  $Z = 2.2$

$n_j$	0.998826	0.998234	0.002341	0.000598
$A_{ij}$	0.565517	-0.741619	-0.607137	0.0
	0.0	0.0	0.0	0.0
	0.565517	0.741619	-0.607137	0.0
	0.0	0.0	0.0	0.0
	0.248822	0.0	1.200043	0.0
	0.0	0.0	0.0	0.0
	0.0	0.0	0.0	1.0
	0.0	0.0	0.0	0.0

Table III(f) The Hamilton-like system where  $B_z = 2.0$

$n_j$	0.984839	0.993253	0.014302	0.007605
$A_{ij}$	0.716836	0.467293	-0.611820	0.0
	0.0	0.0	0.0	0.0
	-0.716836	0.467293	-0.611820	0.0
	0.0	0.0	0.0	0.0
	0.0	0.511747	0.977468	0.0
	0.0	0.0	0.0	0.0
	0.0	0.0	0.0	1.0
	0.0	0.0	0.0	0.0

Table III(g) The Hamilton-like system where  $B_z = 2.5$

$n_j$	0.998980	0.997747	0.002872	0.000400
$A_{ij}$	0.576716	-0.709580	-0.476402	0.0
	0.0	0.0	0.0	0.0
	0.576716	0.709580	-0.476402	0.0
	0.0	0.0	0.0	0.0
	0.362217	0.0	0.997652	0.0
	0.0	0.0	0.0	0.0
	0.0	0.0	0.0	1.0
	0.0	0.0	0.0	0.0

Table III(h) The Hamilton-like system where  $B_z = 3.0$

$n_j$	0.999802	0.999677	0.000501	0.000020
$A_{ij}$	0.641335	-0.707599	-0.355920	0.0
	0.0	0.0	0.0	0.0
	0.641335	0.707599	-0.355920	0.0
	0.0	0.0	0.0	0.0
	0.241871	0.0	1.009443	0.0
	0.0	0.0	0.0	0.0
	0.0	0.0	0.0	1.0
	0.0	0.0	0.0	0.0

REFERENCES

1. E.Schrodinger, Ann.der Physik, 79, 361 (1926)
2. W.R.Hamilton, C.G.J.Jacobi, see G.Joos, Theoretical Physics, Blackie and Son Ltd., London (1934).
3. J.L.Powell and B.Crasemann, Quantum Mechanics, Addison Wesley Publishing Co., Reading, Mass. (1961).
4. D.R.Hartree, Proc.Camb.Phil.Soc., 24, 89 (1928).
5. V.Fock, Z.Physic 61, 126 (1930).
6. J.C.Slater, Phys.Rev., 36, 57 (1930).
7. C.C.J.Roothaan, Rev.Mod.Phys. 23, 69 (1951).
8. F.O.Ellison, N.T.Huff and J.C.Patel, J.Am.Chem.Soc. 85, 3544 (1963).
9. R.E.Christoffersen, J.Chem.Phys. 41, 960 (1964),
10. H.Conroy, J.Chem.Phys. 40, 603 (1964).
11. J.R.Hoyland, J.Chem,Phys. 41, 1370 (1964).
12. K.E.Banyard and H.Shull, J.Chem.Phys. 44, 384 (1966).
13. K.E.Banyard and A.D.Tait, J.Chem.Phys. 49, 3050 (1968).
14. P.O.Lowdin and H.Shull, Phys.Rev. 101, 1730 (1956).
15. R.S.Mulliken, J.Chem.Phys. 23, 1833 (1955).
16. K.W.Hedberg and V.Schomaker, J.Amer.Chem.Soc. 73, 1482 (1951).
17. W.C.Hamilton, Proc.Roy.Soc. A235, 395 (1956).
18. R.S.Mulliken, J.Chim.Phys. 46, 500 (1949).
19. M.Born and J.R.Oppenheimer, Ann.der Phys.84, 457 (1927).
20. H.Shull and G.G.Hall, Nature, 184, 1559 (1959).
21. W.Pauli, Z.Physik, 31, 765 (1925).
22. G.Goudsmit and S.Uhlenbeck, Naturwissenschaften, 13, 953 (1925).
23. H.Eyring, J.Walter and G.E.Kimball, Quantum Chemistry, John Wiley and Sons, Inc., New York (1944).
24. P.O.Lowdin, Adv.in Phys., 5, 1 (1956).

25. W.Kauzman, Quantum Chemistry, Academic Press Inc., New York (1957).
26. J.C.Slater, Quantum Theory of Molecules and Solids, Vol.1, McGraw-Hill Book Company, Inc., New York (1963), p.285.
27. Atlas Computer Lab., Chilton, Didcot, Berks.
28. M.P.Barnett et al., J.Chem.Phys., 40, 3082 (1964).
29. A.Macias, J.Chem.Phys., 48, 3464 (1968).
30. H.Conroy and G.Malli, J.Chem.Phys. 50, 5049 (1969).
31. R.Hoffmann, J.Chem.Phys. 49, 3739 (1968).
32. K.E.Banyard, J.Chem.Phys. 44, 4645 (1966).
33. E.W.Hobson, Theory of Spherical and Ellipsoidal Harmonics, Cambridge (1931).
34. C.A.Coulson, Proc.Camb.Phil.Soc. 33, 104 (1934).
35. C.A.Coulson and M.P.Barnett, Conference on Quantum Mechanical Methods in Valence Theory, 238, Office of Naval Research (1951).
36. R.M.Pitzer, J.P.Wright and M.P.Barnett, Technical Note No.23, Co-operative Computing Lab., M.I.T.
37. Quantum Chemistry Programme Exchange, Chem.Dept., Indiana University, U.S.A.